TITLE AND SUBTITLE (CITE IN FULL)

NIST Research Program on the Seismic Resistance of Partially-Grouted Masonry Shear Walls

CONTRACT OR GRANT NUMBER	TYPE OF REPORT AND/OR PERIOD COVERED

AUTHOR(S) (LAST NAME, FIRST INITIAL, SECOND INITIAL)

Schultz, A. E.

PERFORMING ORGANIZATION (CHECK (X) ONE BOX)
[X] NIST/GAITHERSBURG
[ ] NIST/BOULDER
[ ] JILA/BOULDER

LABORATORY AND DIVISION NAMES (FIRST NIST AUTHOR ONLY)
Building and Fire Research Laboratory, Structures Division (861)

NIST CATEGORY # 140

SPONSORING ORGANIZATION NAME AND COMPLETE ADDRESS (STREET, CITY, STATE, ZIP)
NIST
Gaithersburg, MD 20899

PROPOSED FOR NIST PUBLICATION
[ ] JOURNAL OF RESEARCH (NIST JRES)
[ ] J. PHYS. & CHEM. REF. DATA (JPCRD)
[ ] HANDBOOK (NIST HB)
[ ] SPECIAL PUBLICATION (NIST SP)
[ ] TECHNICAL NOTE (NIST TN)
[ ] MONOGRAPH (NIST MN)
[ ] NATL. STD. REF. DATA SERIES (NIST NSRDS)
[ ] FEDERAL INF. PROCESS. STDS. (NIST FIPS)
[ ] LIST OF PUBLICATIONS (NIST LP)
[X] NIST INTERAGENCY/INTERNAL REPORT (NISTIR)
[ ] LETTER CIRCULAR
[ ] BUILDING SCIENCE SERIES
[ ] PRODUCT STANDARDS
[ ] OTHER _____

PROPOSED FOR NON-NIST PUBLICATION (CITE FULLY)
[ ] U.S. [ ] FOREIGN

PUBLISHING MEDIUM
[X] PAPER
[ ] DISKETTE (SPECIFY)
[ ] OTHER (SPECIFY)
[ ] CD-ROM

SUPPLEMENTARY NOTES

ABSTRACT (A 2000-CHARACTER OR LESS FACTUAL SUMMARY OF MOST SIGNIFICANT INFORMATION. IF DOCUMENT INCLUDES A SIGNIFICANT BIBLIOGRAPHY OR LITERATURE SURVEY, CITE IT HERE. SPELL OUT ACRONYMS ON FIRST REFERENCE.) (CONTINUE ON SEPARATE PAGE, IF NECESSARY.)

A review of the current status of research on masonry structures at the Building and Fire Research Laboratory of the National Institute of Standards and Technology (NIST) is presented, and an ongoing project on partially-grouted masonry shear walls is summarized. This report draws from previous work conducted at NIST including a comprehensive literature review, simulated seismic load tests of unreinforced and reinforced masonry walls, and numerical analyses employing empirical formulations and finite element models. The previous NIST research culminates with a preliminary draft outlining a research program on partially-grouted masonry walls and numerical analyses.

The existing preliminary draft of the research plan on partially-grouted masonry shear walls is revised in response to recent findings on the cyclic load behavior of masonry shear walls and to better reflect laboratory requirements for simulated seismic load tests at the NIST tri-directional testing facility. Specimen configuration, test setup, instrumentation, testing procedure, and numerical modeling are presented, along with a discussion of the shear strength of the specimens calculated using expressions available in the technical literature. The issue of minimum horizontal reinforcement in masonry shear walls is addressed in an appendix, and expressions are derived to serve as a guideline for the program. Potential directions for future research are discussed in a second appendix.

KEY WORDS (MAXIMUM OF 9; 28 CHARACTERS AND SPACES EACH; SEPARATE WITH SEMICOLONS; ALPHABETIC ORDER; CAPITALIZE ONLY PROPER NAMES)
bond beam; building technology; cyclic load tests; finite element; horizontal reinforcement; masonry; partial grouting; seismic design; shear wall

AVAILABILITY
[X] UNLIMITED [ ] FOR OFFICIAL DISTRIBUTION - DO NOT RELEASE TO NTIS
[ ] ORDER FROM SUPERINTENDENT OF DOCUMENTS, U.S. GPO, WASHINGTON, DC 20402
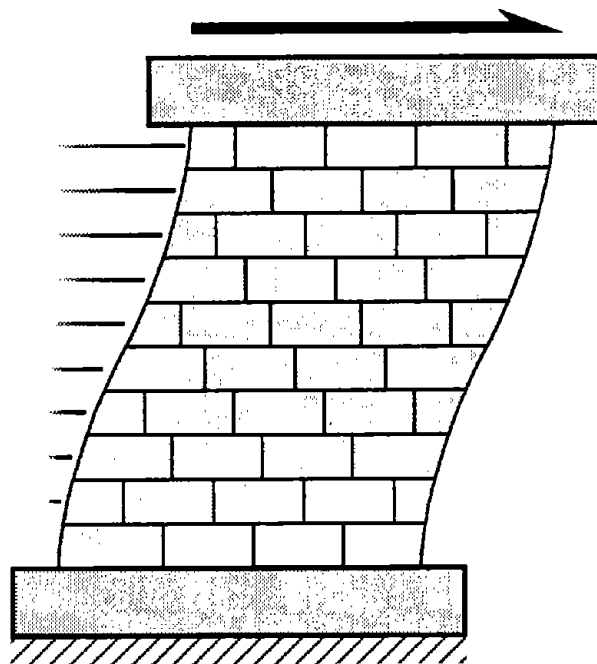[X] ORDER FROM NTIS, SPRINGFIELD, VA 22161

NOTE TO AUTHOR(S): IF YOU DO NOT WISH THIS MANUSCRIPT ANNOUNCED BEFORE PUBLICATION, PLEASE CHECK HERE. [ ]

NISTIR 5481

NIST Research Program
on the Seismic Resistance of
Partially-Grouted Masonry Shear Walls

Building and Fire Research Laboratory
Gaithersburg, Maryland 20899

NIST

United States Department of Commerce
Technology Administration
National Institute of Standards and Technology

NISTIR 5481

NIST Research Program
on the Seismic Resistance of
Partially-Grouted Masonry Shear Walls

Arturo E. Schultz

June 1994
Building and Fire Research Laboratory
National Institute of Standards and Technology
Gaithersburg, MD 20899

U.S. Department of Commerce
Ronald H. Brown, *Secretary*
Technology Administration
Mary L. Good, *Under Secretary for Technology*
National Institute of Standards and Technology
Arati Prabhakar, *Director*

ABSTRACT

A review of the current status of research on masonry structures at the Building and Fire Research Laboratory of the National Institute of Standards and Technology (NIST) is presented, and an ongoing project on partially-grouted masonry shear walls is summarized. This report draws from previous work conducted at NIST, including a comprehensive literature review (Yancey et al., 1991), simulated seismic load tests of unreinforced masonry walls (Woodward and Rankin, 1983; 1984a; 1984b; 1985a; 1985b) and reinforced masonry walls (Yancey and Scribner, 1989), and numerical analyses employing empirical formulations (Fattal and Todd, 1991; Fattal, 1993a; Fattal, 1993c) and finite element models (Yancey). The previous NIST research culminates with a preliminary draft outlining a research program on partially-grouted masonry shear walls (Fattal, 1993b). This program calls for simulated seismic load experiments of partially-grouted masonry walls, and numerical analyses, both empirical and finite element modeling of shear wall behavior.

The existing preliminary draft of the research plan on partially-grouted masonry shear walls is revised in response to recent findings on the cyclic load response of masonry shear walls and to better reflect laboratory requirements for simulated seismic load tests at the NIST tri-directional testing facility (TTF). Specimen configuration, test setup, instrumentation, testing procedure, and numerical modeling are presented, along with a discussion of the shear strength of the specimens calculated using expressions available in the technical literature. The issue of minimum horizontal reinforcement in masonry shear walls is addressed in an appendix, and expressions are derived to serve as a guideline for the experimental program. Potential directions for future research are discussed in a second appendix.

Key Words: bond beam, building technology, cyclic load tests, finite element, horizontal reinforcement, masonry, partial grouting, seismic loading, shear wall

ACKNOWLEDGEMENTS

TABLE OF CONTENTS

LIST OF TABLES

LIST OF FIGURES

1. INTRODUCTION

For nearly one decade, the Building and Fire Research Laboratory at the National Institute of Standards and Technology has maintained an active research program on the seismic behavior and design of masonry walls. This effort, which is part of the U.S. National Earthquake Hazard Reduction Program (NEHRP), has been one of the few coordinated research programs on the seismic resistance of masonry shear walls (Yancey et al., 1991), and the results it has generated have found their way to design practice through codes and standards. The experimental thrust of the program has focused on unreinforced concrete block walls, and study has been undertaken to investigate the influence on shear wall strength of factors such as cyclic loading (Woodward and Rankin, 1983), vertical compression stress (Woodward and Rankin, 1984a), wall aspect ratio (Woodward and Rankin, 1985b), and strengths of block and mortar (Woodward and Rankin, 1985a). A recent project on the cyclic load behavior of concrete block walls with horizontal reinforcement, but with no vertical steel is the first effort at the BFRL to investigate the seismic performance of reinforced masonry walls (Yancey and Scribner, 1989). Masonry research at NIST has also addressed numerical analysis of shear wall behavior, including validation of finite element methods for modeling shear wall response to cyclic lateral loads (Yancey) and development of empirical equations for predicting ultimate shear strength (Fattal, 1993a; 1993c; Fattal and Todd, 1991).

Because of the longstanding commitment of the BFRL to assist the construction industry through the development of design codes and standards, industry participation in the development of the NIST Masonry Research Program has been invited and fostered through informal contacts between BFRL staff and industry representatives, as well as through formal channels such as joint workshops. In a recent workshop (Fattal, 1993b), a number of suggestions were proposed by the Council for Masonry Research to enhance the competitiveness of the U.S. masonry construction industry. The concerns that were voiced most prominently in the workshop were related to construction costs, and total costs in masonry construction are most seriously impacted by labor than any other factor. Fully-grouted, reinforced masonry construction, as used in regions of high seismic risk of the U.S., is much more labor-intensive than other types of masonry construction, yet, the degree of seismic resistance it affords is not necessary for use in regions of moderate seismicity if a more economical alternative (i.e. less labor-intensive) can be identified. A potential alternative was discussed during the workshop, and it was suggested that NIST investigate the seismic behavior of partially-grouted masonry shear walls.

1

Partially-grouted masonry is defined as construction using hollow units in which only those vertical and horizontal cells that contain reinforcement are grouted. To further limit the amount of grouting, vertical reinforcement can be concentrated in fewer cells, particularly along the edges of wall panels (i.e. the jambs). A second issue of high priority that was identified by the Council for Masonry Research in the NIST workshop (Fattal, 1993b) is the replacement of horizontal reinforcement in bond beams with bed joint reinforcement in the form of welded wire grids. This practice promises to reduce the labor costs associated with forming and grouting bond beams, as well as accelerate the erection of masonry walls.

Study of these two construction issues, and how they affect the seismic performance of masonry shear walls, have become the principal objectives of the current phase of the NIST Masonry Research Program. A preliminary plan of the research program for partially-grouted masonry shear walls which focuses on these two issues was drafted by Fattal (1993b). The present document refines and further develops the partially-grouted masonry phase of the NIST Masonry Research Program. Changes are made to the existing draft plan primarily in response to recent research on the influence of bed joint reinforcement to in-plane shear strength. However, other issues such as the current schedule of tri-directional testing facility (TTF), practical concerns regarding construction and testing of masonry walls, and budgetary constraints also entered the decision making process. The changes do not affect the goals and objectives of the existing plan, rather, they are meant to increase the utility of the program

The following sections (1) summarize the preliminary draft of the plan by Fattal (1993b), (2) discuss and justify the changes to the preliminary draft plan, (3) summarize the revised research plan, (4) discuss the expected influences of the key variables on shear wall strength, (5) describe the test specimens and testing procedure, and (6) discuss the complementary numerical analyses. The document also addresses the issue of minimum horizontal reinforcement in masonry shear walls, and presents potential directions for future masonry research at NIST. Consultation with the Council for Masonry Research is of utmost importance in establishing the priory of these and other future directions.

2

2.   LITERATURE REVIEW

An extensive literature review conducted by NIST researchers on masonry shear wall tests (Yancey et al., 1991) serves as the backdrop for research activities at NIST on the seismic resistance of masonry construction. However, two noteworthy papers (Luders and Hidalgo, 1986; Hidalgo and Luders, 1987) were published prior to the initial draft of the NIST Masonry Research Plan (Fattal, 1993), and two others were published subsequently (Sanchez et al., 1992; Shing and Noland, 1992). These papers are of particular significance because they describe simulated seismic load tests of masonry shear walls which are reinforced horizontally with ladder-type wire grids in the bed joints. The observations and conclusions in these studies have an influence on the selection of the amount and type of horizontal reinforcement for the shear walls to be tested in the NIST Masonry Research Program.

2.1 Hidalgo and Luders (1987)

Hidalgo and Luders (1987) tested 29 reinforced masonry shear wall specimens under cyclic lateral load histories and constant vertical load. The specimens included fully-grouted and partially-grouted walls made using either concrete block or hollow clay brick. Some of the specimens were reinforced horizontally with welded wire grids, while others utilized hot-rolled, deformed reinforcing bars in grouted bond beams. Horizontal reinforcement ratios varied from 0 to 0.12% of gross vertical area, and masonry compression strength and shear-span-to depth ratio were the other major variables. Hidalgo and Luders note that due to the low ductility of the wire reinforcing grids, not all of the horizontal steel was able to participate in the resistance to lateral loads. Brittle fracture of the longitudinal wires at the welded intersections was observed in those bars that attracted load first, even though other longitudinal bars had not reached nominal capacity.

2.2 Luders and Hidalgo (1986)

In an earlier paper on the same experimental study, Luders and Hidalgo (1986) report the results of the first 17 shear wall tests. Based on experimental observations, they note that the effectiveness of bed-joint reinforcement, in the form of wire grids, is lower than that of deformed bars when used as shear reinforcement for masonry shear walls. In essence, the contribution of bed-joint reinforcement to peak shear strength is less than the force calculated at nominal yield. Luders and Hidalgo recommend the use of welded bed

joint reinforcement for masonry shear walls, but at a lower efficiency ratio than hot-rolled reinforcing bar. They observed masonry shear wall strength to be linearly proportional to the total cross-sectional area of wire reinforcing grids, but, for equal amounts of horizontal reinforcement, this reinforcement enhanced shear wall strength by only 55% of the increase provided by hot-rolled reinforcing bars.

2.3 Sanchez et al. (1992)

Sanchez et al. (1992) report the results of three cyclic load tests of confined masonry shear walls. Confined masonry, which is a popular type of construction in Latin America, comprises unreinforced masonry walls which are erected between vertical gaps for tie columns. A "confinement" frame of lightly-reinforced tie columns and tie beams is cast after the mortar in the masonry walls has hardened. This system has been reasonably successful throughout Latin American in mitigating seismic damage to low-rise masonry structures (one to three stories), but, for mid-rise structures (4 to 10 stories), inclined cracking of the masonry panels have been observed during strong ground shaking. For this reason, attempts have been made to introduce horizontal reinforcement in the bed joints of the masonry panels, as the use of bond beams is not considered cost-effective in countries where confined masonry is popular.

The shear wall specimens tested by Sanchez featured a window and a door opening, making them unsymmetrical in elevation. Of the three specimens, one had no horizontal reinforcement, while the other two had either bed joint reinforcement, in the form of wire grids, or less brittle, cold-drawn deformed (corrugated) wire reinforcement. The horizontal reinforcement in the latter specimen was embedded in the bed joint mortar rather than being placed in grouted bond beams. Sufficient horizontal steel was used to provide horizontal reinforcement ratios of approximately 0.11%.

The horizontally-reinforced specimens, regardless of the type of shear reinforcement, exhibited the same deformation capacity, and this amount was twice as large as that of the specimen with no horizontal reinforcement. However, the specimen with cold-drawn wire demonstrated 50% more lateral load capacity than did the wire grid specimen, even though both specimens had the same amount of horizontal steel. It was also observed that the wire reinforcing grids failed in a brittle manner at the welded intersections, whereas the cold-drawn wire displayed a "necked down" region at the fracture points, thus indicating more ductile behavior. Sanchez surmises that the premature

4

rupture of the wire reinforcing grids prevented widespread development of horizontal steel strength, resulting in the reduced shear strength of the masonry panels, thus confirming the conclusions set forth by Hidalgo and Luders. It is interesting to note, however, that tension tests of the horizontal reinforcement indicated approximately the same elongation in both the cold-drawn wire and the welded wire grids.

2.4 Shing and Noland (1992)

Shing and Noland (1992) recently reported on reinforced masonry shear wall tests designed to illustrate the behavior of welded wire grids as bed-joint reinforcement, as well as to investigate the influence of heat treatment on the behavior of the girds. Two specimens were built with a horizontal reinforcement equal to 0.07%, but one was reinforced with heat-treated wire grids, and the other utilized untreated grids. Both reinforcements were supplied by the same manufacturer, and the shear wall specimens were nearly identical to another specimen tested by Shing et al. (1989; 1990a; 1990b) as part of the TCCMAR program. Horizontal reinforcement in the TCCMAR specimen, comprising hot-rolled deformed bars in fully-grouted bond beams, provided a horizontal reinforcement ratio equal to 0.14%. Due to greater yield strengths of the wire reinforcing grids than the hot-rolled bar, the difference in horizontal steel forces at nominal yield is not as large as the horizontal reinforcement ratios suggest.

Observed global behavior, including cracking and ultimate shear strengths, deformation capacity, and hysteretic characteristics, was nearly identical for all three specimens. Shing and Noland conclude that in order to achieve ductile behavior in shear-critical walls, it is not sufficient for horizontal reinforcement to be ductile: The amount of steel must exceed some minimum threshold value. Shing and Noland do not elaborate on the minimum horizontal reinforcement concept, nor on a procedure to calculate this quantity. But, they suggest that it is difficult, if not impossible, to provide the necessary amount of horizontal reinforcement for ductile behavior in masonry shear walls when using the commonly-available wire grids. Shing and Noland postulate that welded bed-joint reinforcement could be used to supplement horizontal steel in grouted bond beams.

2.5 Requirements for Horizontal Reinforcement

The preceding studies clearly demonstrate that welded bed-joint reinforcement, as it is commonly produced, may not be conducive to ductile shear wall response. Rapid

cooling of the molten metal at the welded intersections embrittles the steel, and premature fracture is inevitable at these locations due to limited strain capacity. This property tends to make welded bed-joint reinforcement unsuitable for horizontal reinforcement in masonry shear walls subjected to earthquake forces, because premature fracture prevents widespread bridging of cracks, and this feature is necessary for the redistribution of shear stresses and uniform distribution of cracks that are sought in ductile wall behavior. It is also apparent increasing the ductility of bed joint reinforcement alone is not sufficient: The amount of horizontal reinforcement also affects the behavior of masonry shear walls. To modify the brittle nature of masonry walls reinforced with welded bed-joint reinforcement, it is imperative that both the quality of reinforcing steel and the amount of horizontal reinforcement be addressed.

Several alternatives can be exercised to improve steel quality in reference to welded bed-joint reinforcement. First, bed-joint reinforcement can be heat-treated after fabrication to eliminate the embrittlement produced by rapid cooling during the welding process. Or, the welding process can be improved by controlling weld heat and rate of cooling. Alternatively, a tougher steel can be used to fabricate this reinforcement. For example, stainless steels typically have maximum elongations that are two to three times as large as those for low-carbon structural steels. Furthermore, through the addition of alloying agents (such as in 321 and 347 stainless steels), or by limiting the carbon content (such as in 304L stainless steel), commercially-produced stainless steels are commonly modified to allow for welding (Flinn and Trojan, 1986). It is also noted that the use of bed-joint reinforcement manufactured from stainless steel is now commonplace in the U.K. and Canada, as improved corrosion resistance is sought. It may not be necessary, however, to resort to the use of exotic steels, as carbon wire can be cold-drawn under strict quality controls to ensure a minimum elongation on the order of 8% to 12%.

In addition to ductile horizontal steel, a shear wall must have a minimum amount of horizontal steel, if this reinforcement is to participate in the resistance to cyclic, in-plane lateral loads. The minimum horizontal reinforcement ratio concept has not been studied in a systematic manner for masonry walls, but it has been suggested that horizontal reinforcement in shear-critical masonry walls be sufficient to: (1) resist the shear force that produces the first diagonal crack, and (2) absorb, without fracturing, the elastic strain energy stored in the masonry. These conceptual approaches to minimum horizontal reinforcement ratio are investigated in Appendix A.

Assuming that the minimum amount of horizontal reinforcement can be defined in an accurate and reliable manner, the feasibility and practicality of using large amounts of bed joint reinforcement still remains a contentious issue. Shing and Noland (1992) used heat treated, bed-joint reinforcement welded using No. 9 gage wire (3.8-mm or 0.15-in. diameter) at every bed joint and still could not provide enough horizontal reinforcement for ductile shear wall response. The largest nominal wire size that is most commonly used for bed joint reinforcement is No. 9 gage, yet, it is possible to fabricate grids using larger diameter wires, such as No. 6 gage wire (4.8-mm or 0.19-in diameter), and such reinforcement should fit within a bed joint. This wire gage provides a modest increase of 27% in wire diameter, but, it gives rise to a 60% increase in wire cross-sectional area. Even larger wires can be used if the cross wires are butt-welded to the longitudinal wires so as to minimize overall thickness of the grids. Other alternatives include grids in which longitudinal wires have a low-profile rectangular section and grids with two longitudinal wires on either side of the cross wires. The former have been used in western Europe to minimize joint thickness (M. Catani, personal communication, 1994), and the latter are available commercially in the U.S.A.

3.   SUMMARY OF EXISTING DRAFT PLAN

The preliminary draft of the existing research plan developed by Fattal (1993b) was designed to demonstrate by experiment the resistance of partially-grouted masonry walls to cyclic, in-plane load histories. The program features selection of the most critical variables, close control of parametric variations, and repetition of particular combinations. In addition to the effect of partial grouting, the plan was designed to investigate the influence of other parameters, including type and amount of horizontal reinforcement, magnitude of vertical stress, height-to-length aspect ratio, and type of masonry (hollow clay unit or concrete block). The parametric ranges selected for study were chosen to supplement the existing database with carefully controlled series of tests to illustrate conclusive trends. A secondary objective of the plan is the validation of an empirical expression developed by Fattal for prediction of the shear strength of partially-grouted masonry shear walls (1993a; 1993c).

The existing plan is designed around six research priorities regarding the existing experimental database (Table 2.1), and each priority comprises evaluation of the influence of a single variable while all others are held constant (Fattal; 1993b). The parametric combinations identified in the existing draft research plan are summarized in Table 2.2a for the concrete block series, and in Table 2.2b for the hollow clay unit tests. The plan calls for a total of 52 shear wall tests, 30 of which are concrete block masonry and the remaining 22 are hollow clay unit masonry. The program includes replicate shear wall tests for each parametric combination, such that two tests for each of 26 independent parametric combinations are outlined.

Two height-to-length aspect ratios are included, one for stocky wall panels (r_1 = 0.6) which have height H = 1626 mm (64 in.) and length L = 2235 mm (88 in.), and another for square panels (r_2=1.0) with $H = L$ = 1829 mm (72 in.). Two types of horizontal reinforcement (either hot-rolled, deformed reinforcing bars or welded, ladder-type bed joint reinforcement) are included to study the feasibility of replacing bond beams with bed joint reinforcement. Specimens with four horizontal reinforcement ratios are considered, including some with no horizontal reinforcement (ρ_{h0} = 0), both bond beam and bed joint specimens with ρ_{h1} = 0.05%, ρ_{h2} = 0.12%, and bond beam specimens with ρ_{h3} = 0.26%. There are two vertical stress intensities in the existing plan, σ_{c0} = 0 and σ_{c1} = 1.38 MPa (200 psi). The second of these stress intensities is deemed representative of long-term loads in typical masonry construction.

8

A nominal compression strength equal to 138 MPa (2000 psi) is selected for the concrete block walls, while the hollow clay unit specimens are slated to have a nominal compression strength equal to 276 MPa (4000 psi). These compression strengths were suggested by the Council for Masonry Research (CMR), and they represent for the concrete block and clay unit masonry, respectively, a median value and a lower limit for the usual range encountered in masonry construction practice in the U.S.A.

A single vertical reinforcement ratio ($\rho_v = 0.3\%$) is specified for all specimens regardless of aspect ratio. This value was selected to ensure that flexural strength exceeds shear strength in all specimens. After studying the existing database of shear wall tests, Fattal (1993b) concludes that the influence of vertical reinforcement on shear wall strength is less sensitive and better understood than that of other variables in this study.

4. CHANGES TO EXISTING DRAFT PLAN

4.1 Background

The experimental activities outlined by Fattal (1993b) constitute a sound program which seeks to characterize the cracking and ultimate limit states of partially-grouted masonry shear walls. The values chosen for horizontal reinforcement ratio, type of horizontal reinforcement, and masonry compression strength are sound and defensible. Shear strength test data on partially-grouted masonry walls with horizontal reinforcement ratios in the selected range of 0% to 0.26% is scarce. Lightly-reinforced walls are appropriate for regions of low to moderate seismic risk, yet, design guidelines, or even consensus on expected or desired seismic response, do not currently exist in the U.S. Tests of specimens that are identical except for the type of horizontal reinforcement, are highly advisable to determine if bed joint reinforcement can replace, on a direct basis, horizontal reinforcing bars in grouted bond beams. For many reasons, use of the former is more economical than that of the latter. Single values of compression strength are selected for each type of masonry (clay or concrete), and these fall within the usual, and rather narrow, range of strengths used currently in masonry construction.

The changes discussed below are incorporated to increase the utility of the NIST research program on partially-grouted masonry shear walls. Rather than changing the nature of the research priorities (Table 2.1) or the general outline of the parametric combinations to be studied (Tables 2.2a and 2.2b), the following changes comprise mostly an increase of the parametric combinations to be studied at the expense of the replicate specimens. Additional parametric values are recommended in regions of variable space where either existing test data is nonexistent, and/or significant changes in the nature of shear wall behavior are expected.

4.2 Replication

The replicate specimens were eliminated. These were introduced originally to reduce statistical error in experimental data (Fattal, 1993b). Yet, repetition is generally not practiced in structural testing due to the complexity and cost of such tests. The situation is even more acute for large-scale tests. The time and expense required for an additional test are better invested on a specimen with a different parametric combination, and there should be enough flexibility in the testing program to repeat tests which generate questionable data.

4.3 Aspect Ratio

A third height-to-length aspect ratio (r) was added to the program increasing the total number of aspect ratios to three. Walls between floors in low-rise construction tend to be longer than they are high, making it commonplace for aspect ratios to be smaller than unity. Fattal (1993b) recognizes that little experimental information is available for aspect ratios less than unity, and the scarce information available suggests that the greatest influence of aspect ratio on shear strength takes place in this region. In addition, there is reason to believe that the increase in shear strength with decreasing aspect ratio reaches a saturation point, and that this limit exists in the range of $0 < r < 1$.

It is difficult to test stocky masonry walls ($r < 1$) in the NIST Tri-directional Test Facility if realistic wall heights are employed, because the required specimen length exceeds the horizontal clearance of the TTF. As a compromise, height-to-length aspect ratios r_0 = 0.5, r_1 = 0.7 and r_2 = 1.0 are selected for this program to cover a wide range of aspect ratios. It is noted that the original research plan calls for a nominal aspect ratio equal to 0.6, but the dimensions given for the stocky test specimens corresponds to an aspect ratio equal to 0.73.

4.4 Specimen Dimensions

For modularity in testing, the height of the specimens was kept constant while the length is varied. Variations in specimen height are not easily accommodated in the TTF, as it is designed for a few, discrete heights. A single height H = 1626 mm (64 in.) is preferred to maintain uniformity with the bulk of previous masonry shear wall tests at NIST, yet, a height H = 1422 mm (56 in.) is selected for all specimens for the following reasons. First, specimens that are 1626 mm (64 in.) tall require a length of 3252 mm (128 in.) to produce an aspect ratio equal to 0.5, but the maximum practical width that can be accommodated in the TTF is 2845 mm (112 in.). Second, in erecting the panels, an odd number of courses are sought so that the single bond beam may be placed at mid-height rather than at a non-zero vertical offset from mid-height. It is also deemed undesirable to use more than one bond beam per specimen as "concentration of reinforcement" is one of the goals of the partially-grouted masonry research program. To generate the three aspect ratios equal to 0.5, 0.7 and 1.0, respectively, lengths equal to 2845 mm (112 in.), 2032 mm (80 in.), and 1422 mm (56 in.) were selected.

11

4.5 Vertical Reinforcement Ratio

In the existing plan, vertical reinforcement ratio (ρ_v) was eliminated as a test variable and a single value of ρ_v was recommended for all specimens. From the viewpoint of parametric control, selection of a single vertical reinforcement ratio for all specimens is desirable, but it is impractical for walls with different aspect ratios. It is difficult, if not impossible, to fit enough vertical bars in the exterior cells of the stocky specimens ($r_1 = 0.5$) to produce the desired reinforcement ratio. In order to limit the use of grouting, the research plan recommends that all vertical reinforcement be contained in the exterior cells of the test specimens. Yet, the amount of vertical reinforcement that can be provided in this manner is constrained by dimensional limitations regarding the placement of several bars in a single cell.

If a constant vertical reinforcement ratio is deemed desirable, as called for in the original research plan, this ratio must be increased from the recommended value of 0.3% to at least 0.4% for the concrete block and clay unit specimens. This increase is necessary to ensure a margin of safety against flexural failure equal to at least 1.6. This follows from an expected upper bound of $\pm$ 60% on the error in shear strength estimates of the masonry walls (Fattal, 1993a). However, larger vertical reinforcement ratios only worsen the congestion problem.

A different approach is adopted in the revised plan: A single vertical reinforcement configuration is used for all specimens. By using a cross-sectional area of vertical steel, the reinforcement congestion problem is avoided in the stocky specimens ($r_1 = 0.5$). By selecting the required area on the basis of the slender panel ($r_3 = 1.0$), all specimens are guaranteed to fail in shear, as the flexural strength criterion is most severe for the slender panels. However, it is noted that this measure will not ensure a constant vertical reinforcement ratio for all specimens. The details of the analyses are documented in Chapter 6.

4.6 Horizontal Reinforcement Ratio

The largest horizontal reinforcement ratio was reduced from 0.26% to 0.21% for several reasons. First and foremost, it is difficult to guarantee shear failure of the slender clay specimens ($r = 1.0$) if these are endowed with a horizontal reinforcement ratio $\rho_{h3} = 0.26\%$, even if a vertical reinforcement ratio $\rho_v = 0.4\%$ were to be used. Second, it is

12

impractical to place the amount of horizontal reinforcement needed in a single bond beam to provide a horizontal reinforcement ratio equal to 0.26%. As demonstrated in Chapter 5, a horizontal reinforcement ratio equal to 0.26% greatly exceeds the requirements developed in Appendix A for partially-grouted masonry.

4.7 Axial Compression Stress

The axial compression stress (σ_c) equal to 1.38 MPa (200 psi) was retained in the revised research plan, however, it is specified as a net area stress. In the original research plan, axial compression stresses are assumed to act on the gross area, even though the resulting compression forces are unrealistically large when compared with current code provisions for allowable compression stresses in masonry. A compression stress equal to 1.38 MPa (200 psi) on the gross area translates to a net area stress σ_c equal to at least 2.76 MPa (400 psi), if the masonry is fully-bedded using 50% solid units, and may exceed 4.14 MPa (600 psi), for face-shell bedded masonry using units with minimum face shell thickness.

Current code provisions for masonry (MSJC, 1992; ICBO, 1991) do not allow compression service stresses in excess of $0.225f_m$ on the net area, and this requirement translates to 3.10 MPa (450 psi) for the concrete block masonry in the NIST research plan (f_m = 13.8 MPa, or 2000 psi). In addition, bending compression and slenderness effects may further reduce this allowable stress. Consequently, it appears more likely that the net area compression stress associated with long-term loads in a masonry wall is on the order of 1.38 MPa (200 psi), rather than 4.14 MPa (600 psi), or even 2.76 MPa (400 psi).

For the clay unit masonry specimens, a third compression stress σ_{c2} = 2.76 MPa (400 psi) was selected. This will ensure that there be test data for clay unit masonry with axial compression stress σ_c equal to 10% of masonry compression strength f_m. Since the compression strength of the clay unit masonry in the NIST research plan is nominally twice as large as that of the concrete block masonry, a single axial compression stress 1.38 MPa (200 psi) places only one-half as much demand on the clay masonry than it does on the concrete masonry. In addition, by retaining specimens with axial compression stress σ_{c1} = 1.38 MPa (200 psi), a more complete picture can be drawn regarding the influence of axial stress on shear wall strength.

4.8 Diagonal Compression Tests

Diagonal tension tests, as described in the ASTM E519 specification (ASTM, 1988b), were dropped from the revised research plan. The existing plan for research (Fattal, 1993b) calls for ASTM E519 tests to determine the diagonal tension strength of the masonry. Yet, there is clear evidence demonstrating that these tests do not correlate well with shear wall strength. For this reason, structural masonry researchers in the U.S. have all but abandoned the ASTM E519 test as a necessary component of experimental research on masonry shear walls. Diagonal tension tests do not accurately simulate the conditions of a wall, including aspect ratio, uniform shear transfer at top of wall, and mixed failure modes. Furthermore, design standards for masonry (ICBO, 1991; MJSC, 1992; *NEHRP*, 1994) correlate shear wall strength with masonry compression strength f_m.

4.9 Type of Masonry

The concrete block tests and hollow clay unit tests are separated into two independent, self-contained groups of modules, with the first of these groups being dedicated to the concrete block walls. With the exception of the west coast of the U.S.A., where strict seismic design provisions require all new load-bearing masonry construction to be reinforced and fully-grouted, clay brick producers sell mostly architectural units for unreinforced construction. However, many brick producers have the capacity to manufacture hollow structural clay units (hollow brick, structural tile and clay block), and would probably do so if a viable market existed. Since the current work on partially-grouted masonry is intended for regions of moderate risk, the concrete block component enjoys the strongest justification. However, the NIST research program on masonry construction includes a component on partially-grouted, hollow-unit clay masonry because there are indications that the availability and use of hollow clay masonry appears to be increasing markedly.

5. REVISED RESEARCH PLAN

5.1 General

The changes presented in the previous section were incorporated to define the revised masonry program. The overall goals and objectives of the research plan, as well as the variables selected for study, remain unchanged. Due to the magnitude and scope of the NIST Masonry Research Program on the Seismic Resistance of Partially-Grouted Masonry Shear Walls, a note is in order to justify the breadth and depth of this program.

The amount of experimental research dedicated to the in-plane shear strength of masonry walls has grown considerably during the last two decades, yet, a complete understanding of masonry shear wall behavior still proves to be elusive. There are marked differences in the observed influence of certain parameters when comparing shear strength test results from different sources (Yancey et al., 1991; Fattal and Todd, 1991). These discrepancies can be attributed to differences in testing programs (loading conditions, specimen configuration, test setup, etc.), as well as the large number of parameters which influence the behavior of masonry shear walls. Given this assessment of the current state-of-the-art, strict control of parametric variations in experimental investigations of masonry shear wall behavior becomes a necessity.

5.2 Description of the Plan

The six research priorities in the existing plan (Table 2.1) are retained, but a seventh priority is added (Table 5.1) to the revised plan. This last priority concerns the influence of axial compression stress, and addressing this issue is both possible and desirable due to the larger nominal compression strength selected for the clay unit masonry when compared with that selected for the concrete block masonry.

The parametric combinations selected for study are summarized in Table 5.2a for the concrete block wall specimens, and in Table 5.2b for the clay masonry specimens. Twenty-two concrete block wall tests are included, as well as 20 hollow clay unit specimens, for a total of 42 shear wall tests. This represents a reduction of nearly 20% over the existing plan which calls for 52 tests, even though the number of aspect ratios and axial compression stress levels are increased from two to three in the revised plan. These savings and additional flexibility are afforded by the elimination of the replicate specimens.

15

Three height-to-length aspect ratios are included, one for stocky wall panels (r_1 = 0.5) which have length L = 2845 mm (112 in.), another for intermediate wall panels (r_2 = 0.7) with L = 2032 (80 in.), and a third ratio for square wall panels (r_3 = 1.0) with L = 1422 mm (56 in.). All specimens have a nominal height H = 1422 mm (56 in.).

As in the existing plan, two types of horizontal reinforcement are called for, either hot-rolled reinforcing bar in grouted bond beams, or welded bed-joint reinforcement. However, the bed joint reinforcement must be fabricated from steel that is moderately ductile, and this can be assured through either (1) heat treating, or (2) using stainless steel, or (3) requiring a minimum specified elongation. Four horizontal reinforcement ratios are retained (ρ_{h0} = 0, ρ_{h1} = 0.05%, ρ_{h2} = 0.12%, and ρ_{h3} = 0.21%), but the largest value has been reduced to minimize congestion of reinforcement at the intersection of the bond beams and the grouted vertical cells, and to ensure that all of the specimens will fail in shear rather than flexure.

Expressions for minimum horizontal reinforcement ratio are derived in Appendix A for two criteria: one is based on strength and the other on energy. The strength criterion requires enough horizontal steel so that the resultant shear force released by the masonry upon diagonal cracking can be resisted by the reinforcement. The energy criterion requires sufficient horizontal reinforcement so that the elastic strain energy release associated with diagonal cracking of the masonry can be absorbed by the horizontal steel without fracture. Tables 5.3a and 5.3b summarize the ratios required by each criterion for all specimens. In calculating these ratios, the height, effective thickness and gross thickness of masonry in all specimens was taken as 1422 mm (56 in.), 64 mm (2 1/2 in.), and 194 mm (7 5/8 in.), respectively. For the concrete block specimens, the controlling minimum ratios are clustered around 0.03% to 0.07%, while, the range for the clay unit specimens is wider, with minimum ρ_h falling between 0.04% and 0.12%. The horizontal reinforcement ratios in the experimental program should serve to provide additional validation for the minimum ρ_h expressions in Appendix A.

The nominal compression strengths of 13.8 MPa (2000 psi) and 27.6 MPa (4000 psi) remain unchanged, as do the nominal compression stresses σ_{c0} = 0 and σ_{c1} = 1.38 MPa (200 psi). However, a third compression stress σ_{c2} = 2.76 MPa (400 psi) is added to the program. The third axial compression stress is used only with the clay masonry series of shear wall specimens.

A single vertical reinforcement scheme was adopted for all specimens in the revised plan. Two #6 hot-rolled, deformed bars, providing 568 mm² (0.88 in.²) of cross-sectional area, are used to reinforce each exterior cell of the partially-grouted masonry shear wall specimens.

5.3 Specimen Designations

The specimen designations used in Tables 5.2a and 5.2b comprise four descriptive groups of characters separated by hyphens. The first group of characters refers to the type of masonry, and is either CO for concrete block or CL for clay unit. The second group, which begins with the letter R, indicates aspect ratio and includes the numerical pairs 05, 07 or 10 which represent aspect ratios equal to 0.5, 0.7 and 1.0, respectively. The third group identifies with the letter B those specimens with horizontal reinforcement in bond beams, and those with bed-joint reinforcement with the letter J. The next pair of numbers are the first two decimal digits of the horizontal reinforcement ratios expressed in percentages, with 00, 05, 12 and 21 representing horizontal reinforcement ratios equal to 0%, 0.05%, 0.12%, and 0.21%, respectively. The last group of characters (beginning with the letter Q) indicate axial stress, and the two subsequent numbers are the first two decimal digits of axial compression stress when expressed as a fraction of masonry compression strength. The digit pairs 00, 05 and 10, respectively, represent 0%, 5% and 10% of masonry compression strength.

Consider, for example, the test specimen with the designation CO-R07-B21-Q10. This is a concrete block wall (as indicated by CO) with an aspect ratio equal to 0.7 (as noted by R07). The wall has a bond beam which contains horizontal reinforcement equal to 0.21% of the gross area of a vertical section of the wall (as specified by B21), and it sustains an axial compression stress equal to 10% of masonry compression strength (as defined by Q10).

17

6. CALCULATION OF WALL STRENGTH

In planning an experimental program on the in-plane shear strength of masonry walls, flexural failure must be prevented with a high degree of certainty. Requiring the flexural strength of a masonry shear wall to exceed shear strength is a necessary departure from seismic design practice in which flexure is preferred over shear as a mode of failure. However, the present research program seeks to study shear strength, so shear failure must be obtained in all specimens. This exercise entails the prediction of the shear and flexural strengths for various choices of wall dimensions and reinforcement amounts. Because the strength of the partially-grouted masonry walls cannot be predicted with a high degree of accuracy, particularly in-plane shear strength, a large margin of safety is used as a means of safeguarding against premature flexural failure of the specimens.

One of the objectives of the research program described in this document is to validate an empirical expression for predicting the in-plane shear strength of partially-grouted masonry walls (Fattal, 1993a). Thus, a computational tool is available for estimating the in-plane shear strength of the specimens. However, this expression needs validation, so its accuracy does not suffice for the purpose of safeguarding against flexural failure. Fattal (1993a) indicates that the maximum error range for this expression, when applied to partially-grouted masonry tests, is on the order of ±60%, which implies that the margin of safety against flexural failure should be at least 1.6. If the accuracy of the flexural strength estimate is also taken into account, then an even larger margin of safety is needed. In preparing the present plan for research, a target value of 2 was adopted as the margin of safety against flexural failure.

6.1 General

The following sections document shear strength estimates that were made in planning the present program. Shear strength estimates for specimens with a constant ratio of vertical reinforcement (ρ_v = 0.3%), as called for in the existing plan by Fattal (1993b), were used to show that the resulting margins of safety were too small to ensure shear failure in all cases. Shear strength estimates and margins of safety were also computed for two other vertical reinforcing schemes, including ρ_v = 0.4% for all specimens, and 2-#6 bars in each exterior cell of all specimens. The latter scheme was eventually adopted as a way of guaranteeing shear failure in all specimens while simultaneously minimizing congestion of vertical reinforcement. Three other expressions for in-plane shear strength of

masonry walls, one by Shing et al. (1990), and two others contained in the UBC (ICBO, 1991) and the proposed 1994 edition of the NEHRP recommended provisions (*NEHRP*, 1994), were used for comparative purposes in the strength analyses.

6.2 Fattal (1993a)

As part of the NIST masonry research program, Fattal (1993a, 1993c) developed an empirical expression for predicting the shear strength of fully-grouted and partially-grouted masonry shear walls. Data from a variety of experimental programs was used for the development of this expression (Yancey et al., 1991). The expression is a modification of one developed as part of the Japanese TCCMAR effort (Matsumura, 1985; 1987; 1988), and Fattal demonstrates measurable improvements in accuracy of shear strength predictions with these modifications.

According to Fattal (1993a), nominal shear stress at ultimate (v_n) is given by

$$v_n = v_m + v_s + v_a \tag{6.1}$$

where v_m, v_s, and v_a, respectively, are the contributions of masonry, horizontal reinforcement, and axial compression to shear strength. These quantities are given by

$$v_m = k_0 \, k_u \left[\left(\frac{0.5}{r + 0.8} \right) + 0.18 \right] \sqrt{f'_m f_{yv}} \, \left(\rho_v \right)^{0.7} \tag{6.2}$$

$$v_s = 0.011 k_0 \, \gamma \, \delta f_{yh} \, \rho_h^{0.31} \tag{6.3}$$

$$v_a = 0.012 \, k_0 \, f'_m + 0.2 \sigma_c \tag{6.4}$$

where ρ_v and ρ_h are the ratios of vertical and horizontal reinforcement, respectively, and f_{yv} and f_{yh} are the nominal yield stresses of these reinforcements. The dimensionless factors k_0, k_u, and γ are given in Table 6.1. The factor δ is equal to 1.0 for walls with points of inflection at mid-height, and 0.6 for cantilever walls. The nominal in-plane shear strength of a wall (V_n) is the product of v_n and the area (A) of a horizontal section of the wall based on gross dimensions. In fact, all of the parameters in Eq. (6.1) - (6.4) which are proportional to masonry area, including f_m, ρ_v, ρ_h, and σ_c, must be defined in terms of gross area of masonry (Matsumura 1987, 1988).

6.3 Shing et al. (1990)

As part of the U.S. component of the TCCMAR program, Shing et al. (1990a; 1990b) proposed an expression for estimating the in-plane shear strength of fully-grouted, reinforced masonry walls. This approach recognizes the contribution of masonry, horizontal reinforcement, and axial compression stress. However, the contribution of the latter is combined with the shear strength component of the masonry. Total shear strength of a section (V_n) is given by

$$V_n = V_m + V_s \tag{6.5}$$

where V_m and V_s, respectively, are the shear strength contributions of the masonry and horizontal reinforcement. These strengths are given by

$$V_m = \left[c_1 \left(\rho_v f_{yv} + \sigma_c \right) + c_2 \right] A_n \sqrt{f_m'} \tag{6.6}$$

and

$$V_s = \left[\left(\frac{L - 2d'}{s} \right) - 1 \right] A_b f_{yh} \tag{6.7}$$

where L is the length of the wall, d' is the centroidal distance of the vertical tension reinforcement to the nearest jamb, and s is the spacing of horizontal reinforcement. The empirical constants c_1 and c_2, respectively, are equal to 0.0217 $1/\sqrt{\text{MPa}}$ (0.0018 $1/\sqrt{\text{psi}}$) and 0.166 $\sqrt{\text{MPa}}$ (2.0 $\sqrt{\text{psi}}$).

The cross-sectional area of the wall (A_n) in Eq. 6.6 is based on a net horizontal section. However, the ratio of vertical reinforcement ρ_v and the axial compression stress σ_c must be defined in a consistent manner, because the products of these two parameters and the net area must be equal to the total area of vertical steel (A_{sv}) and the net compression force P_c, respectively. Since this expression was developed by Shing for fully-grouted walls, the distinction between net and gross section was not necessary. However, for partially-grouted masonry walls, care must be exercised when applying this formula.

The steel strength (V_s) is based on a 45° truss idealization of the masonry wall, in which horizontal reinforcing bars with area A_b are placed at a uniform spacing s along the height of the wall. In the present study, for specimens with bed joint reinforcement, application of Eq. (6.7) is straightforward. But, for bond beam specimens, s is taken as one-half the height of the panel (in the assumption that the top and bottom boundaries represent the edges of adjacent bond beams), and A_b is taken as the total area of steel in the bond beam.

6.4 UBC (ICBO, 1991)

The 1991 edition of the Uniform Building Code (ICBO, 1991) includes a formula for the shear strength of masonry walls which recognizes the contributions provided by horizontal reinforcement (V_s) and masonry (V_m). Nominal shear strength at ultimate is given by

$$V_n = V_m + V_s \tag{6.8}$$

where

$$V_m = C_d\, A_n\, \sqrt{f'_m} \tag{6.9}$$

$$V_s = A\, \rho_h\, f_{yh} \tag{6.10}$$

When using SI units, the coefficient C_d is taken as either 0.2 $\sqrt{\text{MPa}}$, for shear-span-to-depth ratios (M/Vd) less than or equal to 1/4, or 0.1 $\sqrt{\text{MPa}}$, for M/Vd greater than or equal to 1. The corresponding C_d limits in U.S. Customary units are 2.4 $\sqrt{\text{psi}}$ and 1.2$\sqrt{\text{psi}}$, respectively, for M/Vd equal to 1/4 and 1. Linear interpolation is used to define C_d for values of M/Vd between limits of 1/4 and 1. For aspect ratios equal to 0.5, 0.7, and 1.0 in the present study, values of 0.198, 0.184 and 0.161 $\sqrt{\text{MPa}}$ (2.385, 2.211, and 1.939 $\sqrt{\text{psi}}$), respectively, are used for C_d.

The ratio of horizontal reinforcement ρ_h is determined with respect to a vertical section through the wall. If gross sections are used to define this area of masonry, then the horizontal area A in Eq. 6.10 must also be calculated using gross sections.

21

6.5 Proposed NEHRP Provisions (*NEHRP* 1994)

Proposed changes to the 1994 Edition of the NEHRP Provisions (*NEHRP*, 1994) include a modified version of the shear strength formula for reinforced masonry walls. Nominal shear strength (V_n) is given by

$$V_n = V_m + 0.5V_s \qquad (6.11)$$

where the nominal shear strength of the masonry (V_m) is

$$V_m = c_3\,(4 - 1.75\frac{M}{Vd})\,A_n\,\sqrt{f'_m} + 0.25A_n\,\sigma_c \qquad (6.12)$$

and the shear strength of the horizontal reinforcement (V_s) is

$$V_s = A\,\rho_h\,f_{yh} \qquad (6.13)$$

The constant c_3 in Eq. (6.12) is equal to 0.083 $\sqrt{MPa}$ (1.0 $\sqrt{psi}$), and the axial compression stress σ_c must be calculated using net area if A_n is used for the second term in Eq. (6.12).

The expression for nominal strength of shear reinforcement (Eq. 6.13) is identical to that in the UBC (Eq. 6.10), but only 50% of this strength is assumed to participate effectively in the overall mechanism of shear resistance at ultimate conditions (Eq. 6.11).

6.6 Flexural Strength

The flexural strength of the masonry wall specimens in this study was calculated using the ACI rectangular stress block, as recommended by Shing et al. (1990b). Since all of the vertical reinforcement is concentrated in the exterior cells, only one-half of the vertical steel is effective in tension. The resistance afforded by vertical reinforcement in compression is ignored, and strain hardening is neglected. The mortar beds walls are assumed to cover only the face shells, and an effective face shell thickness (t_f) equal to 32 mm (1 1/4 in.) is assumed.

Equilibrium of vertical forces on the wall requires that the following condition be satisfied

$$0.85 f'_m A^*_n = 0.5A \, \rho_v \, f_{yv} + A_n \, \sigma_c \qquad (6.14)$$

where the first term is the resultant compression force in the masonry, the second term is the net force of vertical reinforcement in tension, and the last term is the net axial compression force on the wall. The masonry compression force (first term) is computed on the basis of the net area of masonry in compression (A^*_n), whereas the net compression force (third term) is based on the net horizontal area of the entire wall (A_n), and the ratio of vertical reinforcement (second term) is based on gross area of masonry in a horizontal section (A).

The depth of the effective compression block (a) is obtained by solving Eq. (6.14), which gives

$$a = \frac{(\rho_v \, f_{yv} + 2\sigma_c)}{1.7 f'_m} L \qquad (6.15)$$

if $a \le L_g$, and

$$a = \left(\frac{t}{2 t_f}\right) \left(\frac{\rho_v \, f_{yv} + 2\sigma_c}{1.7 f'_m}\right) L + \left(1 - \frac{t}{2 t_f}\right) L_g \qquad (6.16)$$

if $a > L_g$, where L_g is the distance from the jamb to the edge of the nearest ungrouted cell, and t is the nominal (gross) thickness of the wall.

Knowing the depth of the effective rectangular compression block (a), the internal resisting moment can be computed about the neutral axis of the wall section. Approximating the centroidal distance of the vertical tension steel to the nearest jamb as $0.5L_g$, allows the nominal moment capacity of the wall to be obtained as

$$M_n = \left(\frac{t L}{2}\right) \left[\rho_v \, f_{yv} \left(L - \frac{L_g + a}{2}\right) + \sigma_c (L - a)\right] \qquad (6.17)$$

The shear force at nominal flexural capacity (V_f) is calculated as $2M_n/H$, as the masonry specimens, which are fixed from rotation at both ends, are subjected to a symmetric state of reverse bending.

6.7 Observations

The calculated shear strengths of all for the specimens are summarized in Tables 6.3, 6.4, and 6.5 for three different schemes of vertical reinforcement. These schemes are described in Table 6.2. Vertical reinforcement scheme 1 is the one called for in the original research plan, i.e. $\rho_v = 0.3\%$. However, review of the calculated strengths in Table 6.3 indicates that for specimens with large amounts of horizontal reinforcement and no axial stress, shear failure cannot be guaranteed. In particular, specimens 19 and 29 have inordinately low margins of safety (MOS), which are defined as the ratio of V_f to V_n. Even though the margin of safety, when calculated using Fattal's formula, is nearly equal to the target value of 2 for specimen 19, the very small MOS values calculated using the other three shear strength formulas indicates a high likelihood of flexural failure or, at least marked flexural yielding.

To overcome the marginal flexural strengths of some of the specimens, a second vertical reinforcing scheme was devised. In scheme 2, vertical reinforcement ratio is increased by one-third of the original amount to 0.4% (Table 6.2). The calculated margins of safety for specimens 19 and 29 are still somewhat low, but, with the exception of the UBC formula, the computed MOS values are equal to at least 1.6. The increase in flexural strength afforded by scheme 2, however, comes at the expense of congestion of vertical reinforcement. This is particularly true for the stocky specimens ($r = 0.5$), in which one #8 bar and one #9 bar must be placed in each exterior cell. Complete grouting of such cells may be difficult, and the ability of the grout to develop bar strength is questionable.

As a compromise to the problems associated with vertical reinforcement schemes 1 and 2, a third scheme was devised (Table 6.2). The vertical reinforcing arrangement for the slender panels ($r = 1.0$), namely, two #6 bars in each exterior cell, is used for all of the specimens in scheme 3. Since the flexural strength criterion is most severe for the slender panels, this amount of vertical reinforcement is sufficient to guarantee flexural failure in the intermediate walls ($r = 0.7$) and the stocky specimens ($r = 0.5$).

It is also of interest to compare the various formulas for shear strength. Calculated shear strengths for several series of specimens (vertical reinforcement scheme 3) are plotted against aspect ratio, horizontal reinforcement ratio, and axial compression stress, respectively, in Fig. 6.1, 6.2, and 6.3. For each series of specimens, the only parameter which is varied is the horizontal ordinate, except for Fig. 6.1, in which specimens with

each of the three aspect ratios have different ratios of vertical reinforcement. Also, results for concrete block specimens are segregated from those for clay unit specimens. Generally, the UBC, NEHRP, and Shing formulas predict similar estimates of shear strength, while Fattal's formula produces smaller estimates and indicates less pronounced influences from the parameters studied.

Aspect ratio has a large effect on calculated shear strength, with Shing's formula demonstrating more than 100% increase in shear strength as r is decreased from 1 to 0.5 (Fig. 6.1). It is interesting to note that Shing's shear strength formula exhibits the same dependency on aspect ratio as do the other formulas, even though Shing's' formula for V_c does not explicitly include either aspect ratio ($r=H/L$) or shear-span-to-depth ratio (M/Vd). Horizontal reinforcement ratio has an equally important effect on predicted shear strength. An increase in ρ_h from 0.05% to 0.2% increases calculated shear strength more than 100% according to the UBC and Shing formulas.

Fattal's expression predicts the lowest shear strengths, and for the previously mentioned range of ρ_h, less than 20% increase in shear strength is observed. Fattal's formula, however, exhibits the largest influence of axial compression stress on shear strength (Fig. 6.3), and this expression demonstrates the same rate of shear strength increase with σ_c that is exhibited by the NEHRP formula. The UBC formula, in contrast, does not recognize this phenomenon.

7. SPECIMEN DETAILS

The partially-grouted shear wall specimens are described in the following. Panel configuration and geometry are described, along with test setup, reinforcement details, fabrication procedure, material tests, and the header/footer precast beams.

7.1 Masonry Wall Panel Configuration

To achieve the objectives of the experimental phase of the NIST research program on partially-grouted masonry shear walls, the wall elevations shown in Fig. 7.1 were selected for the three aspect ratios in the study. All concrete block specimens are to be made using blocks with 194 mm (75/8 in.) x 397 mm (15 5/8 in.) nominal dimensions and which satisfy the ASTM C90 specification for load-bearing concrete block (ASTM, 1985a). Hollow clay units satisfying ASTM C652 (ASTM, 1989a), and with dimensions similar to those of the concrete block, are to be used for the clay masonry specimens. Due to differences in the actual dimensions of the concrete block and the hollow clay units, the actual dimensions of the clay panels may differ slightly from those for the concrete panels. Head and bed joints with an approximate thickness of 9.5 mm (3/8 in.) are used to provide effective masonry unit dimensions of 203 mm (8 in.) x 406 mm (16 in.).

All masonry is to be face-shell bedded using Type S mortar which satisfies ASTM C270 (ASTM, 1989b). Cells containing reinforcement will be filled with coarse grout which meets the requirements of ASTM C476 (ASTM, 1983). Standard tests for material properties are given in Section 7.6.

A total of seven courses in each panel are used to provide a nominal height of masonry equal to 1422 mm (56 in.). The 2845 mm (112 in.), 2032 mm (80 in.) and 1422 mm (56 in.) lengths, respectively, for the stocky ($r_1 = 0.5$), intermediate ($r_2 = 0.7$) and slender ($r_3 = 1.0$) panels is achieved by varying the number of masonry units in each course (Fig. 7.1). All panels are to have a nominal thickness of 203 mm (8 in.).

The grouting pattern is shown in Fig. 7.2 for a slender panels specimen ($r_3 = 1.0$). For all of the specimens, only the exterior cells contain vertical reinforcement, and only these cells are to be grouted. For the bond beam specimens, the bond beam is located at mid-height, and it is formed using bond beam masonry units. Horizontal reinforcement for these specimens is concentrated in these single grouted elements. Bond beams are not

provided at the top and bottom of the panels, as these panels are to be connected to precast concrete header/footer beams described in section 7.4.

7.2 Vertical Reinforcement

Two #6 hot-rolled, deformed reinforcing bars, providing 568 mm^2 (0.88 in.^{2}) of steel area, are used to reinforce each exterior cell of the concrete block and clay unit masonry walls. These vertical reinforcement schemes provide a total cross-sectional area equal to 1136 mm^2 (1.76 in.^{2}). Because the lengths of the specimens vary with aspect ratio, these steel areas provide different vertical reinforcement ratios, depending on the aspect ratio of the wall. The vertical reinforcement ratios, based on gross area of horizontal sections, is given in Table 5.3. All vertical steel must comprise Grade 60 hot-rolled, deformed reinforcing bar.

Two straight pieces of #6 reinforcing bar, approximately 2210 mm (87 in.) long, are placed in each exterior cell of the specimens. The bars extend above and below the 1422-mm (56 in.) height of masonry, and the ends of the bars extend into pockets in the precast concrete header/footer beams. High-strength, non-shrink grout serves to anchor the bars in these pockets, as described in section 7.4. The ends of the vertical bars are threaded over a 51-mm (2 in.) length at either end. A pair of steel nuts and a steel plate serve to anchor the bar securely in the grout pocket.

7.3 Horizontal Reinforcement

The bond beam specimens have either 2-#3, 1-#4 and 1-#5, or 2-#6 hot-rolled, deformed reinforcing bars in a single bond beam to provide horizontal reinforcement ratios of 0.05%, 0.12% or 0.21%, respectively. One bar is placed above the other in the grout pocket, and one bar is placed on either side of the plane defined by the vertical bars (Fig. 7.3). The horizontal bars are continuous over the length of the panel. The ends are bent into 180° hooks, and the hooks are looped around the nearest vertical bar in the exterior cell at each end of the wall (Fig. 7.3).

The above detail was selected over 90°hooks because it has been shown to provide superior anchorage (Sveinsson et al., 1985). Furthermore, due to limitations on the number of specimens in the present program, anchorage detail could not be included as an experimental variable. However, this decision is not to be taken as an endorsement of 180°

hooks at the expense of the 90° counterpart, nor are the former being promoted as a necessary feature of partially-grouted masonry construction. Future research on partially-grouted masonry shear walls should address anchorage details for horizontal reinforcement.

The specimens with bed joint reinforcement have welded (ladder-type) wire reinforcing grids that meet ASTM A82 specifications (ASTM, 1985b) placed in the bed joints. The wire grids are to be made using cold-drawn carbon steel wire with a minimum specified elongation of 8%. In addition, the cross wires will be butt-welded to the longitudinal wires, so that the overall thickness will be one wire diameter, and the welding process is controlled to minimize embrittlement from rapid cooling of the welded intersections.

Two different wire grids are to be used. For the specimens with $\rho_{hl} = 0.05\%$, a grid with No. 9 Gage (3.76 mm or 0.148 in. diameter) longitudinal wires and cross wires is used, while a grid with No. 5 Gage (5.26 mm or 0.207 in. diameter) longitudinal wires and cross wires is used for the specimens with $\rho_{h2} = 0.12\%$. The latter utilizes slightly larger longitudinal wires than are typically allowed in 9.5 mm (3/8 in.) bed joints, so, it may be necessary to use a slightly thicker bed joint. Even though the diameter of No. 5 Gage wire exceeds that of 4.76-mm (3/16 in.) wire by only 1/2 mm (0.02"), the difference in cross-sectional area exceeds 20%. Whenever possible, bed joint reinforcement is to be placed such that cross wires engage at least one of the vertical bars in the grouted cells.

7.4 Precast Concrete Header/Footer Beams

In-plane shear and vertical compression stresses will be applied to the walls by means of stiff precast concrete header/footer beams (Fig. 7.2). It is customary for masonry shear walls specimens for use in-plane cyclic load tests to feature large concrete footers to anchor vertical reinforcement. Often, the header beams are either eliminated if the specimen is a cantilever wall. In the present study, the specimens are fixed against rotation top and bottom, so a header beam is required as well as the footer. These beams also serve the auxiliary purposes of anchoring the vertical reinforcement and providing easy connection to the TTF upper and lower crossheads.

Previous experimental studies at NIST on masonry shear walls did not utilize such header/footer beams. However, all but one of these studies involved unreinforced walls,

and the only study on reinforced masonry utilized walls that had only horizontal reinforcement (Scribner and Yancey, 1989). It is essential that vertical reinforcement in masonry shear wall specimens be anchored such that the ultimate strength of the vertical bars can be developed. Otherwise, uncharacteristically large amounts of slip of reinforcing bars in tension can take place, resulting in uplift of the heel of the wall and reduction in flexural strength. This situation is more acute for slender walls ($r_3 = 1.0$) which have no axial compression ($\sigma_{c0} = 0$).

The header/footer beams are shown in Fig. 7.4. By precasting these members, large savings in labor and materials are gained, as a pair of these beams would otherwise have to be built for each wall specimen. Only one pair of header/footer beams for each of the three aspect ratios are to be built, and these members will be reused for the entire testing program.

The precast concrete header/footer beams (Fig. 7.5) are prismatic members with rectangular cross-section. These members feature multiple vertical openings of small diameter that (1) enable lifting of the specimen using high-strength threaded rods, and (2) allow placement of the high-strength post-tensioning rods to attach the specimen to the TTF. In addition, the header/footer beams feature a pair of pockets in the shape of a truncated right pyramid, in which the vertical reinforcing bars of the wall panel are anchored. A pair of vertical bars are to be anchored in each pocket, and a steel plate, held in place by two steel nuts, serves as mechanical anchorage.

The truncated right pyramid configuration was employed to facilitate the removal of the grout plug following a test. By placing a plastic barrier (i.e. polyethylene sheet) to break bond between the grout and the concrete beam, the plug can be removed without having to apply much force. Vertical stirrup pairs are placed at 76-mm (3 in.) spacing to resist flexural shear in this region. In addition, horizontal ties are used to confine the pyramid, and, shearheads fabricated from structural steel tubes are used to resist punching shear stresses in the concrete above the pockets.

The header/footer beams are to be cast using a lightweight concrete, with a 28-day compression strength equal to 34.5 MPa (5000 psi) and a weight density of 1920 kg/m³ (120 lb/ft³). This is done to reduce the overall weight of the header/footer beams while still retaining sufficient strength to withstand the rigors of transportation and testing in the laboratory.

7.5 Fabrication Procedure

The masonry walls will be built by a licensed mason. Groups of approximately six masonry panels will be built at one time, and companion prisms (grouted and ungrouted), mortar cubes and grout cubes will be made simultaneously. The masonry will be laid on platforms to provide a smooth, level surface, and to allow placement of the vertical reinforcing bars. Once the vertical bars are properly located, units along the edges of the panels can be placed over these bars.

Wire grids for bed joint reinforcement will be placed in the bed joint specimens with each course of masonry. Exterior cells will be grouted in these specimens after all seven courses have been placed. For bond beam specimens, the first four courses (3 ungrouted courses plut bond beam) will be laid, after which time the exterior vertical cells and bond beam will be grouted. Subsequently, the top three courses of masonry will be laid, and the top portion of the exterior vertical cells will be grouted. For both bed join and bond beam specimens, external support at the top of the vertical rebars will be necessary when the panels are constructed.

After a period of at least one week, the panels will be positioned on shims in conjunction with a bed of mortar on top of the precast concrete footer. The portions of vertical reinforcing bars which protrude below the masonry panel will be inserted through the access tubes and into the pockets of the footer beam (Fig. 7.4). Anchor plates and steel nuts will be attached at the appropriate location at the bottom of the vertical bars. Shims and another bed of mortar will be placed on top of the masonry panel, and the header beam will be lowered into position. The top of the vertical bars will have been placed through the access tubes and into the pockets of the header beam, and steel nuts and plates will be attached to the bars. Anchorage of the vertical bars will be provided by filling the pockets in the header and footer beams with superplasticized high-strength, non-shrink grout. The grout will be pumped through an inlet, and an outlet will be used to determine by visual inspection when the pockets are filled.

Once the grout in the header/footer pockets has matured at least 7 days, the specimens, which will by now comprise the masonry panel and the header and footer beams, will be placed in the TTF. The specimens will be lifted using the overhead crane by means of high-strength threaded rods that are bolted to the footer beam. A bed of hydraulic lime mortar will be placed below the footer and above the header to provide sufficient

30

surface contact for uniform transfer of stresses between the TTF crossheads and the specimens.

7.6 Material Tests

Prism compression tests, according to ASTM specifications, will be conducted for both concrete block masonry (ASTM, 1980) and clay unit masonry (ASTM, 1990) using a height-to-thickness (h/t) ratio equal to 2. Sufficient tests will be conducted to characterize grouted and ungrouted prisms for both types of masonry. Unit compression tests for concrete block, as described in ASTM C140 (ASTM, 1980), and clay units, as described in ASTM C67 (ASTM, 1990), will also be conducted. Mortar cube tests and grout cube tests, as specified in ASTM C109 (ASTM, 1988a) and ASTM C1019 (ASTM, 1984), respectively, will supplement the tests described above. Tension coupon tests for vertical and horizontal reinforcing steel will also be included in the program.

8. TESTING PROCEDURE

8.1 Test Setup

The assembled specimens will be tested in the tri-directional test facility (TTF) using the setup shown in Fig. 8.1. The TTF is a multiaxial testing machine which is capable of applying force/displacement histories along 6 directions (three translational and three rotational). The TTF comprises a pair of crossheads (one fixed and one moving), six hydraulic actuators, a hydraulic power supply, and electronic controls for the power supply and actuators. The TTF is a closed-loop system which is controlled by dedicated computer, and data are acquired by another dedicated computer. A detailed description of the TTF is found elsewhere (Woodward and Rankin, 1984b).

The specimens will be placed in the TTF such that the plane of the masonry wall is directed along the east-west axis of the TTF. A 457-mm (18 in.) deep concrete beam is placed between the specimen and lower crosshead to span the clear height of the TTF. High-strength post-tensioning rods will be used to connect the header/footer of the specimen to the TTF. These rods will be post-tensioned only after the hydrocal mortar between the header/footer and the TTF crossheads has reached sufficient strength (see section 7.5).

8.2 Loading History

A displacement history will be imposed on the specimen along the east-west axis of the TTF (i.e. along the in-plane horizontal direction of the masonry wall panel), while a constant vertical force resultant is maintained. The lower crosshead of the TTF is fixed, thus all motion of the base of the specimens will be restricted. The top crosshead will be constrained by the TTF control system from rotating along three orthogonal axes and from translating along the north-south axis of the TTF (i.e. perpendicular to the plane of the masonry wall panel).

The east-west displacement history will conform to the Sequential Phased Displacement procedure developed as part of the TCCMAR program (Porter and Tremel, 1987). An idealized plot of this procedure is shown in Fig. 8.2, where it can be seen that cycles of reversing displacements of increasing amplitude are applied to the specimen until failure. The procedure uses as a benchmark the displacement the produces the first major

32

event (FME), which is defined in this program as the formation of the first inclined crack. Two distinct types of displacement cycles are featured in the program, including degradation cycles during which the cycle peak displacement amplitude decreases, and stabilization cycles in which cycle peak displacement amplitude is maintained constant. Failure of the specimens will be defined at the instant when a loss of strength is observed to exceed one-half of peak strength in either loading direction.

8.3 Instrumentation

The shear wall specimens will be instrumented with linear variable differential transformers (LVDT), linear strain transducers (LST), and electrical resistance strain gages (ERSG), respectively, to monitor wall displacements, reinforcing bar strains, and masonry strains. The LVDT, LST and ERSG instrumentation schemes, respectively, are given in Fig. 8.3, 8.4 and 8.5.

Total lateral displacement of the wall will be measured using three LVDT's attached to a steel frame that will be erected adjacent to the TTF (Fig. 8.3). Two other LVDT's will be used to determine the change in length of the principal diagonals, and 6 LVDT's will be used to measure the vertical shortening/elongation of the exterior cells. A pair of LVDT's will also be used to monitor liftoff/crushing of the wall toe/heel. The linear strain indicators (LST), which are strain amplifying devices utilizing strain gages mounted on leaf springs, will be placed at various locations to monitor local strains in the masonry (Fig. 8.4). Electrical resistance strain gages attached to the horizontal and vertical reinforcing bars will be used to monitor strain changes in the reinforcement (Fig. 8.5).

The instruments described above are in addition to the internal load cells and displacement transducers in the hydraulic actuators of the TTF. Note that the control software for the TTF generates global force and displacement signals that define the translation and rotation of the upper crosshead along three orthogonal axes. These signals will be digitized, recorded, and stored along with the strains and displacements measured on the masonry panels.

33

9. NUMERICAL MODELING

One of the underlying goals of the present research program is to identify and enhance analytical methods for the seismic response of partially-grouted masonry shear walls. These methods include predictive formulas amenable for design calculations, as well as sophisticated nonlinear analysis tools. The experimental program has been designed to generate test data with which to 1) calibrate empirical formulas for predicting the shear strength of partially-grouted masonry walls, and 2) verify finite element codes for nonlinear lateral load analysis.

9.1 Empirical Analyses

The empirical equations (6.2-6.4) developed by Fattal (1993a; 1993c) on the basis of previous work by Matsumura (1985; 1987; 1988) will be further validated using the test data produced by the experimental program described in this document. The influence of the experimental variables, including type and amount of horizontal reinforcement, aspect ratio, axial compression, and type of masonry, will be carefully evaluated. Appropriate modifications will be made to Eq. 6.2-6.4 so that they properly reflect the experimental observations.

The predictive capability of the empirical expression developed by Fattal has been shown to match, and, in some cases, exceed that of other available expressions for estimating the in-plane shear strength of masonry walls (Fattal and Todd, 1991). However, it is not likely for this expression to be adopted in structural design practice. Equations 6.2-6.4 include a large number of variables, and they have a format which is considerably more complex that of other available expressions. Furthermore, because Matsumura's original formulation was the direct outcome of statistical analysis of experimental data, Fattal's equations do not reflect a conceptual model of shear wall behavior which is rational. For these reasons, the test data generated by means of the present research program will also be used to verify and calibrate other predictive formulas for shear strength of masonry walls. Likely candidates include the current UBC shear strength formula (ICBO, 1991), as well as the formula in the proposed revision to the NEHRP provisions for masonry (*NEHRP*, 1994).

9.2 Finite Element Studies

Previous work at NIST (Yancey) has shown that an existing finite element code (FEM/I) by Ewing et al. (1987) can reproduce the response of fully-grouted, reinforced masonry shear walls to cyclic load histories with a modest degree of success. The applicability of this code to the analysis of partially-grouted walls will be pursued as part of the present study. However, an updated version of this finite element code, which was released subsequent to Yancey's study, will be used.

The ability of FEM to simulate the response of partially-grouted masonry walls is an issue of importance, as well as speculation. The precursor of FEM was developed for reinforced masonry shear walls with a uniform grid of orthogonal reinforcement at a close spacing. A layered model is used to represent this system, with the steel layer providing most of the strength and stiffness after the masonry has cracked. The partially-grouted masonry walls in this study do not have such a layer of steel, as the flexural reinforcing bars are concentrated in the exterior vertical cells. For the specimens with bond beams, horizontal steel is also concentrated, and, there is no horizontal reinforcement for some specimens. In the process of verifying the applicability of FEM to partially-grouted masonry shear walls, the sensitivity of this code to pertinent variables, such as aspect ratio and horizontal reinforcement ratio, study will be established.

10. SUMMARY

A research program on the seismic performance of partially-grouted masonry shear walls is described in this document. The program combines cyclic load tests of shear wall with numerical modeling in an attempt to define and quantify the shear strength, stiffness and deformation of partially grouted walls at cracking and ultimate. Vertical reinforcement for these shear walls are concentrated in exterior cells, and no other cells are grouted. In addition to studying the practice of partial grouting, the program seeks to verify the feasibility of bond beam replacement with bed joint reinforcement.

This program has its roots in a preliminary draft plan by Fattal (1993b), and it is further developed and refined in this document. The number of specimens, parametric combinations, and selected variables have been modified to increase the utility of the program, and to better utilize the NIST TTF facility. A total of 42 shear wall tests are specified in the research program, and analytical activities include nonlinear finite element analyses and calibration of existing empirical formulas for prediction of shear strength.

This report documents shear strength calculations of the partially-grouted shear wall specimens. Four different predictive formulas are used to calculate shear strength, and the variation in calculated strengths serves to justify the tests. In addition, two criteria for defining the minimum amount of horizontal reinforcement in masonry shear walls are investigated. These expressions illustrate the deficiencies of common types of wire grids for bed joint reinforcement, thus, a case is made for enhancing the toughness of these grids. Calculated minimum horizontal reinforcement ratios serve to support the values selected for this parameter in this study.

The experimental phase of this research program is subdivided into two main series, one for concrete block masonry and the other for clay unit masonry. Each of these series can be further subdivided into two modules, with the experimental activities for Module 1 comprising the twelve shear wall tests in Priority I of the concrete block series (Specimen Nos. 1-12). Module 2 includes the ten shear wall tests in Priorities II-V of the concrete block series (Specimen Nos. 13-22), and the last two modules encompass the clay masonry series, with eleven shear wall tests (specimen nos. 23-29 and 39-42) in Module 3 and nine shear wall tests (specimen nos. 30-38) in Module 4. Each module also includes finite element analysis and empirical formula calibration activities, and seismic design guidelines for partially-grouted masonry shear walls will be developed within each module.

Each Module can stand alone as a self-contained unit, and the numbers assigned to the Modules do not necessarily reflect the chronological order in which these tests will be conducted. In other words, Modules 1 and 3 may be conducted first, followed by Modules 2 and 4. A one-year duration is estimated for each of the four modules in the research program.

11. REFERENCES

ACI Committee 318, "Building Code Requirements for Reinforced Concrete Buildings," ACI Publication 318-89, American Concrete Institute, Detroit, MI, 1989.

American Society for Testing and Materials, "Standard Specification for Grout for Masonry," ASTM C476-83, ASTM, Philadelphia, PA, 1983.

American Society for Testing and Materials, "Standard Specification for Hollow Brick (Hollow Masonry Units Made from Clay or Shale)," ASTM C652-89a, ASTM, Philadelphia, PA, 1989a.

American Society for Testing and Materials, "Standard Specification for Hollow Load-Bearing Concrete Masonry Units," ASTM C90-85, ASTM, Philadelphia, PA, 1985a.

American Society for Testing and Materials, "Standard Specification for Mortar for Unit Masonry," ASTM C270-89, ASTM, Philadelphia, PA, 1989b.

American Society for Testing and Materials, "Standard Specification for Steel Wire, Plain, for Concrete Reinforcement," ASTM A82-85, ASTM, Philadelphia, PA, 1985b.

American Society for Testing and Materials, "Standard Method of Sampling and Testing Grout," ASTM C1019, ASTM, Philadelphia, PA, 1984.

American Society for Testing and Materials, "Standard Methods of Sampling and Testing Concrete Masonry Units," ASTM C140-75 (reapproved 1980), ASTM, Philadelphia, PA, 1980.

American Society for Testing and Materials, "Test Method for Compressive Strength of Hydraulic Cement Mortar," ASTM C109, ASTM, Philadelphia, PA, 1988a.

American Society for Testing and Materials, "Standard Test Method for Diagonal Tension in Masonry Assemblages," ASTM E519-81 (reapproved 1988), ASTM, Philadelphia, PA, 1988b.

American Society for Testing and Materials, "Standard Test Method of Sampling and Testing Brick and Structural Clay Tile," ASTM C67-89a, ASTM, Philadelphia, PA, 1990.

Bonacci, J. F., and Marquez, J., "Tests of Yielding Anchorages under Monotonic Loadings," *Journal of Structural Engineering*, ASCE, Vol. 120, No. 3, March 1994, pp. 965-986.

Drysdale, R. G., Hamid, A. A., and Baker, L. R., *Masonry Structures, Behavior and Design*, Prentice-Hall, Inc., Englewood Cliffs, NJ, 1994, 784 pp.

Englekirk, R. E., and Hart, G. C.,, and the Concrete Masonry Association of California and Nevada, *Earthquake Design of Concrete Masonry Buildings, Vol. 2, Strength Design of One-to-Four Story Buildings*, Prentice-Hall, Inc, Englewood Cliffs, NJ, 1984, 268 pp.

Ewing, R. D., El-Mustapha, A. M., and Kariotis, J. C., "FEM/I, A Finite Element Computer Program for the Nonlinear Static Analysis of Reinforced Masonry Building Components," U.S.-Japan Coordinated Program for Masonry Building Research, Report No. 2.2-1, Ewing/Kariotis/Englekirk & Hart, Rancho Palos Verdes, CA, 118 pp.

Fattal, S. G., "Strength of Partially-Grouted Masonry Shear Walls Under Lateral Loads," NISTIR 5147, National Institute of Standards and Technology, Gaithersburg, MD, June 1993a, 66 pp.

Fattal, S. G., "Research Plan for Masonry Shear Walls," NISTIR 5117, National Institute of Standards and Technology, Gaithersburg, MD, June 1993b, 33 pp.

Fattal, S. G., "The Effect of Critical Parameters on the Behavior of Partially-Grouted Masonry Shear Walls Under Lateral Loads," NISTIR 5116, National Institute of Standards and Technology, Gaithersburg, MD, June 1993c, 45 pp.

Fattal, S. G., and Todd, D. R., "Ultimate Strength of Masonry Shear Walls: Predictions vs Test Results," NISTIR 4633, National Institute of Standards and Technology, Gaithersburg, MD, October 1991, 46 pp.

Flinn, R. A., and Trojan, P. K., *Engineering Materials and their Applications*, 3rd Ed., Houghton Mifflin Co., Boston, MA, 1986, 742 pp.

Hidalgo, P. and Luders, C., "Resistencia al Esfuerzo de Corte de Muros de Albañilería Armada Sometidos a Solicitaciones Sismicas," XXIV Jornadas Sudamericanas de Ingenieria Estructural, Vol. 1, Porto Alegre, Brasil, 1987, pp. 1-15.

International Conference of Building Officials, *Uniform Building Code*, Whittier, CA, 1991.

Langhaar, H. L. *Energy Methods in Applied Mechanics*, J. Wiley and Sons, Inc., New York, NY, 1962, 350 pp.

Luders, C, and Hidalgo, P., "Influencia del Refuerzo Horizontal en el Comportamiento Sismico de Muros de Albanileria Armada," Cuartas Jornadas Chilenas de Sismologia e Ingenieria Antisismica, Vol. 2, Viña del Mar, Chile, pp. H-139 to H-158, 1986.

Masonry Standards Joint Committee, "Building Code Requirements for Masonry Structures," Publication No. ACI 530-92/ASCE 5-92/TMS 420-92, American Concrete Institute, Detroit, MI, American Society of Civil Engineers, New York, NY, and The Masonry Society, Boulder, CO, 1992.

Matsumura, A., "Effectiveness of Shear Reinforcement in Fully Grouted Hollow Clay Masonry Walls," Fourth Meeting of the Joint Technical Coordinating Committee on Masonry Research, U.S.-Japan Coordinated Earthquake Research Program, San Diego, CA, October, 1988.

Matsumura, A., "Shear Strength of Reinforced Hollow Unit Masonry Walls," *Proceedings,* Fourth North American Masonry Conference, Paper No. 50, Los Angeles, CA, 1987.

Matsumura, A., "Effect of Shear Reinforcement in Concrete Masonry Walls," First Meeting of the Joint Technical Coordinating Committee on Masonry Research, U.S.-Japan Coordinated Earthquake Research Program, Tokyo, Japan, August, 1985.

NEHRP Recommended Provisions for the Development of Seismic Regulations for New Buildings, Part 1, Provisions, Federal Emergency Management Agency, proposed revisions to 1994 Edition.

Orangun, C. O., Jirsa, J. O., and Breen, J. E., "A Reevaluation of Test Data on Development Length and Splices," *Journal of the American Concrete Institute*, Vol. 74, March 1977, pp. 114-122.

Porter, M. L. and Tremel, P. M., "Sequential Phased Displacement Procedure for TCCMAR Testing," Third Meeting of the Joint Technical Coordinating Committee on Masonry Research, U.S.-Japan Coordinated Earthquake Research Program, Sapporo, Japan, October 1987.

Sabnis, G. M., Harris, H. G., White, R. N., and Mirza, M. S., *Structural Modeling and Experimental Techniques*, Prentice-Hall, Inc., Englewood Cliffs, NJ, 1983, 585 pp.

Sanchez, T. A., Flores, L., Alcocer, S. M., and Meli, R., "Respuesta Sismica de Muros de Mamposteria Confinada con Diferentes Tipos de Refuerzo Horizontal," Report No. ES/02/92, CENAPRED, Mexico City, March 1992, 49 pp.

Schneider, R. R., and Dickey, W. L., *Reinforced Masonry Design*, Prentice-Hall, Inc., Englewood Cliffs, NJ, 1987, 682 pp.

Schultz, A. E. and Scolforo, M. J., "Engineering Design Provisions for Prestressed Masonry Part 1: Masonry Stresses," *The Masonry Society Journal*, Vol. 10, No. 2, February 1992, pp. 29-47.

Schultz, A. E., and Scolforo, M. J., "Engineering Design Provisions for Prestressed Masonry - Part 2: Steel Stresses and Other Considerations," *The Masonry Society Journal*, Vol. 10, No. 2, February 1992, pp. 48-64.

Schultz, A. E., and Scolforo, M. J., "An Overview of Prestressed Masonry," *The Masonry Society Journal*, Vol. 10, No. 1, August 1991, pp. 6-21.

Shing, P. B., and Noland, J. L., "Shear Behavior of Concrete Masonry Walls with Horizontal Joint Reinforcement," Dept. of Civil, Env. and Arch. Engrg., Univ. of Colorado, Boulder, Oct. 1992, 13 pp.

Shing, P. B., Schuller, M., and Hoskere, V. S., "In-Plane Resistance of Reinforced Masonry Shear Walls," *Journal of Structural Engineering*, ASCE, Vol. 116, No. 3, Mar. 1990, pp. 619-640.

Shing, P. B., Schuller, M., Hoskere, V. S., and Carter, E., "Flexural and Shear Response of Reinforced Masonry Walls," *ACI Structural Journal*, Vol. 87, No. 6, November-December, 1990, pp. 646-656.

Shing, P. B., Noland, J. L., and Klamerus, E., "Inelastic Behavior of Concrete Masonry Shear Walls," *Journal of Structural Engineering*, ASCE, Vol. 115, No. 9, Sept. 1989, pp. 2204-2225.

Sveinsson, B. I., McNiven, H. D., and Sucuoglu, H., "Cyclic Loading Tests of Masonry Single Piers, Volume 1 - Additional Tests with Height to Width Ratio of 1," Report No. UCB/EERC-85/15, Earthquake Engineering Research Center, University of California, Berkeley, December 1985, 163 pp.

Viwathanatepa, S., Popov, E. P., and Bertero, V. V., "Effects of Generalized Loadings on Bond of Reinforcing Bars Embedded in Confined Concrete Blocks," Report No. UCB/EERC-79/22, Earthquake Engineering Research Center, University of California, Berkeley, August 1979, 304 pp.

Woodward, K., and Rankin, F., "Influence of Block and Mortar Strength on Shear Resistance of Concrete Block Masonry Walls," NBSIR 85-3143, National Bureau of Standards, Gaithersburg, MD, April 1985a, 73 pp.

Woodward, K., and Rankin, F., "Influence of Aspect Ratio on Shear Resistance of Concrete Block Walls," NBSIR 84-2993, National Bureau of Standards, Gaithersburg, MD, January 1985b, 65 pp.

Woodward, K., and Rankin, F., "Influence of Vertical Compressive Stress on Shear Resistance of Concrete Block Masonry Walls," NBSIR 84-2929, National Bureau of Standards, Gaithersburg, MD, October 1984a, 61 pp.

Woodward, K., and Rankin, F., "The NBS Tri-Directional Test Facility," NBSIR 84-2879, National Bureau of Standards, Gaithersburg, MD, May 1984b, 44 pp.

Woodward, K., and Rankin, F., "Behavior of Concrete Block Masonry Walls Subjected to Repeated Cyclic Displacements," NBSIR 83-2780, National Bureau of Standards, Gaithersburg, MD, October 1983, 178 pp.

Yancey, C. W. C., Experimental Results Versus Finite Element Predictions for Masonry Shear Walls," NISTIR, National Institute of Standards and Technology, Gaithersburg, MD (in progress).

Yancey, C. W. C., Fattal, S. G. and Dikkers, R. D., "Review of Research Literature on Masonry Shear Walls," NISTIR 4512, National Institute of Standards and Technology, Gaithersburg, MD, February 1991, 99 pp.

Yancey, C. W. C., and Scribner, C. F., "Influence of Horizontal Reinforcement on Shear Resistance of Concrete Block Masonry Walls," NISTIR 89-4202, National Institute of Standards and Technology, Gaithersburg, MD, October 1989, 61 pp.

Table 2.1 Experimental Priorities in Existing Masonry Research Plan

Priority	Objective
I	Effectiveness of bed joint reinf. vs. hot-rolled, deformed bars in bond beams
II	Contribution of vertical reinforcement in the absence of horizontal steel
III	Effect of zero axial compression stress
IV	Influence of horizontal reinforcement
V	Influence of aspect ratio
VI	Characteristics of hollow clay unit masonry

Table 2.2 Schedule of Specimens in Existing Masonry Research Plan
a) Concrete Block Specimens

Priority	Parametric Combination	Aspect Ratio (H/L)	Type of Horizontal Reinforcement	Horizontal Reinforcement Ratio (%)	Compressive Stress (MPa)
I	1	$r_1 = 0.6$	bond beam	$\rho_{h1} = 0.05$	$\sigma_{c1} = 1.38$
	2	$r_1 = 0.6$	joint r/f	$\rho_{j1} = 0.05$	$\sigma_{c1} = 1.38$
	3	$r_2 = 1.0$	bond beam	$\rho_{h1} = 0.05$	$\sigma_{c1} = 1.38$
	4	$r_2 = 1.0$	joint r/f	$\rho_{j1} = 0.05$	$\sigma_{c1} = 1.38$
	5	$r_1 = 0.6$	bond beam	$\rho_{h2} = 0.12$	$\sigma_{c1} = 1.38$
	6	$r_1 = 0.6$	joint r/f	$\rho_{j2} = 0.12$	$\sigma_{c1} = 1.38$
	7	$r_2 = 1.0$	bond beam	$\rho_{h2} = 0.12$	$\sigma_{c1} = 1.38$
	8	$r_2 = 1.0$	joint r/f	$\rho_{j2} = 0.12$	$\sigma_{c1} = 1.38$
II	9	$r_1 = 0.6$	none	$\rho_{h0} = 0$	$\sigma_{c1} = 1.38$
	10	$r_2 = 1.0$	none	$\rho_{h0} = 0$	$\sigma_{c1} = 1.38$
III	11	$r_2 = 1.0$	none	$\rho_{h0} = 0$	$\sigma_{c0} = 0$
	12	$r_2 = 1.0$	bond beam	$\rho_{h2} = 0.12$	$\sigma_{c0} = 0$
	13	$r_2 = 1.0$	bond beam	$\rho_{h3} = 0.26$	$\sigma_{c0} = 0$
IV & V	14	$r_1 = 0.6$	bond beam	$\rho_{h3} = 0.26$	$\sigma_{c1} = 1.38$
	15	$r_2 = 1.0$	bond beam	$\rho_{h3} = 0.26$	$\sigma_{c1} = 1.38$

45

Table 2.2 Schedule of Specimens in Existing Masonry Research Plan
b) Clay Unit Specimens

Priority	Parametric Combination	Aspect Ratio (H/L)	Type of Horizontal Reinforcement	Horizontal Reinforcement Ratio (%)	Compressive Stress (MPa)
II & VI	16	$r_1 = 0.6$	none	$\rho_{h0} = 0$	$\sigma_{c1} = 1.38$
	17	$r_2 = 1.0$	none	$\rho_{h0} = 0$	$\sigma_{c1} = 1.38$
III & VI	18	$r_2 = 1.0$	none	$\rho_{h0} = 0$	$\sigma_{c0} = 0$
	19	$r_2 = 1.0$	bond beam	$\rho_{h2} = 0.12$	$\sigma_{c0} = 0$
	20	$r_2 = 1.0$	bond beam	$\rho_{h3} = 0.26$	$\sigma_{c0} = 0$
IV-VI	21	$r_1 = 0.6$	bond beam	$\rho_{h1} = 0.05$	$\sigma_{c1} = 1.38$
	22	$r_1 = 0.6$	bond beam	$\rho_{h2} = 0.12$	$\sigma_{c1} = 1.38$
	23	$r_1 = 0.6$	bond beam	$\rho_{h3} = 0.26$	$\sigma_{c1} = 1.38$
	24	$r_2 = 1.0$	bond beam	$\rho_{h1} = 0.05$	$\sigma_{c1} = 1.38$
	25	$r_2 = 1.0$	bond beam	$\rho_{h2} = 0.12$	$\sigma_{c1} = 1.38$
	26	$r_2 = 1.0$	bond beam	$\rho_{h3} = 0.26$	$\sigma_{c1} = 1.38$

Table 5.1 Experimental Priorities in Revised Masonry Research Plan

Priority	Objective
I	Effectiveness of bed joint reinf. vs. hot-rolled, deformed bars in bond beams
II	Contribution of vertical reinforcement in the absence of horizontal steel
III	Effect of zero axial compression stress
IV	Influence of horizontal reinforcement
V	Influence of aspect ratio
VI	Characteristics of hollow clay unit masonry
VII	Influence of axial compression stress

Table 5.2 Schedule of Specimens in Revised Masonry Research Plan
a) Concrete Block Specimens

Priority	Specimen		Aspect Ratio	Horizontal Reinforcement		Compressive Stress
	No.	Designation	(H/L)	Type	Ratio (%)	(MPa)
I	1	CO-R05-B05-Q10	$r_1 = 0.5$	bond beam	$\rho_{h1} = 0.05$	$\sigma_{c1} = 1.38$
	2	CO-R05-J05-Q10	$r_1 = 0.5$	joint r/f	$\rho_{h1} = 0.05$	$\sigma_{c1} = 1.38$
	3	CO-R07-B05-Q10	$r_2 = 0.7$	bond beam	$\rho_{h1} = 0.05$	$\sigma_{c1} = 1.38$
	4	CO-R07-J05-Q10	$r_2 = 0.7$	joint r/f	$\rho_{h1} = 0.05$	$\sigma_{c1} = 1.38$
	5	CO-R10-B05-Q10	$r_3 = 1.0$	bond beam	$\rho_{h1} = 0.05$	$\sigma_{c1} = 1.38$
	6	CO-R10-J05-Q10	$r_3 = 1.0$	joint r/f	$\rho_{h1} = 0.05$	$\sigma_{c1} = 1.38$
	7	CO-R05-B12-Q10	$r_1 = 0.5$	bond beam	$\rho_{h2} = 0.12$	$\sigma_{c1} = 1.38$
	8	CO-R05-J12-Q10	$r_1 = 0.5$	joint r/f	$\rho_{h2} = 0.12$	$\sigma_{c1} = 1.38$
	9	CO-R07-B12-Q10	$r_2 = 0.7$	bond beam	$\rho_{h2} = 0.12$	$\sigma_{c1} = 1.38$
	10	CO-R07-J12-Q10	$r_2 = 0.7$	joint r/f	$\rho_{h2} = 0.12$	$\sigma_{c1} = 1.38$
	11	CO-R10-B12-Q10	$r_3 = 1.0$	bond beam	$\rho_{h2} = 0.12$	$\sigma_{c1} = 1.38$
	12	CO-R10-J12-Q10	$r_3 = 1.0$	joint r/f	$\rho_{h2} = 0.12$	$\sigma_{c1} = 1.38$
II	13	CO-R05-B00-Q10	$r_1 = 0.5$	none	$\rho_{h0} = 0$	$\sigma_{c1} = 1.38$
	14	CO-R07-B00-Q10	$r_2 = 0.7$	none	$\rho_{h0} = 0$	$\sigma_{c1} = 1.38$
	15	CO-R10-B00-Q10	$r_3 = 1.0$	none	$\rho_{h0} = 0$	$\sigma_{c1} = 1.38$
III	16	CO-R10-B00-Q00	$r_3 = 1.0$	none	$\rho_{h0} = 0$	$\sigma_{c0} = 0$
	17	CO-R10-B05-Q00	$r_3 = 1.0$	bond beam	$\rho_{h1} = 0.05$	$\sigma_{c0} = 0$
	18	CO-R10-B12-Q00	$r_3 = 1.0$	bond beam	$\rho_{h2} = 0.12$	$\sigma_{c0} = 0$
	19	CO-R10-B21-Q00	$r_3 = 1.0$	bond beam	$\rho_{h3} = 0.21$	$\sigma_{c0} = 0$
IV & V	20	CO-R05-B21-Q10	$r_1 = 0.5$	bond beam	$\rho_{h3} = 0.21$	$\sigma_{c1} = 1.38$
	21	CO-R07-B21-Q10	$r_2 = 0.7$	bond beam	$\rho_{h3} = 0.21$	$\sigma_{c1} = 1.38$
	22	CO-R10-B21-Q10	$r_2 = 1.0$	bond beam	$\rho_{h3} = 0.21$	$\sigma_{c1} = 1.38$

48

Table 5.2 Schedule of Specimens in Revised Masonry Research Plan
b) Clay Unit Specimens

Priority	Specimen		Aspect Ratio	Horizontal Reinforcement		Compres-sive Stress
	No.	Designation	(H/L)	Type	Ratio (%)	(MPa)
II & VI	23	CL-R05-B00-Q05	$r_1 = 0.5$	none	$\rho_{h0} = 0$	$\sigma_{c1} = 1.38$
	24	CL-R07-B00-Q05	$r_2 = 0.7$	none	$\rho_{h0} = 0$	$\sigma_{c1} = 1.38$
	25	CL-R10-B00-Q05	$r_3 = 1.0$	none	$\rho_{h0} = 0$	$\sigma_{c1} = 1.38$
III & VI	26	CL-R10-B00-Q00	$r_3 = 1.0$	none	$\rho_{h0} = 0$	$\sigma_{c0} = 0$
	27	CL-R10-B05-Q00	$r_3 = 1.0$	bond beam	$\rho_{h1} = 0.05$	$\sigma_{c0} = 0$
	28	CL-R10-B12-Q00	$r_3 = 1.0$	bond beam	$\rho_{h2} = 0.12$	$\sigma_{c0} = 0$
	29	CL-R10-B21-Q00	$r_3 = 1.0$	bond beam	$\rho_{h3} = 0.21$	$\sigma_{c0} = 0$
IV - VI	30	CL-R05-B05-Q05	$r_1 = 0.5$	bond beam	$\rho_{h1} = 0.05$	$\sigma_{c1} = 1.38$
	31	CL-R05-B12-Q05	$r_1 = 0.5$	bond beam	$\rho_{h2} = 0.12$	$\sigma_{c1} = 1.38$
	32	CL-R05-B21-Q05	$r_1 = 0.5$	bond beam	$\rho_{h3} = 0.21$	$\sigma_{c1} = 1.38$
	33	CL-R07-B05-Q05	$r_2 = 0.7$	bond beam	$\rho_{h1} = 0.05$	$\sigma_{c1} = 1.38$
	34	CL-R07-B12-Q05	$r_2 = 0.7$	bond beam	$\rho_{h2} = 0.12$	$\sigma_{c1} = 1.38$
	35	CL-R07-B21-Q05	$r_2 = 0.7$	bond beam	$\rho_{h3} = 0.21$	$\sigma_{c1} = 1.38$
	36	CL-R10-B05-Q05	$r_2 = 1.0$	bond beam	$\rho_{h1} = 0.05$	$\sigma_{c1} = 1.38$
	37	CL-R10-B12-Q05	$r_2 = 1.0$	bond beam	$\rho_{h2} = 0.12$	$\sigma_{c1} = 1.38$
	38	CL-R10-B21-Q05	$r_2 = 1.0$	bond beam	$\rho_{h3} = 0.21$	$\sigma_{c1} = 1.38$
VI & VII	39	CL-R10-B00-Q10	$r_2 = 1.0$	none	$\rho_{h0} = 0$	$\sigma_{c2} = 2.76$
	40	CL-R10-B05-Q10	$r_2 = 1.0$	bond beam	$\rho_{h1} = 0.05$	$\sigma_{c2} = 2.76$
	41	CL-R10-B12-Q10	$r_2 = 1.0$	bond beam	$\rho_{h2} = 0.12$	$\sigma_{c2} = 2.76$
	42	CL-R10-B21-Q10	$r_2 = 1.0$	bond beam	$\rho_{h3} = 0.21$	$\sigma_{c2} = 2.76$

Table 5.3 Estimated Minimum Horizontal Reinforcement Ratios
a) Concrete Block Specimens

Specimen		f_m (MPa)	f_{yh} (MPa)	σ_c (MPa)	L (mm)	minimum ρ_h (%)	
No.	Designation					Strength	Energy
1	CO-R05-B05-Q10	13.8	414	1.38	2845	0.057	0.030
2	CO-R05-J05-Q10	13.8	552	1.38	2845	0.043	0.074
3	CO-R07-B05-Q10	13.8	414	1.38	2032	0.057	0.024
4	CO-R07-J05-Q10	13.8	552	1.38	2032	0.043	0.059
5	CO-R10-B05-Q10	13.8	414	1.38	1422	0.057	0.019
6	CO-R10-J05-Q10	13.8	552	1.38	1422	0.043	0.047
7	CO-R05-B12-Q10	13.8	414	1.38	2845	0.057	0.030
8	CO-R05-J12-Q10	13.8	552	1.38	2845	0.043	0.074
9	CO-R07-B12-Q10	13.8	414	1.38	2032	0.057	0.024
10	CO-R07-J12-Q10	13.8	552	1.38	2032	0.043	0.059
11	CO-R10-B12-Q10	13.8	414	1.38	1422	0.057	0.019
12	CO-R10-J12-Q10	13.8	552	1.38	1422	0.043	0.047
13	CO-R05-B00-Q10	13.8	414	1.38	2845	0.057	0.030
14	CO-R07-B00-Q10	13.8	414	1.38	2032	0.057	0.024
15	CO-R10-B00-Q10	13.8	414	1.38	1422	0.057	0.019
16	CO-R10-B00-Q00	13.8	414	0	1422	0.027	0.009
17	CO-R10-B05-Q00	13.8	414	0	1422	0.027	0.009
18	CO-R10-B12-Q00	13.8	414	0	1422	0.027	0.009
19	CO-R10-B21-Q00	13.8	414	0	1422	0.027	0.009
20	CO-R05-B21-Q10	13.8	414	1.38	2845	0.057	0.030
21	CO-R07-B21-Q10	13.8	414	1.38	2032	0.057	0.024
22	CO-R10-B21-Q10	13.8	414	1.38	1422	0.057	0.019

Table 5.3 Estimated Minimum Horizontal Reinforcement Ratios
b) Clay Unit Specimens

Specimen		f_m (MPa)	f_{yh} (MPa)	σ_c (MPa)	L (mm)	minimum ρ_h (%)	
No.	Designation					Strength	Energy
23	CL-R05-B00-Q05	27.6	414	1.38	2845	0.080	0.030
24	CL-R07-B00-Q05	27.6	414	1.38	2032	0.080	0.024
25	CL-R10-B00-Q05	27.6	414	1.38	1422	0.080	0.019
26	CL-R10-B00-Q00	27.6	414	0	1422	0.039	0.009
27	CL-R10-B05-Q00	27.6	414	0	1422	0.039	0.009
28	CL-R10-B12-Q00	27.6	414	0	1422	0.039	0.009
29	CL-R10-B21-Q00	27.6	414	0	1422	0.039	0.009
30	CL-R05-B05-Q05	27.6	414	1.38	2845	0.080	0.030
31	CL-R05-B12-Q05	27.6	414	1.38	2845	0.080	0.030
32	CL-R05-B21-Q05	27.6	414	1.38	2845	0.080	0.030
33	CL-R07-B05-Q05	27.6	414	1.38	2032	0.080	0.024
34	CL-R07-B12-Q05	27.6	414	1.38	2032	0.080	0.024
35	CL-R07-B21-Q05	27.6	414	1.38	2032	0.080	0.024
36	CL-R10-B05-Q05	27.6	414	1.38	1422	0.080	0.019
37	CL-R10-B12-Q05	27.6	414	1.38	1422	0.080	0.019
38	CL-R10-B21-Q05	27.6	414	1.38	1422	0.122	0.019
39	CL-R10-B00-Q10	27.6	414	2.76	1422	0.122	0.031
40	CL-R10-B05-Q10	27.6	414	2.76	1422	0.122	0.031
41	CL-R10-B12-Q10	27.6	414	2.76	1422	0.122	0.031
42	CL-R10-B21-Q10	27.6	414	2.76	1422	0.122	0.031

Table 6.1 Factors for Partially-Grouted Masonry

Factor	Fully-Grouted Walls (Clay or Concrete Masonry)	Partially-Grouted Clay Masonry Walls	Partially-Grouted Concrete Masonry Walls
k_0	1.00	0.80	0.80
k_u	1.00	0.80	0.64
γ	1.00	1.00	0.60

Table 6.2 Alternate Vertical Reinforcement Schemes

Scheme	Aspect Ratio, r	Vertical Reinforcement		
		ρ_v (%)	Bar Combination	Area (mm^2)
1	0.5	0.28	4-#7	1548
	0.7	0.29	4-#6	1135
	1.0	0.29	4-#5	800
2	0.5	0.42	2-#8 & 2-#9	2310
	0.7	0.40	2-#6 & 2-#8	1587
	1.0	0.41	4-#6	1135
3	0.5	0.21	4-#6	1135
	0.7	0.29	4-#6	1135
	1.0	0.41	4-#6	1135

53

Table 6.3 Estimated Shear Strengths for Vertical Reinforcing Scheme 1
a) Concrete Block Specimens

Specimen		Shear Strength, V_n (kN)				Margin of Safety (V_f / V_n)			
No.	Designation	Fattal	Shing	UBC	NEH RP	Fattal	Shing	UBC	NEH RP
1	CO-R05-B05-Q10	302	316	250	319	5.28	5.04	6.36	5.00
2	CO-R05-J05-Q10	305	293	260	323	5.23	5.44	6.12	4.92
3	CO-R07-B05-Q10	210	206	172	220	4.01	4.08	4.88	3.82
4	CO-R07-J05-Q10	212	205	179	223	3.97	4.10	4.69	3.76
5	CO-R10-B05-Q10	141	122	113	146	2.88	3.32	3.61	2.79
6	CO-R10-J05-Q10	143	138	118	148	2.85	2.94	3.46	2.75
7	CO-R05-B12-Q10	336	491	405	396	4.74	3.25	3.93	4.02
8	CO-R05-J12-Q10	333	402	387	387	4.78	3.96	4.11	4.11
9	CO-R07-B12-Q10	234	303	283	275	3.59	2.77	2.97	3.05
10	CO-R07-J12-Q10	232	278	270	269	3.62	3.03	3.11	3.13
11	CO-R10-B12-Q10	158	161	190	184	2.57	2.52	2.14	2.20
12	CO-R10-J12-Q10	157	184	181	180	2.59	2.21	2.24	2.26
13	CO-R05-B00-Q10	187	183	133	260	8.53	8.68	11.98	6.13
14	CO-R07-B00-Q10	127	132	88	178	6.60	6.37	9.53	4.72
15	CO-R10-B00-Q10	84	93	54	116	4.86	4.39	7.53	3.49
16	CO-R10-B00-Q00	59	82	54	85	5.10	3.64	5.55	3.52
17	CO-R10-B05-Q00	116	112	113	115	2.57	2.67	2.66	2.61
18	CO-R10-B12-Q00	134	151	190	153	2.24	1.98	1.57	1.95
19	CO-R10-B21-Q00	151	220	326	221	1.98	1.36	0.92	1.35
20	CO-R05-B21-Q10	372	798	678	532	4.28	2.00	2.35	2.99
21	CO-R07-B21-Q10	260	474	477	373	3.24	1.77	1.76	2.26
22	CO-R10-B21-Q10	176	230	326	253	2.31	1.77	1.25	1.61

Table 6.3 Estimated Shear Strengths for Vertical Reinforcing Scheme 1
b) Clay Unit Specimens

Specimen		Shear Strength, V_n (kN)				Margin of Safety (V_f / V_n)			
No.	Designation	Fattal	Shing	UBC	NEH RP	Fattal	Shing	UBC	NEH RP
23	CL-R05-B00-Q05	257	259	188	342	6.55	6.50	8.97	4.93
24	CL-R07-B00-Q05	175	187	125	233	4.94	4.64	6.95	3.71
25	CL-R10-B00-Q05	115	131	76	152	3.65	3.21	5.49	2.77
26	CL-R10-B00-Q00	90	117	76	120	3.37	2.61	3.98	2.52
27	CL-R10-B05-Q00	148	146	135	150	2.06	2.08	2.25	2.03
28	CL-R10-B12-Q00	165	185	213	189	1.84	1.64	1.43	1.61
29	CL-R10-B21-Q00	183	254	349	257	1.66	1.19	0.87	1.18
30	CL-R05-B05-Q05	373	392	305	400	4.52	4.30	5.52	4.21
31	CL-R05-B12-Q05	407	567	460	478	4.14	2.97	3.66	3.53
32	CL-R05-B21-Q05	443	874	733	614	3.81	1.93	2.30	2.74
33	CL-R07-B05-Q05	258	261	209	275	3.36	3.33	4.15	3.15
34	CL-R07-B12-Q05	282	358	319	331	3.07	2.42	2.71	2.62
35	CL-R07-B21-Q05	308	529	514	428	2.82	1.64	1.69	2.03
36	CL-R10-B05-Q05	173	161	135	181	2.43	2.61	3.11	2.32
37	CL-R10-B12-Q05	190	200	213	220	2.21	2.10	1.97	1.91
38	CL-R10-B21-Q05	208	269	349	288	2.02	1.56	1.20	1.46
39	CL-R10-B00-Q10	140	145	76	183	3.79	3.65	6.95	2.90
40	CL-R10-B05-Q10	198	175	135	212	2.69	3.03	3.93	2.50
41	CL-R10-B12-Q10	215	214	213	251	2.47	2.48	2.50	2.12
42	CL-R10-B21-Q10	233	283	349	319	2.28	1.87	1.52	1.66

Table 6.4 Estimated Shear Strengths for Vertical Reinforcing Scheme 2
a) Concrete Block Specimens

Specimen		Shear Strength, V_n (kN)				Margin of Safety (V_f / V_n)			
No.	Designation	Fattal	Shing	UBC	NEH RP	Fattal	Shing	UBC	NEH RP
1	CO-R05-B05-Q10	338	341	250	319	6.07	6.01	8.20	6.44
2	CO-R05-J05-Q10	341	318	260	323	6.02	6.46	7.90	6.35
3	CO-R07-B05-Q10	229	221	172	220	4.66	4.83	6.20	4.85
4	CO-R07-J05-Q10	231	220	179	223	4.61	4.85	5.96	4.78
5	CO-R10-B05-Q10	154	134	113	146	3.38	3.91	4.63	3.58
6	CO-R10-J05-Q10	156	149	118	148	3.35	3.49	4.44	3.52
7	CO-R05-B12-Q10	373	516	405	396	5.51	3.98	5.07	5.18
8	CO-R05-J12-Q10	369	427	387	387	5.56	4.81	5.30	5.30
9	CO-R07-B12-Q10	254	318	283	275	4.21	3.36	3.78	3.88
10	CO-R07-J12-Q10	252	293	270	269	4.24	3.65	3.96	3.97
11	CO-R10-B12-Q10	171	173	190	184	3.04	3.02	2.74	2.83
12	CO-R10-J12-Q10	170	195	181	180	3.07	2.68	2.88	2.90
13	CO-R05-B00-Q10	223	209	133	260	9.20	9.83	15.5	7.90
14	CO-R07-B00-Q10	147	147	88	178	7.26	7.26	12.1	6.00
15	CO-R10-B00-Q10	97	104	54	116	5.40	5.03	9.66	4.49
16	CO-R10-B00-Q00	72	94	54	85	5.85	4.49	7.78	4.93
17	CO-R10-B05-Q00	129	123	113	115	3.25	3.41	3.73	3.67
18	CO-R10-B12-Q00	147	163	190	153	2.87	2.59	2.21	2.74
19	CO-R10-B21-Q00	164	231	326	221	2.55	1.82	1.29	1.90
20	CO-R05-B21-Q10	408	823	678	532	5.03	2.49	3.03	3.86
21	CO-R07-B21-Q10	279	489	477	373	3.82	2.18	2.24	2.87
22	CO-R10-B21-Q10	189	242	326	253	2.76	2.16	1.60	2.07

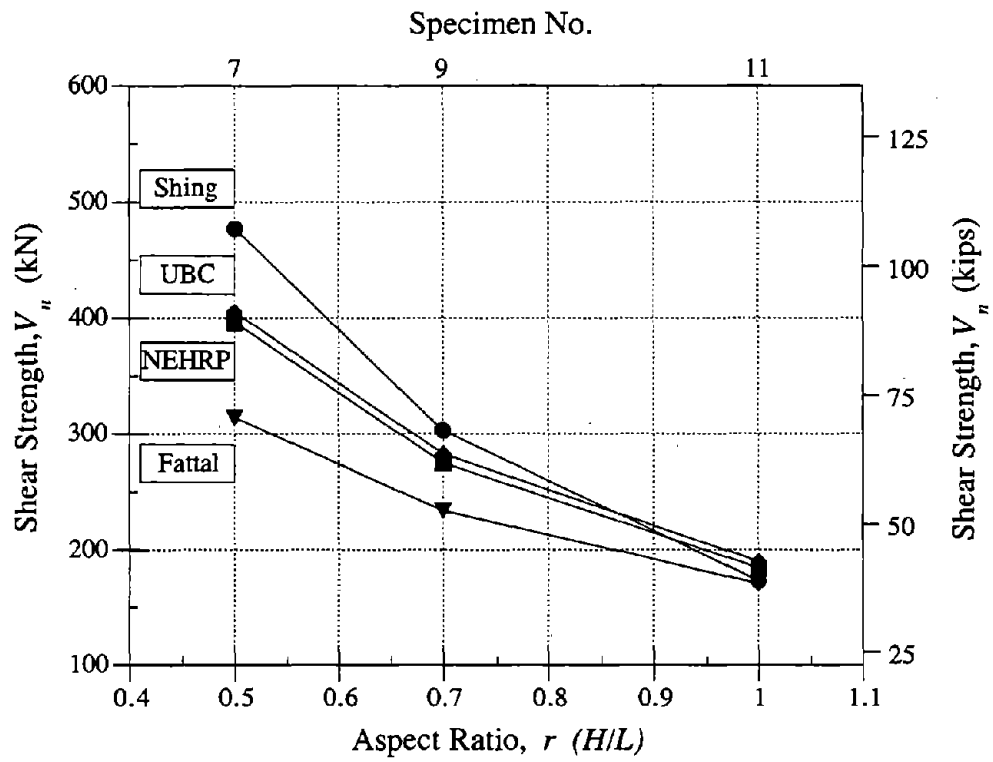Table 6.4 Estimated Shear Strengths for Vertical Reinforcing Scheme 2
b) Clay Unit Specimens

Specimen		Shear Strength, V_n (kN)				Margin of Safety (V_f / V_n)			
No.	Designation	Fattal	Shing	UBC	NEH RP	Fattal	Shing	UBC	NEH RP
23	CL-R05-B00-Q05	309	295	188	342	7.32	7.66	12.04	6.62
24	CL-R07-B00-Q05	203	208	125	233	5.45	5.32	8.88	4.75
25	CL-R10-B00-Q05	133	147	76	152	4.06	3.69	7.09	3.57
26	CL-R10-B00-Q00	109	132	76	120	3.95	3.24	5.61	3.56
27	CL-R10-B05-Q00	166	162	135	150	2.58	2.65	3.17	2.86
28	CL-R10-B12-Q00	183	201	213	189	2.34	2.13	2.02	2.27
29	CL-R10-B21-Q00	201	270	349	257	2.13	1.59	1.23	1.67
30	CL-R05-B05-Q05	424	428	305	400	5.33	5.29	7.41	5.65
31	CL-R05-B12-Q05	458	603	460	478	4.94	3.75	4.91	4.73
32	CL-R05-B21-Q05	494	910	733	614	4.58	2.49	3.09	3.68
33	CL-R07-B05-Q05	286	282	209	275	3.88	3.93	5.31	4.02
34	CL-R07-B12-Q05	310	379	319	331	3.57	2.92	3.47	3.35
35	CL-R07-B21-Q05	336	550	514	428	3.30	2.01	2.15	2.59
36	CL-R10-B05-Q05	191	176	135	181	2.84	3.07	4.01	2.99
37	CL-R10-B12-Q05	208	216	213	220	2.60	2.51	2.55	2.47
38	CL-R10-B21-Q05	226	285	349	288	2.40	1.90	1.55	1.88
39	CL-R10-B00-Q10	158	161	76	183	4.11	4.03	8.51	3.56
40	CL-R10-B05-Q10	216	191	135	212	3.01	3.41	4.81	3.06
41	CL-R10-B12-Q10	233	230	213	251	2.79	2.83	3.06	2.59
42	CL-R10-B21-Q10	251	299	349	319	2.59	2.17	1.86	2.04

Table 6.5 Estimated Shear Strengths for Vertical Reinforcing Scheme 3
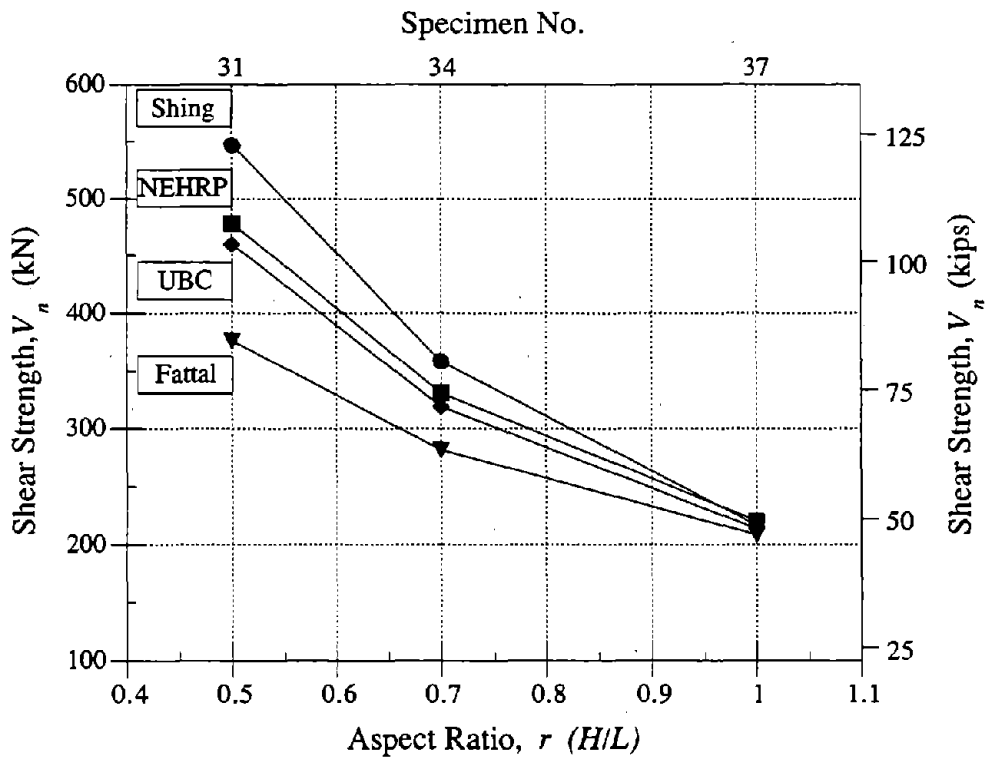a) Concrete Block Specimens

Specimen		Shear Strength, V_n (kN)				Margin of Safety (V_f / V_n)			
No.	Designation	Fattal	Shing	UBC	NEH RP	Fattal	Shing	UBC	NEH RP
1	CO-R05-B05-Q10	280	302	250	319	4.73	4.38	5.28	4.15
2	CO-R05-J05-Q10	283	279	260	323	4.68	4.74	5.09	4.09
3	CO-R07-B05-Q10	210	206	172	220	4.01	4.08	4.88	3.82
4	CO-R07-J05-Q10	212	205	179	223	3.97	4.10	4.69	3.76
5	CO-R10-B05-Q10	154	134	113	146	3.38	3.91	4.63	3.58
6	CO-R10-J05-Q10	156	149	118	148	3.35	3.49	4.44	3.52
7	CO-R05-B12-Q10	314	477	405	396	4.21	2.77	3.26	3.34
8	CO-R05-J12-Q10	311	388	387	387	4.25	3.41	3.42	3.42
9	CO-R07-B12-Q10	234	303	283	275	3.59	2.77	2.97	3.05
10	CO-R07-J12-Q10	232	278	270	269	3.62	3.03	3.11	3.13
11	CO-R10-B12-Q10	171	173	190	184	3.04	3.02	2.74	2.83
12	CO-R10-J12-Q10	170	195	181	180	3.07	2.68	2.88	2.90
13	CO-R05-B00-Q10	165	170	133	260	8.04	7.80	9.96	5.09
14	CO-R07-B00-Q10	127	132	88	178	6.60	6.37	9.53	4.72
15	CO-R10-B00-Q10	97	104	54	116	5.40	5.03	9.66	4.49
16	CO-R10-B00-Q00	72	94	54	85	5.85	4.49	7.78	4.93
17	CO-R10-B05-Q00	129	123	113	115	3.25	3.41	3.73	3.67
18	CO-R10-B12-Q00	147	163	190	153	2.87	2.59	2.21	2.74
19	CO-R10-B21-Q00	164	231	326	221	2.55	1.82	1.29	1.90
20	CO-R05-B21-Q10	350	784	678	532	3.78	1.69	1.95	2.49
21	CO-R07-B21-Q10	260	474	477	373	3.24	1.77	1.76	2.26
22	CO-R10-B21-Q10	189	242	326	253	2.76	2.16	1.60	2.07

Table 6.5 Estimated Shear Strengths for Vertical Reinforcing Scheme 3
b) Clay Unit Specimens

| Specimen		Shear Strength, V_n (kN)				Margin of Safety (V_f / V_n)			
No.	Designation	Fattal	Shing	UBC	NEH RP	Fattal	Shing	UBC	NEH RP
23	CL-R05-B00-Q05	226	240	188	342	6.06	5.71	7.29	4.01
24	CL-R07-B00-Q05	175	187	125	233	4.94	4.64	6.95	3.71
25	CL-R10-B00-Q05	133	147	76	152	4.06	3.69	7.09	3.57
26	CL-R10-B00-Q00	109	132	76	120	3.95	3.24	5.61	3.56
27	CL-R10-B05-Q00	166	162	135	150	2.58	2.65	3.17	2.86
28	CL-R10-B12-Q00	183	201	213	189	2.34	2.13	2.02	2.27
29	CL-R10-B21-Q00	201	270	349	257	2.13	1.59	1.23	1.67
30	CL-R05-B05-Q05	341	373	305	400	4.01	3.68	4.48	3.42
31	CL-R05-B12-Q05	376	547	460	478	3.65	2.50	2.98	2.87
32	CL-R05-B21-Q05	412	855	733	614	3.33	1.60	1.87	2.23
33	CL-R07-B05-Q05	258	261	209	275	3.36	3.33	4.15	3.15
34	CL-R07-B12-Q05	282	358	319	331	3.07	2.42	2.71	2.62
35	CL-R07-B21-Q05	308	529	514	428	2.82	1.64	1.69	2.03
36	CL-R10-B05-Q05	191	176	135	181	2.84	3.07	4.01	2.99
37	CL-R10-B12-Q05	208	216	213	220	2.60	2.51	2.55	2.47
38	CL-R10-B21-Q05	226	285	349	288	2.40	1.90	1.55	1.88
39	CL-R10-B00-Q10	158	161	76	183	4.11	4.03	8.51	3.56
40	CL-R10-B05-Q10	216	191	135	212	3.01	3.41	4.81	3.06
41	CL-R10-B12-Q10	233	230	213	251	2.79	2.83	3.06	2.59
42	CL-R10-B21-Q10	251	299	349	319	2.59	2.17	1.86	2.04

a) Concrete Block Specimens

b) Clay Unit Specimens

Fig. 6.1 Influence of Aspect Ratio on Shear Strength

60

Specimen No.
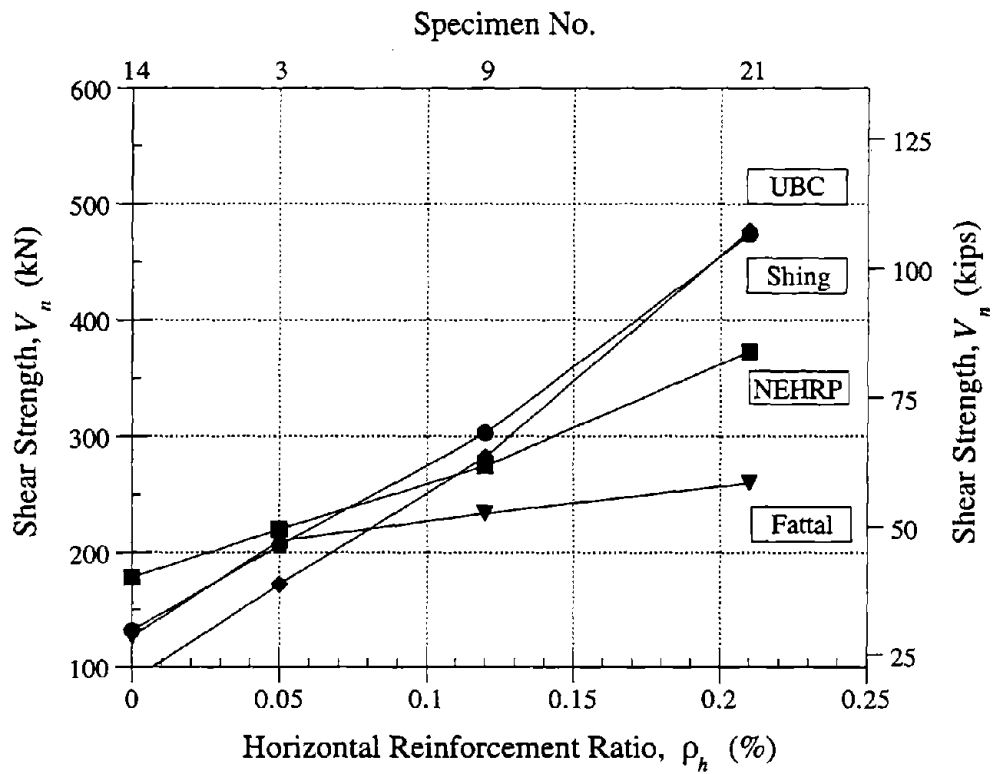
a) Concrete Block Specimens
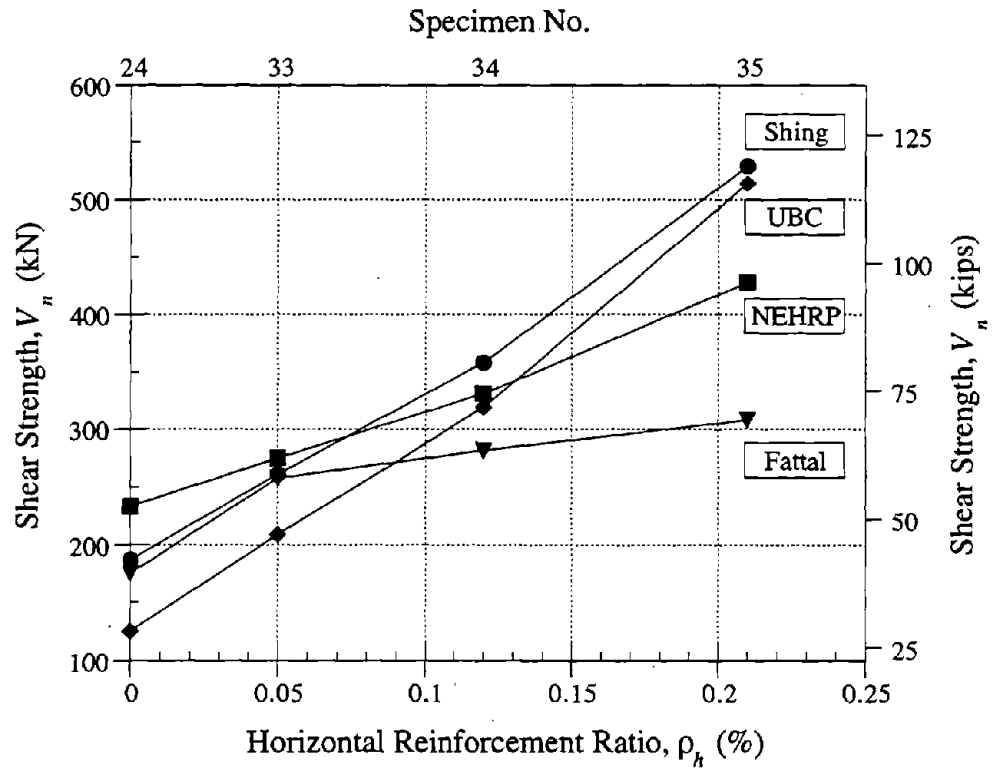
Specimen No.

b) Clay Unit Specimens

Fig. 6.2 Influence of Horizontal Reinforcement on Shear Strength

61

a) Concrete Block Specimens

b) Clay Unit Specimens

Fig. 6.3 Influence of Axial Compression on Shear Strength

a) $r = 0.5$

$7 @ 203^* = 1422$
$(7 @ 8 = 56)$

$7 @ 406^* = 2845$
$(7 @ 16 = 112)$

b) $r = 0.7$

$7 @ 203^* = 1422$
$(7 @ 8 = 56)$

$5 @ 406^* = 2032$
$(5 @ 16 = 80)$

c) $r = 1.0$

$7 @ 203^* = 1422$
$(7 @ 8 = 56)$

$3.5 @ 406^* = 1422$
$(3.5 @ 16 = 56)$

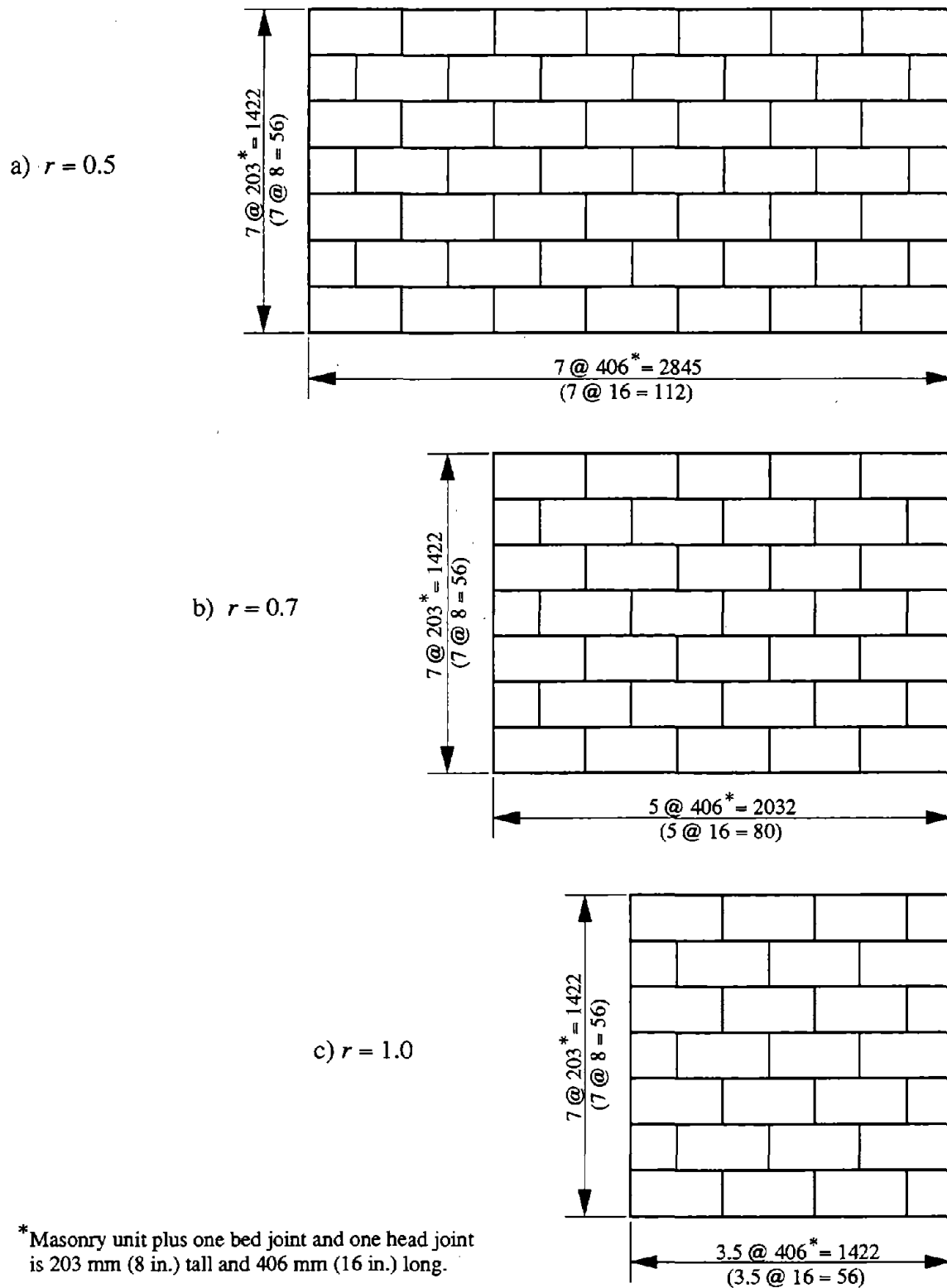*Masonry unit plus one bed joint and one head joint is 203 mm (8 in.) tall and 406 mm (16 in.) long.
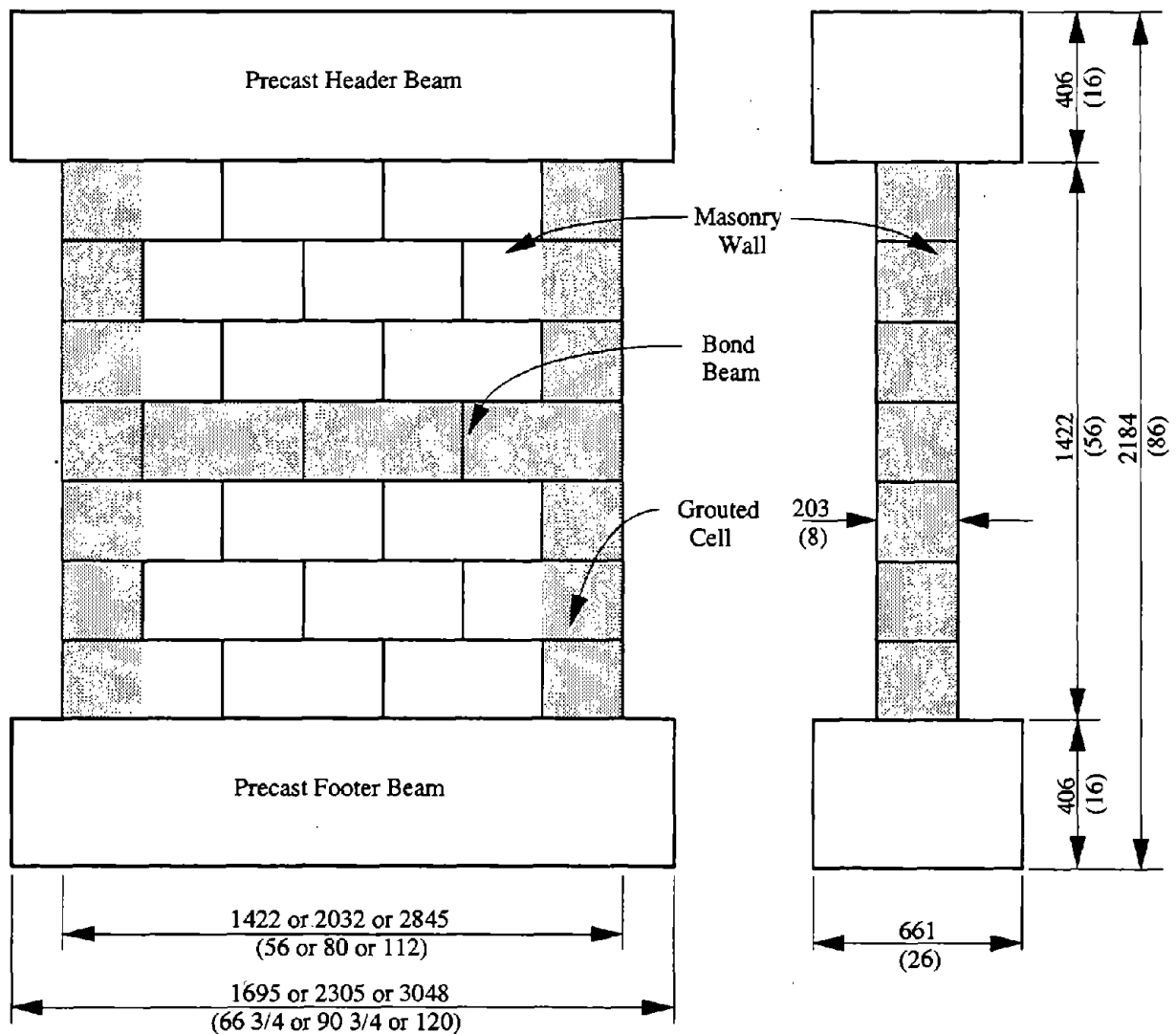
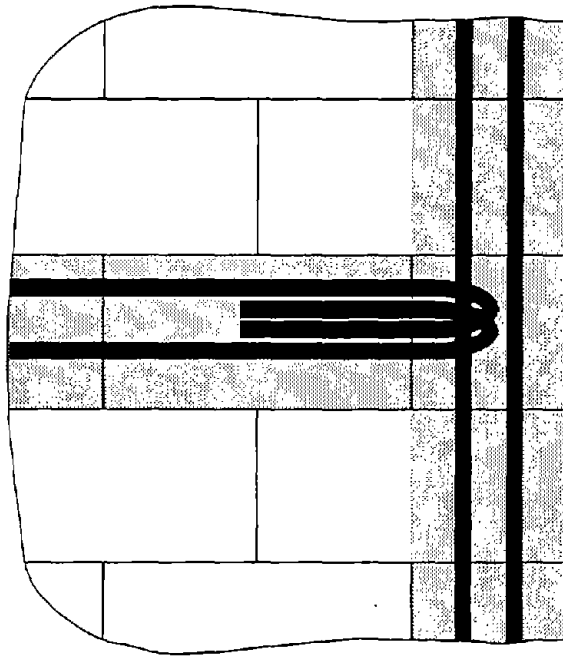Fig. 7.1 Masonry Wall Panel Configurations
All dimensions in mm (in.)

63

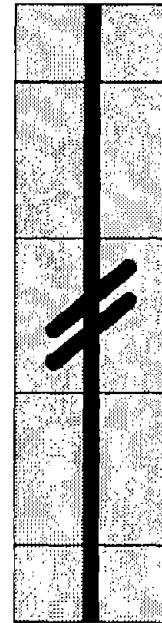Shaded areas represent grouted, reinforced elements.
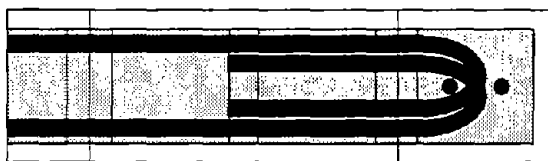
a) Elevation

b) Side View

Fig. 7.2 Grouting Pattern for Bond Beam Specimens
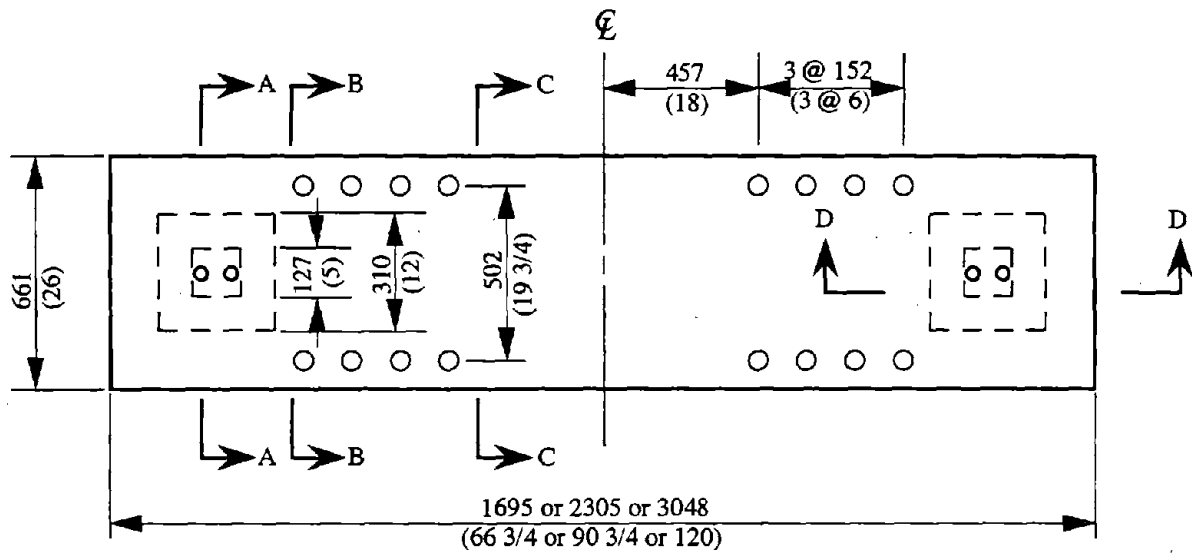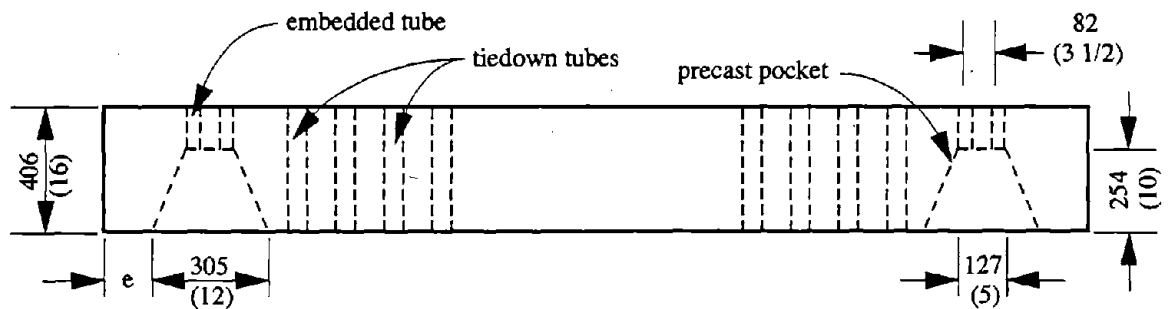All dimensions in mm (in.)

a) Elevation

b) Side View

c) Section

Fig. 7.3 Bond Beam Reinforcement Details

a) Plan

$e = 68$ (2 11/16) for $r = 0.5$; $e = 86$ mm (3 3/8) for $r = 0.7$ and 1.0

b) Elevation

Fig. 7.4 Precast Concrete Header/Footer Beam
All dimensions in mm (in.)

76 x 51 x 4.8 steel
tube (3 x 2 x 3/16)

76 x 51 x 6 steel
tube (3 x 2 x 1/4)

#8 bar

#3 bar

vertical rebar

embedded tube

#3 vertical stirrups

#3 horizontal ties

nut and plate assembly

bond breaker

a) Section A-A

#3 bars (section B-B only)

#3 supplementary vertical
stirrups (section B-B only)

#3 vertical stirrups
(sections B-B and C-C)

#8 bar (sections
B-B and C-C)

b) Sections B-B and C-C

76 x 51 x 4.8 steel
tube (3 x 2 x 3/16)

76 x 51 x 6 steel
tube (3 x 2 x 3/16)

#3 vertical stirrups

vertical rebar

embedded tube

#8 bar

#3 bar

#3 horizontal ties

nut and plate assembly

bond breaker

c) Section D-D

Fig. 7.5 Header/Footer Beam Details
All dimensions in mm (in.)

67

Constant Vertical Compression Stress

Lateral
Load
History

Top (Moving) Head

Precast
Header
Beam

Masonry Panel

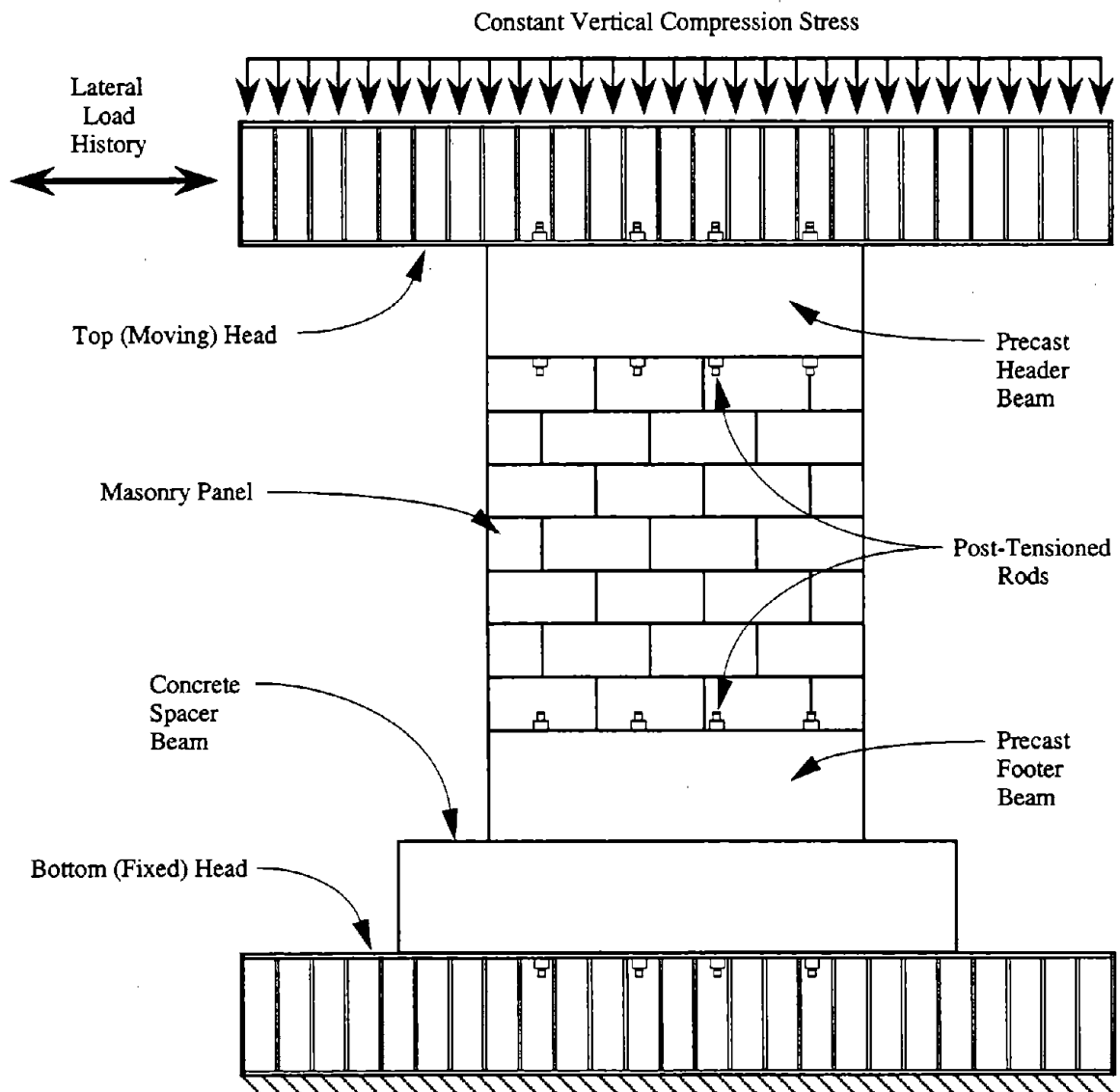Post-Tensioned
Rods

Concrete
Spacer
Beam

Precast
Footer
Beam

Bottom (Fixed) Head

Fig. 8.1 Test Setup for Partially-Grouted Masonry Shear Wall Specimens

68
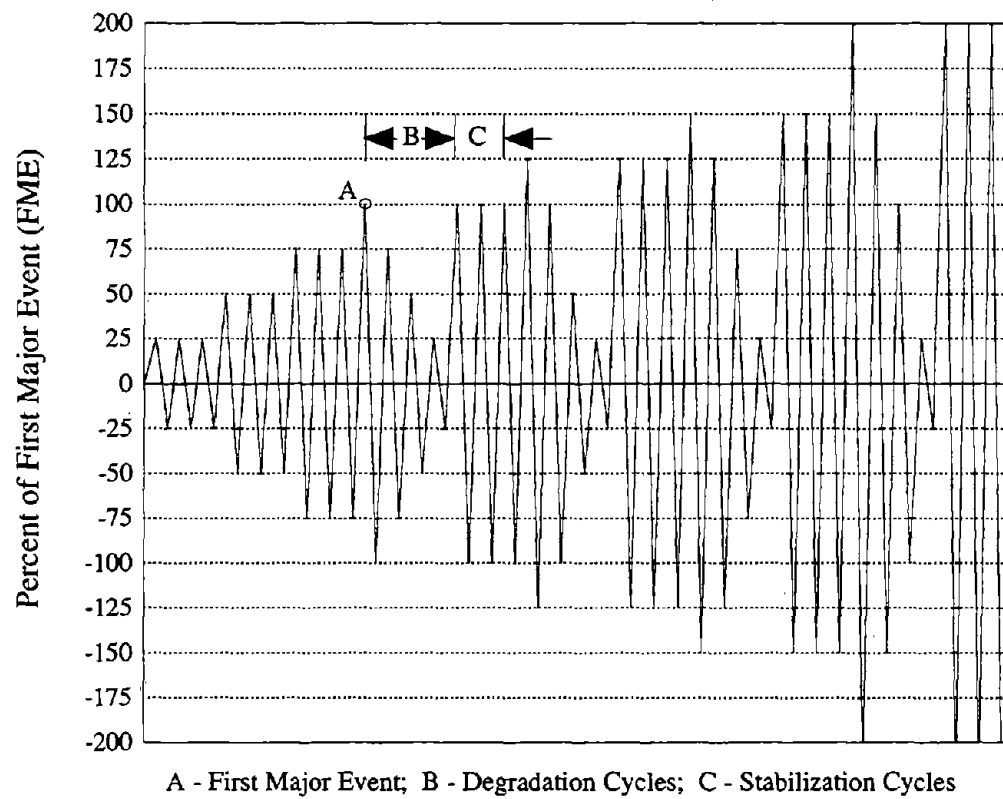
Fig. 8.2 Idealized Displacement History

A - First Major Event; B - Degradation Cycles; C - Stabilization Cycles
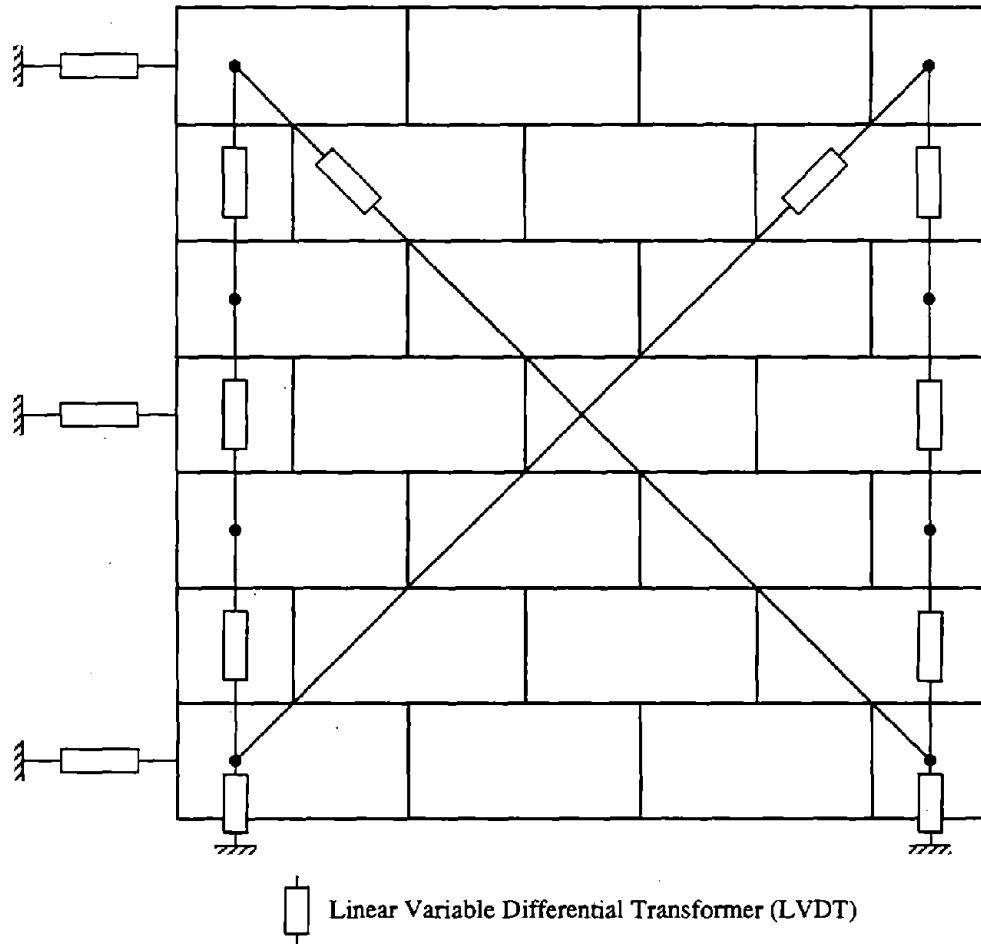
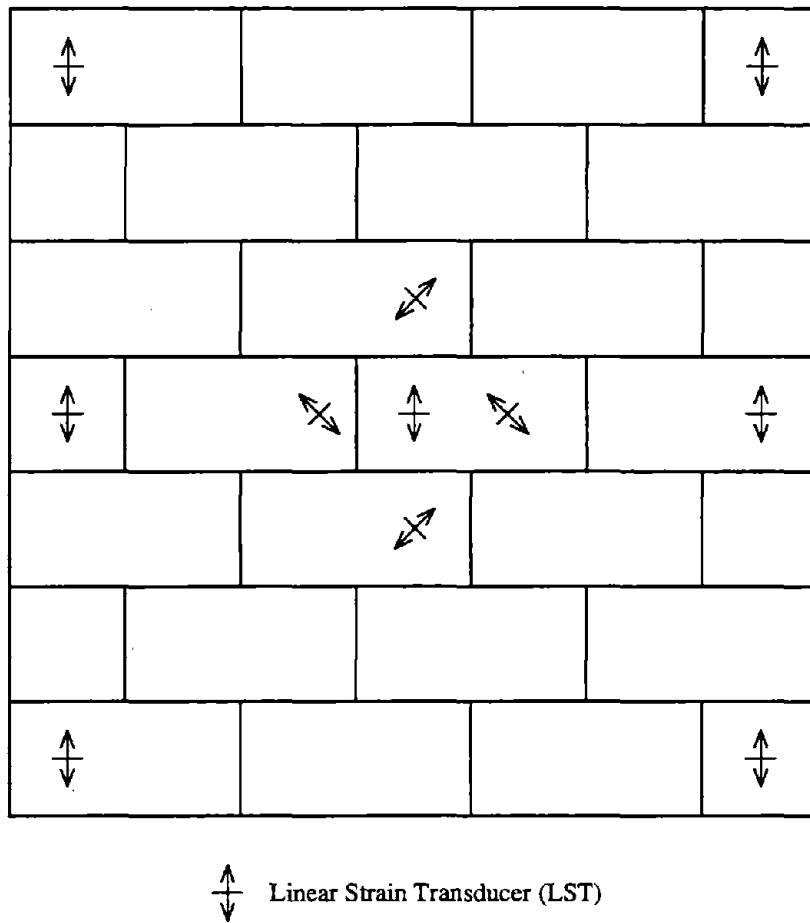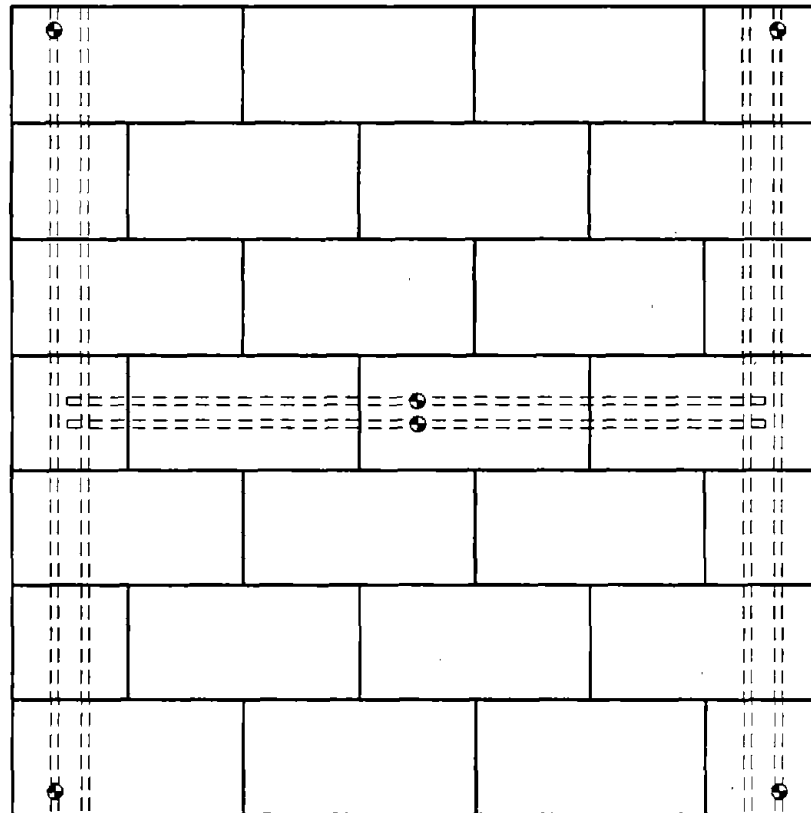Fig. 8.3 Displacement Transducer Locations on North Face of Masonry Specimens

Fig. 8.4 Strain Transducer Locations on South Face of Masonry Specimens

⊙ Electric Resistance Strain Gage (ERSG)

Fig. 8.5 Strain Gage Locations on Shear Wall Reinforcement

APPENDIX A. MINIMUM HORIZONTAL REINFORCEMENT RATIO

In this appendix, expressions are derived for the minimum amount of horizontal reinforcement in masonry walls needed to prevent the onset of premature shear failure upon inclined cracking. The ability of a cracked shear wall to resist the lateral force producing inclined cracking has been shown experimentally to affect ductile behavior after cracking (Englekirk et al., 1984). Horizontal reinforcement is the principal measure whereby post-cracking strength of a wall can be increased for the purpose of enhancing ductile response. Thus, rational limits on minimum horizontal reinforcement in masonry walls must be based, in part, on reliable transfer of force and energy from an uncracked state to a cracked one.

Limits on the minimum amount of horizontal reinforcement in masonry shear walls have appeared in building codes and standards of practice for many years. However, the historical development of these limits have been based on the control of cracking due to shrinkage and temperature changes, rather than on the behavior of masonry walls subjected to lateral loads. Current provisions in the UBC (ICBO, 1991) requiring a minimum horizontal reinforcement ratios equal to 0.07% appears to have arisen from this concept. The current recommendations of the Masonry Joint Standards Committee also require a minimum horizontal reinforcement ratio equal to 0.07% for UBC Seismic Zones 2, 3 and 4 (MSJC, 1992).

Recently proposed revisions to the NEHRP provisions for masonry (*NEHRP*, 1994) retain a minimum horizontal reinforcement ratio equal to 0.07% for seismic performance categories C and D (UBC seismic zones 2b and 3). For exposure to the highest seismic risk (seismic performance category E), masonry walls that do not form part of the lateral load resisting system are required by the proposed NEHRP proposed provisions to have a minimum horizontal reinforcement ratio equal to 0.15%, while those members which are engineered to resist lateral loads must have a ratio equal to at least 0.25%. These requirements are 2 and 3.5 times, respectively, as large as the minimum ratio required for NEHRP categories C and D, as well as the UBC code requirement. This discrepancy raises questions regarding both the applicability and goal of existing limits on horizontal reinforcement in masonry shear walls.

Englekirk et al. (1984) suggested a strength-based criterion for the minimum amount of shear reinforcement in concrete masonry shear walls based an analogy between

73

reinforced concrete and concrete masonry. The ACI minimum shear reinforcement requirements for concrete beams (ACI 318, 1989) were converted into a minimum reinforcement requirement for concrete masonry walls. The recommendation given by Englekirk et al. can be stated as a minimum horizontal reinforcement ratio equal to k/f_{yh} where k is equal to 0.207 MPa (30 psi). For Grade 60 reinforcement, minimum ρ_h is equal to 0.05% of the gross area of a vertical section through the wall. Yet, this formulation ignores a number of variables affecting masonry wall strength, and it recommends minimum reinforcement ratios that, experience has shown, are too small for certain conditions.

Two independent criteria are investigated for the formulation of rational limits on minimum horizontal reinforcement in masonry shear walls. In the first criterion, the shear strength of a cracked masonry wall must match or exceed the shear force which produces initial inclined cracking. In the second criterion, the horizontal reinforcement must possess sufficient toughness to absorb the elastic shear strain energy which is released when a diagonal crack forms in a masonry wall.

The formulas proposed by Shing et al. (1989; 1990a; 1990b) for cracking (V_c) and ultimate (V_m) strengths of masonry and steel strength (V_s) are used in the present study for several reasons. First, these formulas enjoy the same degree of accuracy as other available expressions (Fattal and Todd, 1991), and they produce similar variations in masonry compression strength with the most important variables, as noted in Chapter 6. In addition, Shing's extensive experimental investigation included not only the formulation of analytical expressions for masonry and steel shear strengths, but also generated carefully calibrated diagonal cracking strengths (Shing et al., 1989). An accurate assessment of diagonal cracking strength, which is compatible with the masonry and steel shear strength expressions, is as important to the strength and energy criteria in this appendix as are those for V_m and V_s.

A.1 Strength Criterion

To prevent the undesirable effects of insufficient shear strength, it is assumed that horizontal reinforcement must have sufficient capacity V_s to resist that portion of the cracking shear strength V_c that cannot be resisted by the masonry after cracking V_m, or

$$V_m + V_s \geq V_c \qquad\qquad (A.1)$$

To guarantee that the condition in (A.1) is satisfied, the cracking strength V_c is augmented by a dimensionless overstrength factor ϕ as follows

$$V_m + V_s \geq \phi V_c \tag{A.2}$$

where $\phi > 1$.

Recalling that Shing's formula for masonry shear strength (Eq. 6.6) was developed for fully-grouted masonry, and recognizing that the ratio of vertical reinforcement ρ_v is usually defined in terms of gross area, the following modification to Shing's expression for V_m is needed for partially-grouted masonry

$$V_m = \left[a_1 \left(\left(\frac{t}{t_e} \right) \rho_v f_{yv} + \sigma_c \right) + b_1 \right] A_n \sqrt{f'_m} \tag{A.3}$$

where t is the nominal (gross) thickness of the wall, and t_e is the effective thickness based on net area of masonry.

The contribution of horizontal reinforcement to ultimate shear strength is given by Eq. 6.7. After some rearrangement this expression becomes

$$V_s = \left(L - 2d' - s \right) \left(\frac{A_b}{s} \right) f_{yh} \tag{A.4}$$

After multiplying the right side of (A.4) by the unit fraction A/tL and simplifying, Shing's steel strength component can be expressed as

$$V_s = \frac{2}{3} A \rho_h f_{yh} \tag{A.5}$$

where the term $(L-2d'-s)$ is taken equal to $2L/3$. No single value for this dimension can represent the full range of masonry shear wall dimensions that can be expected in practice, so, the choice of $2L/3$ is arbitrary. It is intended as a median value for $(L-2d'-s)$ which is typically in the range of $L/2$ and $4L/5$. Had the lower limit of $L/2$ been selected for this dimension, Eq. A.5 would have been identical to the treatment given to horizontal steel in the proposed changes to the NEHRP provisions for masonry (Eq. 6-11 and 6-13).

The diagonal cracking strength of the masonry is represented by the expression

$$V_c = (a_2 \sigma_c + b_2) A_n \sqrt{f'_m} \tag{A.6}$$

in which a_2 and b_2 are equal to 0.0759 1/$\sqrt{\text{MPa}}$ (0.0063 1/$\sqrt{\text{psi}}$) and 0.208 $\sqrt{\text{MPa}}$ (2.5 $\sqrt{\text{psi}}$), respectively. This formula is a best-fit linear regression of experimental observations reported by Shing et al. (1989). It is worth noting that Shing found cracking strength to be proportional to both compression stress σ_c and masonry strength f_m. It is equally important to note that the contributions of masonry and axial compression stress are greater for cracking strength than for post-cracking masonry strength, as evidenced by the larger value for the constants a_2 and b_2 in (A.6) than the corresponding constants a_1 and b_1 in both (6.6) and (A.3).

After substitution of (A.3), (A.5), and (A.6) into (A.2) and some modification, the expression for minimum horizontal reinforcement becomes

$$\rho_h \geq \frac{3}{2}\left(\frac{t_e}{t}\right)\left(\frac{\sqrt{f'_m}}{f_{yh}}\right)\left[(\phi a_2 - a_1)\sigma_c + (\phi b_2 - b_1) - a_1\left(\frac{t}{t_e}\right)\rho_v f_{yv}\right] \tag{A.7}$$

An overstrength factor ϕ equal to 1.15 is assumed as this value is comparable to the usual coefficient of variation in material properties of properly executed masonry construction. Thus, (A.7) becomes

$$\rho_h \geq \frac{3}{2}\left(\frac{t_e}{t}\right)\left(\frac{\sqrt{f'_m}}{f_{yh}}\right)\left[a_3 \sigma_c + b_3 - a_1\left(\frac{t}{t_e}\right)\rho_v f_{yv}\right] \tag{A.8}$$

where a_3 and b_3, respectively, are equal to 0.0656 1/$\sqrt{\text{MPa}}$ and 0.0727 $\sqrt{\text{MPa}}$ (0.0054 1/$\sqrt{\text{psi}}$ and 0.875 $\sqrt{\text{psi}}$).

Equation A.8 can be further simplified if a single-valued estimate is made for the last term on the right side, which corresponds to the dowel resistance of vertical reinforcement. The dowel resistance term reduces minimum horizontal reinforcement ratio, so a relatively small value equal to 0.25% is adopted for ρ_v, and Grade 60 steel is assumed. For fully-grouted construction ($t_e/t = 1$), the dowel term takes on a value of 0.0224 $\sqrt{\text{MPa}}$ (0.270 $\sqrt{\text{psi}}$) for fully-grouted masonry. This quantity is subdivided into roughly equal parts and each of these is combined with the masonry and axial stress terms

76

of Eq. A.8. Assuming an axial stress equal to 0.69 MPa (100 psi), the minimum horizontal reinforcement ratio becomes

$$\rho_h \geq \frac{3}{2}\left(\frac{t_e}{t}\right)\left(\frac{\sqrt{f'_m}}{f_{yh}}\right)\left(a_4\sigma_c + b_4\right) \tag{A.9}$$

where a_4 and b_4, respectively, are equal to 0.0482 $1/\sqrt{\text{MPa}}$ (0.004 $1/\sqrt{\text{psi}}$) and 0.0623 $\sqrt{\text{MPa}}$ (0.75 $\sqrt{\text{psi}}$).

For partially-grouted construction, the dowel contribution of vertical reinforcement is greater than for fully-grouted masonry, as the ratio t/t_e in the dowel term of Eq. A.8 exceeds unity. However, in view of the fact that the dowel resistance term was replaced with a conservatively small estimate, the use of (A.9) for partially-grouted masonry implies only an additional increment in conservatism.

A.2 Energy Criterion

When a masonry wall develops an inclined crack, it is not sufficient for the horizontal reinforcement to meet the strength criterion presented in the previous section. Horizontal reinforcement will survive only if it possesses sufficient toughness to absorb the strain energy released by the masonry upon inclined cracking. This condition can be expressed as

$$U_S \geq U'_M \tag{A.10}$$

where U_S is the strain energy absorbed by the reinforcement and U'_M is that portion of the elastic shear strain energy in the masonry which is released upon inclined crack formation.

a) Elastic Shear Strain Energy in Uncracked Masonry

The elastic shear strain energy that is stored in the masonry at the onset of inclined cracking is calculated assuming the wall is an elastic, homogeneous medium in which flexure and shear response are uncoupled. Elastic strain energy stored in mechanisms of flexural resistance is not considered, as these mechanisms are not interrupted by inclined crack formation. Moreover, should such an interruption take place (i.e. flexural cracking), vertical reinforcement will absorb the flexural strain energy released by the masonry.

77

Langhaar (1962) gives the following expression for elastic shear strain energy U_M

$$U_M = \int_0^H \frac{1}{2}\left(\frac{\kappa V^2}{A_n G_m}\right) dy \qquad (A.11)$$

where V is the horizontal shear force at a distance y from the top of the wall (Fig. A.1), and the dimensionless constant κ is equal to 1.2 for walls with rectangular cross-sections. Net area of masonry A_n in a horizontal section of the wall is given by $t_e L$, and the shear modulus of elasticity G_m is equal to $E_m/2(1+\upsilon)$. Dickey and Schneider (1987) report values of υ equal to 0.4 and 0.23, respectively, for ungrouted and grouted clay masonry, while Drysdale et al. (1993) suggest a value of 0.2 for υ in concrete masonry. Assuming that $\upsilon = 0.25$, the shear modulus takes on the value $0.4E_m$.

After substituting the above values into (A.10), strain energy can be simplified to

$$U_M = \left(\frac{3}{2E_m t_e L}\right)\int_0^H V^2 dy \qquad (A.12)$$

If the shear diagram shape factor β_s is defined as

$$\beta_s = \left(\frac{H}{M_o^2}\right)\int_0^H V^2 dy \qquad (A.13)$$

where M_o is the moment at the base of the wall, then strain energy becomes

$$U_M = \frac{3\beta_s M_o^2}{2E_m t_e LH} \qquad (A.14)$$

The shear diagram shape factor is calculated for a one-story portion of a wall. Since lateral loads are applied by the floor and roof diaphragms, the moment diagram is linear between diaphragms (Fig. A.1). It is further assumed that the moment at the base M_o is larger than the moment at the top λM_o (i.e. $\lambda < 1$). The intensity of the story shear force is obtained from moment equilibrium. So, $V = M_o (1 - \lambda)/H$, and

$$\int_0^H V^2 dy = \int_0^H \left[\frac{M_o}{H}(1-\lambda)\right]^2 dy = \frac{M_o^2}{H}(1-\lambda)^2 \qquad (A.15)$$

78

The corresponding shear diagram shape factor β_s is equal to $(1-\lambda)^2$. At the onset of inclined cracking, M_o is equal to the cracking moment. By equilibrium, this moment is given by $V_cH/(1-\lambda)$. Thus, total shear strain energy in the masonry wall at the onset of inclined cracking is

$$U_M = \frac{3V_c^2 H}{2E_m t_e L} \tag{A.16}$$

Equation A.6 is substituted for V_c, and E_m is replaced with the empirical expression $c_3 f'_m$ which is recommended in the proposed NEHRP provisions for masonry (*NEHRP*, 1994). Recognizing that net area A_n is equal to $t_e L$, and simplifying strain energy gives

$$U_M = \frac{3}{2} \left[\frac{\left(a_2 \sigma_c + b_2\right)^2}{c_3} \right] t_e H L \tag{A.17}$$

where the dimensionless constant c_3 is equal to 750.

It is noted that only some of the elastic shear strain energy in the masonry is transferred to the horizontal reinforcement upon inclined crack formation. The masonry retains the ability to transfer some horizontal shear stress across the inclined crack. Thus, the strain energy that must be absorbed by the reinforcement U'_M is only a fraction of U_M (Eq. A.17), and that fraction is approximated as

$$\frac{U'_M}{U_M} = \frac{V_c - V_m}{V_c} \tag{A.18}$$

In (A.18), it is assumed that total shear strain energy U_M is proportional to cracking shear force V_c, and the strain energy absorbed by the steel is proportional to the shear force resisted by the steel, i.e. the difference between V_c and $V_{m,}$. V_c is given by (A.6), and V_m is given by (A.3), except that the dowel term is dropped for the sake of simplicity. In addition, the overstrength factor ϕ is applied only to the cracking shear force V_c in the numerator of (A.18). After rearranging terms, the strain energy ratio becomes

$$\frac{U'_M}{U_M} = \frac{\left(a_3 \sigma_c + b_3\right)}{\left(a_2 \sigma_c + b_2\right)} \tag{A.19}$$

79

where the constants a_3 and b_3 were given in the previous section. Thus, the strain energy absorbed by the horizontal reinforcement is

$$U_M' = \frac{3}{2} \frac{(a_2 \sigma_c + b_2)(a_3 \sigma_c + b_3)}{c_3} t_e HL \qquad (A.20)$$

and the following expression

$$U_M' = \frac{3}{2} \frac{(a_5 \sigma_c + b_5)^2}{c_3} t_e HL \qquad (A.21)$$

is nearly identical to (A.20) for axial stresses σ_c ranging from 0 to 10.3 MPa (1500 psi). The empirical constants a_5 and b_5 are equal 0.0723 $1/\sqrt{\text{MPa}}$ (0.006 $1/\sqrt{\text{psi}}$) and 0.125 $\sqrt{\text{MPa}}$ (1.5 $\sqrt{\text{psi}}$), respectively.

b) Energy Absorbed by Horizontal Reinforcement

The lengths of horizontal reinforcing bars in a masonry shear wall that participate in energy absorption are controlled by the mechanism of bond stress transfer between the reinforcement and surrounding grout. Horizontal reinforcing bars are assumed to be fully bonded in grouted bond beams, and a constant bond stress distribution is assumed along such bars (Fig. A.2). The resulting distribution of uniaxial stress in the bar is linear, with stresses decreasing in proportion to distance from the critical section (i.e. the intersection of the bar and the inclined crack). The corresponding distribution of bar strain is bilinear, in which a change in slope is present at the location where the bar yields. For simplicity, the reinforcing bar is assumed to be bilinear with elastic and post-yield regimes (Fig. A.3).

In the present idealization, only the bonded portion of the bar which has finite stress can participate in energy absorption. This total bonded length l_b is the sum of an "elastic" bonded length l_e and a "plastic" bonded length l_p. Horizontal equilibrium requires the force developed through bond over the total bonded length $(\pi d_b l_b u_b)$ to be equal to the strength of the bar $(A_b f_u)$, so that the bonded length is given by

$$l_b = \frac{d_b f_u}{4 u_b} \qquad (A.22)$$

and u_b is the constant bond stress. The relation between l_b and l_e is established by exploiting linearity of the distribution of bar stresses, so $l_b/l_e = f_u/f_y$.

The strain energy stored in the bar is subdivided into three components, elastic (U_{el}), plastic (U_{pl}), and post-yield (U_{py}), as noted in the stress and strain diagrams in Fig. A.2. Thus, the strain energy in a bar U_b is obtained by algebraic addition of these quantities

$$U_b = U_{el} + U_{pl} + U_{py} \tag{A.23}$$

and the strain energy components can be obtained by integration such that

$$U_b = 2\left[\int_0^{l_e} \frac{1}{2} f \varepsilon A_b dx + \int_{l_e}^{l_b} f_y \varepsilon_y A_b dx + \int_0^{l_p} \frac{1}{2} \Delta f \Delta \varepsilon A_b dx' \right] \tag{A.24}$$

where the quantity in brackets is doubled to include the energy stored in the portion of the bar on both sides of the inclined crack, and f and ε are bar stress and strain at a distance x from the critical section, and Δf and $\Delta \varepsilon$ are increments in stress and strain at x'. These quantities are given by

$$f = \left(\frac{f_y}{l_e} \right) x \tag{A.25}$$

$$\varepsilon = \left(\frac{\varepsilon_y}{l_e} \right) x$$

$$\Delta f = \left(\frac{f_u - f_y}{l_p} \right) x'$$

$$\Delta \varepsilon = \left(\frac{\varepsilon_u - \varepsilon_y}{l_p} \right) x'$$

Substituting (A.25) into (A.24), integrating and simplifying gives

$$U_b = \frac{A_b f_y \varepsilon_y l_e}{3} \left[1 + 6\left(\frac{l_b}{l_e} - 1 \right) + \left(\frac{l_b}{l_e} - 1 \right)\left(\frac{f_u}{f_y} - 1 \right)\left(\frac{\varepsilon_u}{\varepsilon_y} - 1 \right) \right] \tag{A.26}$$

81

recognizing that $l_b/l_e = f_u/f_y$, substituting (A.22) into (A.26), and replacing ε_y with f_y/E_s and A_b with $\pi d_b^2/4$, strain energy absorbed by the bar becomes

$$U_b = \frac{\pi}{48} \left(\frac{d_b^3 f_y^3}{E_s u_b} \right) \left[6\left(\frac{f_u}{f_y} - \frac{5}{6} \right) + \left(\frac{f_u}{f_y} - 1 \right)^2 \left(\frac{\varepsilon_u}{\varepsilon_y} - 1 \right) \right] \qquad (A.27)$$

For Grade 60 reinforcing bars, with nominal yield stress $f_y = 414$ MPa (60 ksi), ultimate strength f_u is typically on the order of 621 MPa (90 ksi). So $f_u/f_y = 3/2$, and

$$U_b = \frac{\pi}{192} \left(\frac{d_b^3 f_y^3}{E_s u_b} \right)(\mu_\varepsilon + 15) \qquad (A.28)$$

and, for a wall with n such horizontal reinforcing bars, strain energy in the horizontal steel is given by

$$U_s = \frac{\pi n}{192} \left(\frac{d_b^3 f_y^3}{E_s u_b} \right)(\mu_\varepsilon + 15) \qquad (A.29)$$

The preceding derivation, through (A.27) is applicable to wire reinforcing grids as long as a cross wire is not present in the bonded length l_b. The presence of a cross-wire disrupts the assumed bond stress distribution, and effectively anchors the longitudinal wires. Assuming that cross wires are not present in the length l_b, (A.27) can also be tailored for wire reinforcing grids. For most grid reinforcement made using untreated cold-drawn carbon steel, nominal yield stress f_y is on the order of 552 MPa (80 ksi), and ultimate strength is only incrementally larger. Assuming that $f_u = 621$ MPa (90 ksi), so $f_u/f_y = 9/8$, (A.27) can be simplified to

$$U_b = \frac{\pi}{192} \left(\frac{d_b^3 f_y^3}{E_s u_b} \right)\left(\frac{\mu_\varepsilon + 111}{16} \right) \qquad (A.30)$$

For a wall with n wire reinforcing grids, each with two longitudinal wires, strain energy is

$$U_s = \frac{\pi n}{192} \left(\frac{d_b^3 f_y^3}{E_s u_b} \right)\left(\frac{\mu_\varepsilon + 111}{8} \right) \qquad (A.31)$$

82

c) Influence of Longitudinal Wire Diameter in Reinforcing Grids

If the diameter of longitudinal wires in a reinforcing grid is too large, and/or the distance between cross wires is too short, the mechanism of anchorage may be different from that assumed in the previous section. If, on the average, the distance from a critical section to the nearest cross wire is equal to one-half the clear distance between cross wires l_c, then, the longitudinal wires must be developed through bond within the distance $l_c/2$. Otherwise, the assumed stress and strain distributions in the previous section (Fig. A.2) are disrupted, and the previous expression for strain energy in reinforcing grids (Eq. A.31) is not correct.

Given the above idealization, the bond mechanism described in the preceding section is applicable as long as the bond length l_b is less than $l_c/2$. Using results from the preceding section, this condition can be expressed as

$$\frac{l_c}{d_b} \geq \frac{f_u}{2u_b} \tag{A.32}$$

If this condition is not satisfied, then the stress and strain distributions along bonded bar length are truncated, as shown in Fig. A.4. The stress in the bar immediately before the cross wire f_o is obtained by subtracting from f_u the stress change due to bond along the distance $l_c/2$, which can be shown to be equal to $2(l_c u_b/d_b)$, or

$$f_o = f_u \left(1 - \frac{l_c/d_b}{f_u/2u_b}\right) \tag{A.33}$$

As long as f_o is less than f_y, the truncated portions of the stress and strain diagrams represent a fictitious fraction of the elastic strain energy U_{el} in the bar. This quantity can be easily calculated, and the appropriate correction can be made to the strain energy given by (A.23). For f_o to be less than f_y, the following condition must be satisfied

$$\frac{l_c}{d_b} \geq \frac{f_u}{2u_b} \left(1 - \frac{f_y}{f_u}\right) \tag{A.34}$$

The distance x_o represents the difference between the total bonded length l_b (calculated assuming no cross wire) and the dimension $l_c/2$, and it is given by

$$x_o = \left(\frac{f_u / 2u_b}{l_c / d_b} - 1 \right) \frac{l_c}{2} \qquad (A.35)$$

The elastic strain energy U'_{el} associated with the truncated portions of the bar stress and strain diagrams can be shown to equal $\xi(A_b f_y \, \varepsilon_y \, l_e / 3)$, where

$$\xi = \left[\left(\frac{f_u}{f_y} \right) \left(1 - \frac{l_c / d_b}{f_u / 2u_b} \right) \right]^3 \qquad (A.36)$$

Subtracting U'_{el} from the strain energy in (A.26) and simplifying yields

$$U_b = \frac{\pi}{48} \left(\frac{d_b^3 f_y^3}{E_s u_b} \right) \left[6 \left(\frac{f_u}{f_y} - \frac{(5 + \xi)}{6} \right) + \left(\frac{f_u}{f_y} - 1 \right)^2 \left(\frac{\varepsilon_u}{\varepsilon_y} - 1 \right) \right] \qquad (A.37)$$

Assuming that $f_u / f_y = 9/8$ for wire reinforcing grids and simplifying, gives

$$U_b = \frac{\pi}{192} \left(\frac{d_b^3 f_y^3}{E_s u_b} \right) \left(\frac{\mu_\varepsilon + 111 - 64\xi}{16} \right) \qquad (A.38)$$

and for a wall with n wire reinforcing grids, each with two longitudinal wires, strain energy is

$$U_s = \frac{\pi n}{192} \left(\frac{d_b^3 f_y^3}{E_s u_b} \right) \left(\frac{\mu_\varepsilon + 111 - 64\xi}{8} \right) \qquad (A.39)$$

Assuming $f_u = 621$ MPa (90 ksi) and $u_b = 4.1$ MPa (600 psi) for wire reinforcing grids, as noted in the following section, the limit given by (A.32) indicates that the ratio l_c/d_b must exceed 75 if the absorbed energy given by (A.31) is to be applicable. For typical grids with a 406 mm (16 in.) spacing between cross wires, longitudinal wires with a diameter equal to or less than 5.42 mm (0.213 in.) have a bonded length that is smaller than $l_c/2$. Thus, for grids with No. 5 Gage longitudinal wires or smaller, (A.30) and (A.31) are applicable. For longitudinal wires with larger diameter, (A.38) and (A.39) are applicable. Furthermore, the condition given in (A.34) to ensure that $f_o < f_y$, requires that the ratio l_c/d_b exceed 8.3, which is satisfied for longitudinal wire diameters as large as 48.8 mm (1.92 in.).

84

The dimensionless term 64ξ in (A.39) takes on values that range from 0.01 for No. 4 Gage wire, which has a diameter of 5.72 mm (0.225 in.), to 2.5 for No. 0 Gage wire, which has a diameter equal to 7.77 mm (0.306 in.). Even if cross wires are placed at a spacing l_c equal to 203 mm (8 in.), the term 64ξ in (A.39) doe not exceed 11 for wire sizes that can be used for wire reinforcing grids (No. 5 Gage and smaller). Thus, the effect of wire diameter on bonded length is negligible for wire sizes that can be used for reinforcing grids.

d) Combining Effects

To define the minimum ratio of horizontal steel for the energy criterion, the expressions for the energy absorbed by the horizontal reinforcement are combined with the elastic shear strain energy transferred from the masonry according to the condition described in (A.10). For hot-rolled reinforcing bar, the energy absorbed by the reinforcement is given by (A.29). Combining this equation with (A.21) and (A.10), and simplifying gives the following minimum bar diameter

$$
d_b \geq \left[\left(\frac{288}{\pi n} \right) \left(\frac{E_s u_b}{f_y} \right) \left(\frac{t_e HL}{c_3} \right) \frac{(a_5 \sigma_c + b_5)^2}{(\mu_\varepsilon + 15)} \right]^{1/3}
\tag{A.40}
$$

Using this expression to calculate the total horizontal cross-sectional area of n such bars, and dividing by the gross area of a vertical section of the wall (tH), defines the minimum steel ratio

$$
\rho_h \geq \left[64\sqrt{n} \left(\frac{E_s u_b}{c_3 f_y^3} \right) \left(\frac{t_e}{t} \right) \sqrt{\left(\frac{L/t}{H/L} \right)} \frac{(a_5 \sigma_c + b_5)^2}{(\mu_\varepsilon + 15)} \right]^{2/3}
\tag{A.41}
$$

Similarly, for wire grids, combining (A.10), (A.21), and (A.31), and simplifying yields

$$
d_b \geq \left[\left(\frac{2304}{\pi n} \right) \left(\frac{E_s u_b}{f_y} \right) \left(\frac{t_e HL}{c_3} \right) \frac{(a_5 \sigma_c + b_5)^2}{(\mu_\varepsilon + 111)} \right]^{1/3}
\tag{A.42}
$$

and, obtaining the total for $2n$ such wires, and dividing by tH gives

$$\rho_h \geq \left[1445\sqrt{n} \; \left(\frac{E_s u_b}{c_3 f_y^3}\right)\left(\frac{t_e}{t}\right)\sqrt{\left(\frac{L/t}{H/L}\right)} \frac{\left(a_5\sigma_c + b_5\right)^2}{\left(\mu_\varepsilon + 111\right)} \right]^{2/3} \qquad (A.43)$$

The minimum horizontal reinforcement ratios given by (A.41) and (A.43) are further simplified by assuming constant quantities for certain variables. The dimensionless constant c_3 is taken equal to 750, as recommended in the proposed NEHRP provisions for masonry (*NEHRP*, 1994), and assuming 207,000 MPa (30,000,000 psi) for the modulus of elasticity of steel. Yield stresses f_y equal to 414 MPa (60 ksi) and 552 MPa (80 ksi) are assumed for hot-rolled bars and wire reinforcing grids, respectively. Constant values are assumed for $\sqrt{n}$, and, since ρ_h is proportional to the cube root of n, there is little error associated with this approximation. For walls reinforced horizontally with bars in grouted bond beams, n often varies from 2 to 6, with an approximate mean value of 2 for $\sqrt{n}$, whereas, for wire grids, n usually takes on values between 5 and 15, with a mean value for $\sqrt{n}$ closer to 3.

It is not uncommon for Grade 60 hot-rolled bars to develop elongations of 20% or more, while, reinforcing grids fabricated from cold-drawn wire seldom display elongations in excess of 4-8%. Elongations of 15% and 5%, respectively, were assumed for hot-rolled Grade 60 bar and wire grids in this study, and since the bonded lengths (l_b) for this reinforcement are of the same order as the gage lengths used in standard tension tests, these elongations are considered appropriate. The associated strain ductility factors μ_ε are equal to 75 and 19, respectively, for hot-rolled bar and wire grids.

The use of a single-valued bond stress u_b is probably the greatest source of error in this study. In reality, local bond stresses for embedded bars are far from constant (Viwathanatepa et al., 1979; Bonacci and Marquez, 1994), but assuming a constant value is computationally expedient. This idealization has been used extensively in reinforced concrete design (Orangun et al., 1977), and ample experimental data has been developed regarding this parameter. Harris et al. (1983) report a wide range of average ultimate bond stresses obtained from pullout tests for a variety of hot-rolled deformed bar and cold-drawn wire reinforcement. Average ultimate bond stresses range from 8.3 MPa (1200 psi) to 15.2 MPa (2200 psi) for small diameter hot-rolled deformed bar (#4 to #7), and a median bond stress equal to 10.3 MPa (1500 psi) is assumed in the present study. Average

ultimate bond stresses typically range from 2.1 MPa (300 psi) to 6.9 MPa (1000 psi) for wire embedded in concrete (Sabnis et al. 1983), and an approximate average value of 4.1 MPa (600 psi) is assumed for wire reinforcing grids. It is worth noting that it is preferable to overestimate bond stress in the present study than it is to underestimate this parameter, as the former leads to conservatism in minimum reinforcement ratio calculations.

After substituting the values given above for c_3, E_s, f_y, $\sqrt{n}$, μ_ε, and u_b into Eq. A.41, and simplifying, the minimum reinforcement ratio expression becomes

$$\rho_h \geq \left[c_4 \left(\frac{t_e}{t}\right) \sqrt{\left(\frac{L/t}{H/L}\right)} \left(a_s \sigma_c + b_s\right)^2 \right]^{2/3} \tag{A.44}$$

where c_4 is equal to 5.70×10^{-5} 1/MPa (3.95×10^{-7} 1/psi) and 2.24×10^{-4} 1/MPa (1.56×10^{-6} 1/psi) for hot-rolled bar and wire reinforcing grids, respectively.

A.3 Verification

The reinforced masonry shear wall specimens tested by Shing et al. (1989; 1990a; 1990b; 1992) are used to verify the accuracy of the minimum horizontal reinforcement ratio expressions derived in this appendix. These cantilever shear walls were loaded using the TCCMAR in-plane cyclic load history (Porter and Tremel, 1987), and a uniform axial compression stress. The tests include 16 concrete block specimens with deformed reinforcing bars in grouted bond beams (Wall Nos. 1-16), 6 hollow clay brick specimens with deformed reinforcing bars in grouted bond beams (Wall Nos. 17-22), and 2 concrete block specimens with wire grid reinforcement in bed joints (Wall Nos. D1 and D2).

The dimensions, material properties, reinforcement ratios and axial compression stresses for these shear wall specimens are summarized in Table A.1. The calculated minimum values of ρ_h for the strength and energy criteria are given in Table A.2, along with the ratios of provided to required horizontal reinforcement. The failure mode, displacement ductility factors, and energy dissipation factors reported by Shing et al. are also listed in Table A.2.

The flexure failure mode includes the specimens that exhibited flexural yielding of vertical steel and compressive crushing of masonry at wall toes, while those specimens failing in shear exhibited diagonal tensile cracking that governed ultimate strength. The

sliding failure is documented as relative horizontal movement between wall and footing which accounted for 25% or more of the total horizontal deformation of the specimen. The specimens failing by rupture of horizontal reinforcement did so only after the formation of diagonal cracks over the full height of the specimens. The rows in Tables A.1 and A.2 that correspond to specimens failing purely in a shear mode have been highlighted for easy identification.

It is noted that for all 24 specimens in Table A.2, the strength criterion controls minimum reinforcement ratio, as the strength equation (A.9) requires reinforcement ratios that are at least four times as large as those required by the energy equation (A.44). Even for the walls with wire grid reinforcement (D1 and D2), the strength criterion supersedes the toughness requirements of the energy criterion. However, Wall Nos. D1 and D2, having less than 50% of the steel needed for toughness, are the only two specimens that do not meet the energy criterion. Wall Nos. 1-22 were provided with at least twice the amount of horizontal steel required by the energy criterion.

The minimum horizontal reinforcement ratio expressions developed in this appendix (A.9 and A.44) are seen to serve as reasonably accurate indicators of shear critical walls (Table A.2). Nine of the twelve (75%) specimens that eventually failed in shear (Wall Nos. 3, 5, 7, 9, 14, 21, 22, D1, D2) require horizontal reinforcement ratios, according to the present study, that exceed the amount of horizontal steel that was actually provided. Furthermore, the ratio of provided-to-required horizontal reinforcement for the remaining three walls that failed in pure shear (Wall Nos. 4, 13, 16) is only marginally larger than unity (1.37, 1.02, 1.17). Ten of the twelve (83%) specimens that eventually failed in either flexure (Wall Nos. 1, 12, 17-20) or a mixed mode (Wall Nos. 6, 8, 11, 15) were provided with more horizontal reinforcement than was needed, according to this study. For the remaining specimen that failed in flexure (Wall No. 2), the provided-to-required horizontal reinforcement ratio was relatively close to unity (0.91), while the remaining specimen (Wall No. 10) failing in a mixed mode (flexure/shear) demonstrated some shear distress.

The shear distress of specimens D1 and D2 is clearly predicted by the discrepancy between the reinforcement ratios provided (0.07% for both D1 and D2) and the required horizontal reinforcement ratios required for the strength criterion (0.21% for D1 and 0.19% for D2). However, these two specimens failed in a more brittle and sudden manner than any of the other walls, as the horizontal reinforcement (wire grids) ruptured shortly after

88

diagonal crack formation. Curiously enough, Wall Nos. D1 and D2 are the only two specimens that were provided less horizontal reinforcement than required by the energy criterion. Clearly, the consequences of not satisfying the two criteria differ.

Insufficient reinforcement to meet the strength criteria will result in strength deterioration upon inclined crack formation. This does not necessarily imply a sudden, catastrophic failure, only a decrease in lateral load capacity. This behavior can be seen in those walls in Table A.2 which fail in shear, but which exhibited modest displacement ductility ratios and normalized energy dissipation factors. These two parameters were defined by Shing et al. (1989) for that portion of the load history in which the wall maintained at least 50% of its peak strength. It is also noted that the most ductile and tough specimens were those failing in flexure, or a combination of flexure and one of the other modes.

Insufficient steel to meet the toughness requirements of the energy criterion is a more serious matter altogether. Should an inclined crack form in such a wall, the horizontal steel will be unable to absorb the strain energy released by the wall. Rupture of the horizontal reinforcement must follow such a condition. Once the horizontal reinforcement ruptures, a sudden, catastrophic failure of the wall is most certain. In fact, this behavior was observed only in those specimens not meeting the energy criterion (Wall Nos. D1 and D2). It is essential to require masonry shear walls to contain sufficient horizontal reinforcement to exceed the energy criterion by an ample margin.

A.4 Discussion

Minimum horizontal reinforcement based on the strength criterion (Eq. A.9) and the energy criterion (Eq. A.44), respectively, are illustrated in Fig. A.5 and A.6 for hot-rolled reinforcing bar and wire reinforcing grids. It is worth noting that for both criteria, axial compression stress has a strong influence on minimum horizontal reinforcement ratio, and over a range of σ_c from 0 to 2 MPa (290 psi), minimum ρ_h more than doubles: In some cases, it nearly triples. Also, for partially-grouted masonry, minimum ρ_h is, for all practical purposes, proportional to t_e/t. However, besides σ_c and t_e/t, the parameters affecting ρ_h differ for the two criteria, with f'_m and f_{yh} influencing the strength criterion, while a greater number of variables affect the energy criterion, including f_u/f_y, μ_ε, E_s, and u_b.

In all cases considered, minimum horizontal reinforcement ratios for hot-rolled reinforcing bars are controlled by the strength criterion (Fig. A.5a), rather than the energy criterion (Fig. A.6a). The strength criterion suggests that fully-grouted walls require reinforcement ratios as large as 0.25%, if the masonry has high compression strength (f_m=27.6 MPa=4000 psi) and large axial compression stresses (σ_c=1.38 MPa=200 psi) are applied. However, a constant ρ_h equal to 0.15% satisfies the strength criterion for hot-rolled reinforcing bar for the usual ranges of f_m ($\leq$20.7 MPa=3000 psi) and σ_c ($\leq$0.69 MPa=100 psi).

For wire reinforcing grids, the computed ranges of minimum horizontal reinforcement ratios for the strength and energy criteria are similar. However, since different variables control these criteria, the strength criterion may control in some cases (fully-grouted walls with high compression strengths and axial stresses), while the energy criterion may control for other parametric combinations (long, low-rise walls that are fully grouted). Yet, a horizontal reinforcement ratio of 0.25% appears to be conservative for all cases considered, and a ratio equal to 0.15% satisfies both criteria for wire grids with typical values for f_m ($\leq$20.7 MPa=3000 psi) and moderately low values for σ_c ($\leq$0.69 MPa=100 psi).

If a single-valued, conservative estimate is sought for ρ_h, and σ_c is not expected to greatly exceed 0.69 MPa (100 psi), then a value of 0.15% appears to be justified for fully-grouted masonry. If added safety is sought, or if large axial compression stresses are expected, 0.25% horizontal reinforcement ratio seems justified for fully-grouted masonry. These suggested minimum horizontal reinforcement ratios imply that current UBC and NEHRP requirement of 0.07% horizontal reinforcement ratio is too low for fully-grouted masonry. This current requirement appears to apply to masonry with compression strength that does not exceed 10.3 MPa (1500 psi), which is reinforced horizontally with hot-rolled Grade 60 reinforcing bars, and which does not have significant axial compression ($\sigma_c \sim 0$). In addition, for partially-grouted masonry, these ratios should be multiplied by t_e/t.

In light of this study, the use of wire reinforcing grids as shear reinforcement in masonry shear walls appears to be justified, as long as sufficient horizontal reinforcement can be detailed to satisfy the requirements outlined in this appendix. For partially grouted masonry, it is possible to meet these requirements using wire grids in the commonly-available configurations. However, for fully-grouted masonry, it may be difficult to provide sufficient horizontal steel in typically-available grids to meet the necessary

requirements. Variations of the commonly-used wire grids with modified material properties are needed.

The typically high yield strength of wire reinforcing grid, when compared with hot-rolled bar, helps to reduce minimum ratio required by the strength criterion. However, to further relax the energy requirements, increases in both strain ductility (μ_ε) and strain-hardening stress range (f_u/f_y) are needed. For example, if wire grids can be manufactured with the assurance that $f_y \geq 552$ MPa (80 ksi), $f_u/f_y \geq 1.25$, and $\varepsilon_u \geq 0.10$, then, the constant c_4 in Eq. A.44 becomes 9.56 x 10^{-5} 1/MPa (6.59 x 10^{-7} 1/psi), and reinforcement ratios for the energy criterion are rendered smaller than those for the strength criterion in all cases considered (Fig. A.5b). In fact, required horizontal reinforcement ratios for wire grids with the preceding properties are roughly one-half as large as the ratios given in Fig. A.6b.

A.5 Recommended Code Provision

It is of value to use the formulas for minimum ρ_h derived in this appendix to calibrate code provisions for minimum horizontal reinforcement. Undoubtedly, the minimum horizontal reinforcement ratio expressions derived in this appendix require further verification with experimental observations, even though the validity of these expressions was established partially in this appendix through comparison with Shing's shear wall test data. But, test results are needed over a wider range of the pertinent variables, in particular, more data is needed on walls with bed joint reinforcement in the form of wire grids. The experimental research outlined in this document was designed to fulfill this goal, in addition to the other experimental priorities described in Chapter 5.

The energy criterion is eliminated in view of the dominance of the strength criterion for Grade 60, hot-rolled reinforcing bar. In the preceding section, minimum requirements for the mechanical properties of wire reinforcing grids are suggested so that the energy criterion controls the proportioning of this type of reinforcement as well. Even though axial compression stress has a marked influence on the minimum horizontal reinforcement requirement, it is desirable, for several reasons, to eliminate σ_c from a code provision based on the expression for the strength criterion (A.9). Simplicity in code provisions, particularly for limiting conditions, is always desirable. At the time that reinforcement ratio limits are being established during preliminary design, a designer may not have an accurate estimate of axial compression stress. Also, minimum ρ_h given by (A.9) is likely to differ for similar walls in a masonry structure. Thus, it is worthwhile to use a single-valued,

91

conservative estimate of axial compression stress σ_c to eliminate the dependency of minimum horizontal reinforcement ratio ρ_h on this variable.

The NEHRP minimum ratio of 0.25% for seismic performance category E is used as a benchmark for simplifying the strength formula for minimum ρ_h. This ratio agrees with the minimum ratio required by Eq. A.9 for fully-grouted masonry with grade 60 horizontal reinforcement, and with f_m=27.6 MPa (4000 psi) and σ_c=1.38 MPa (200 psi). Using this reinforcement ratio as a benchmark, and retaining the influence of t_e/t and f_m/f_{yh}, the strength requirement in (A.9) is replaced by

$$\rho_h \geq c_5 \left(\frac{t_e}{t}\right)\frac{\sqrt{f_m'}}{f_{yh}} \tag{A.45}$$

where c_5 is equal to 0.2 $\sqrt{\text{MPa}}$ (2.4 $\sqrt{\text{psi}}$).

For fully grouted masonry reinforced horizontally with grade 60 steel, the ratios required by (A.45) varies from 0.13% for f_m=6.9 MPa (1000 psi) to 0.25% for f_m =27.6 MPa (4000 psi). If wire reinforcing grids with f_{yh}=552 MPa (80 ksi), the variation in minimum ρ_h is 0.095% to 0.19% for the same range of masonry compression strengths. These ratios are further reduced for partially-grouted masonry. For example, the face-shell bedded masonry in this study has an effective thickness t_e=64 mm (2.5 in.) and a gross thickness t=194 mm (7.625 in.), for a ratio t_e/t=0.33, and Eq. A.45 requires minimum horizontal reinforcement ratios varying from 0.04% for f_m=6.9 MPa (1000 psi) to 0.08% for f_m =27.6 MPa (4000 psi) for grade 60 steel. For wire reinforcing grids (f_{yh}=552 MPa=80 ksi), the corresponding range is 0.031% to 0.063%.

Table A.1 Properties of Shing's Shear Wall Test Specimens

Wall No.	t (mm)	L (mm)	H (mm)	f'_m (MPa)	Horizontal Steel		Vertical Steel		σ_c (MPa)
					f_{yh} (MPa)	ρ_h (%)	f_{yv} (MPa)	ρ_v (%)	
1	143	1830	1830	20	462	0.24	441	0.38	1.38
2	143	1830	1830	20	386	0.24	441	0.38	1.86
3	143	1830	1830	20.7	386	0.14	496	0.74	1.86
4	143	1830	1830	17.9	386	0.14	496	0.74	0
5	143	1830	1830	17.9	386	0.14	496	0.74	0.69
6	143	1830	1830	17.9	386	0.14	441	0.38	0
7	143	1830	1830	20.7	386	0.14	496	0.74	0.69
8	143	1830	1830	20.7	462	0.24	441	0.38	0
9	143	1830	1830	20.7	386	0.14	441	0.38	1.86
10	143	1830	1830	22.1	386	0.14	441	0.38	0.69
11	143	1830	1830	22.1	462	0.24	496	0.74	0
12	143	1830	1830	22.1	462	0.24	441	0.38	0.69
13	143	1830	1830	22.8	462	0.24	448	0.54	1.86
14	143	1830	1830	22.8	386	0.14	448	0.54	1.86
15	143	1830	1830	22.8	462	0.24	448	0.54	0.69
16	143	1830	1830	17.2	462	0.24	496	0.74	1.86
17	137	1830	1830	26.2	462	0.26	441	0.40	1.93
18	137	1830	1830	26.2	462	0.26	441	0.40	1.93
19	137	1830	1830	26.2	462	0.26	441	0.40	1.93
20	137	1830	1830	26.2	462	0.26	441	0.40	1.93
21	137	1830	1830	26.2	386	0.14	448	0.56	1.93
22	137	1830	1830	26.2	386	0.14	448	0.56	0.69
D1	143	1830	1830	28.3	572	0.07	510	0.54	1.86
D2	143	1830	1830	28.3	641	0.07	510	0.54	1.86

Table A.2 Minimum Reinforcement Ratios for Shing's Shear Walls

Wall No.	Minimum ρ_h		Prov'd ρ_h /Req'd ρ_h		Failure Mode[†]	Disp. Duct. Factor	Energy Dissip. Factor
	Strength (%)	Energy (%)	Strength	Energy			
1	0.187	0.047	1.28	5.11	F	9	16
2	0.264	0.057	0.91	4.21	F	11	17
3	0.268	0.057	0.92	2.46	Sh	11	17
4	0.102	0.022	1.37	6.36	Sh	5	9
5	0.157	0.034	0.89	4.12	Sh	4	8
6	0.102	0.022	1.37	6.36	F/Sh/Sl	18	65
7	0.169	0.034	0.83	4.12	Sh	6	10
8	0.092	0.022	2.61	10.91	F/Sl	11	40
9	0.268	0.057	0.52	2.46	Sh	7	7
10	0.174	0.034	0.80	4.12	F/Sh	11	26
11	0.095	0.022	2.53	10.91	Sh/Sl	5	10
12	0.146	0.034	1.65	7.06	F	16	55
13	0.235	0.057	1.02	4.21	Sh	11	14
14	0.282	0.057	0.50	2.46	Sh	6	9
15	0.148	0.034	1.62	7.06	F/Sh	14	39
16	0.205	0.057	1.17	4.21	Sh	6	12
17	0.258	0.060	1.01	4.33	F	---	---
18	0.258	0.060	1.01	4.33	F	---	---
19	0.258	0.060	1.01	4.33	F	---	---
20	0.258	0.060	1.01	4.33	F	---	---
21	0.309	0.060	0.45	2.33	Sh	---	---
22	0.190	0.034	0.74	4.12	Sh	---	---
D1	0.212	0.144	0.33	0.49	R	---	---
D2	0.189	0.144	0.37	0.49	R	---	---

†F - flexure, Sh - shear (diagonal cracking), Sl - sliding (base), R - rupture (horiz. steel)

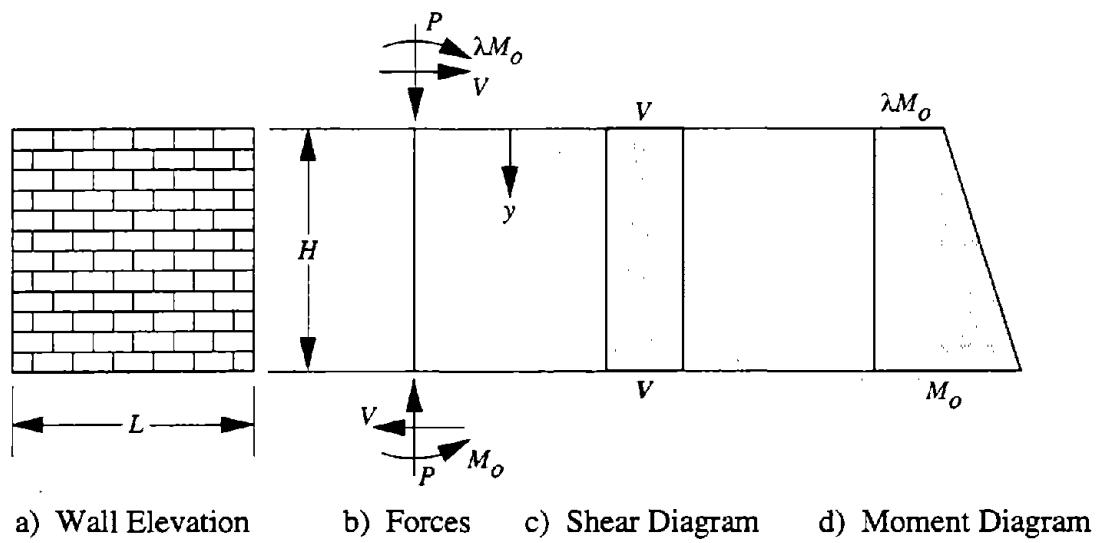a) Wall Elevation   b) Forces   c) Shear Diagram   d) Moment Diagram
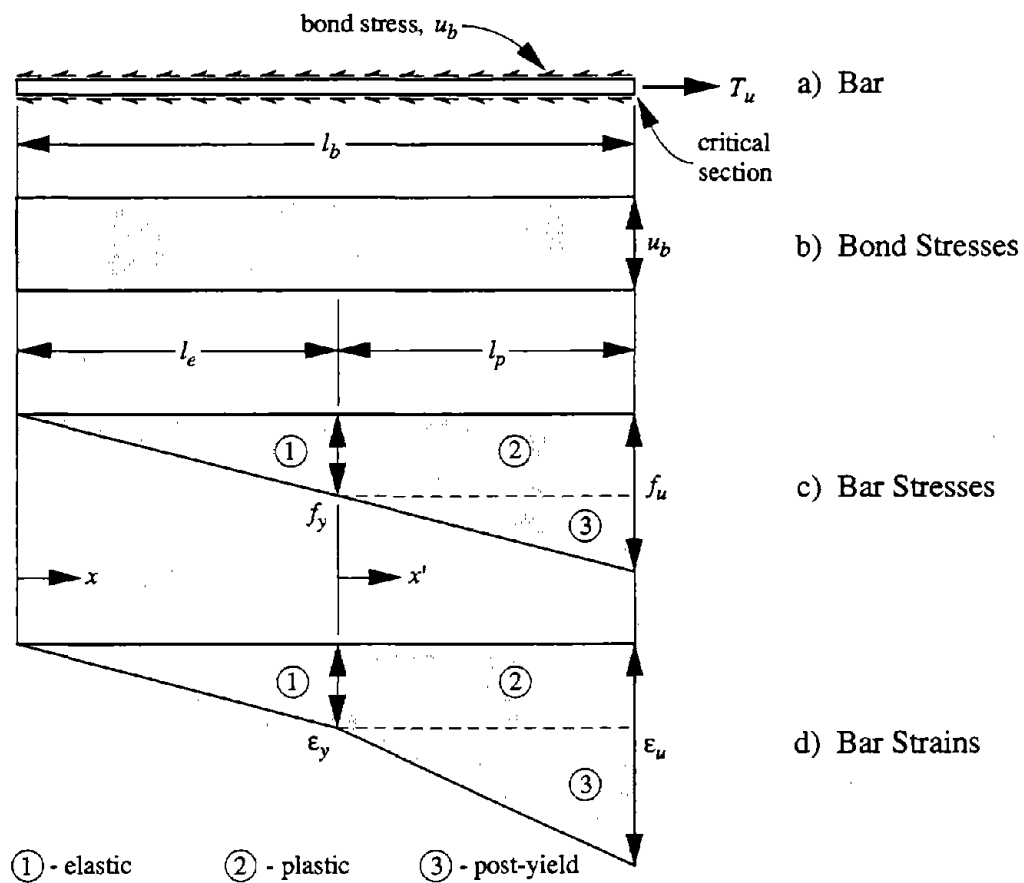
Fig. A.1 Forces in Masonry Shear Wall

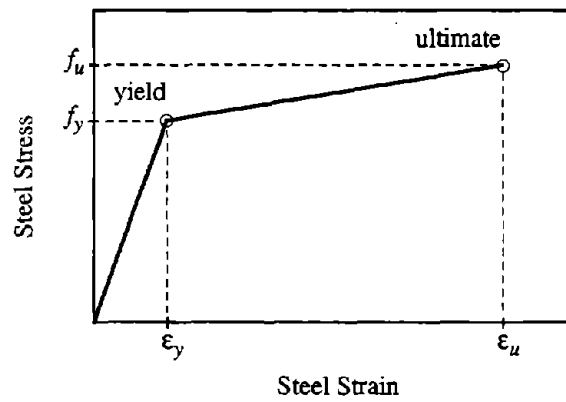Fig. A.2 Stresses and Strains in Bonded Reinforcement

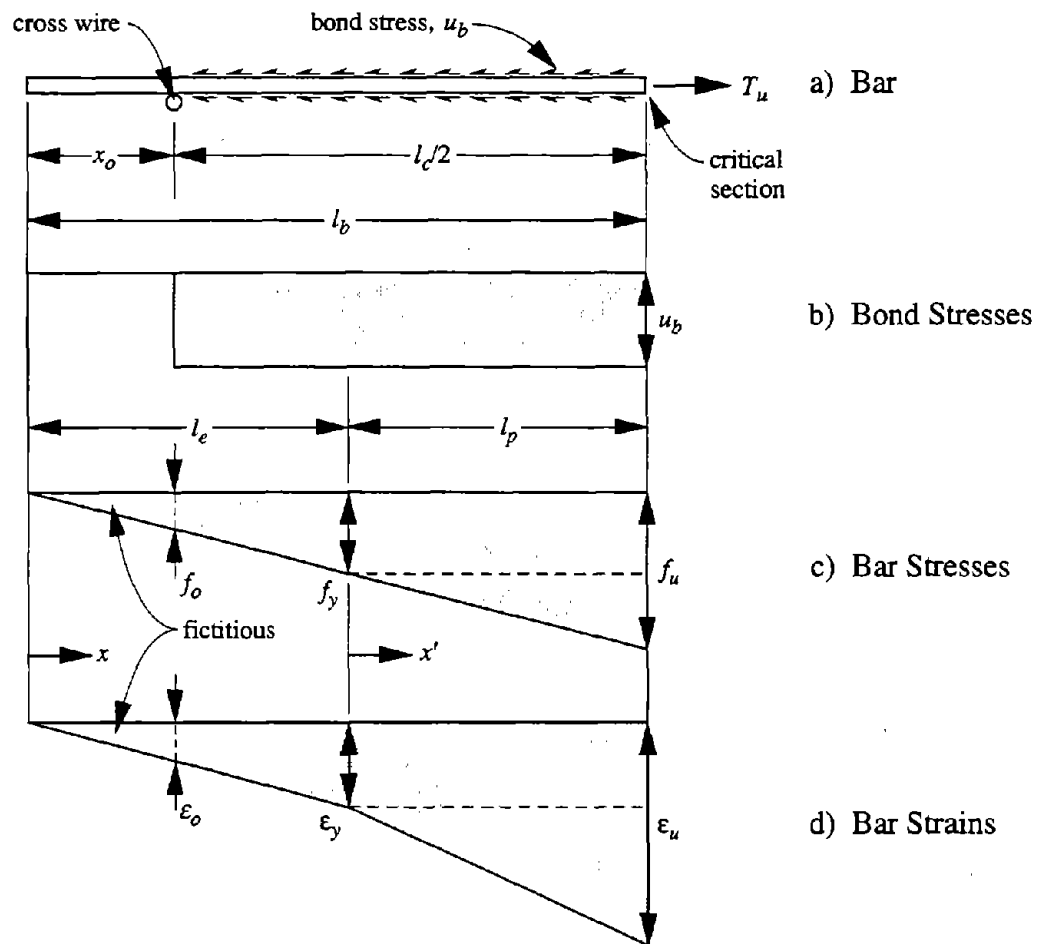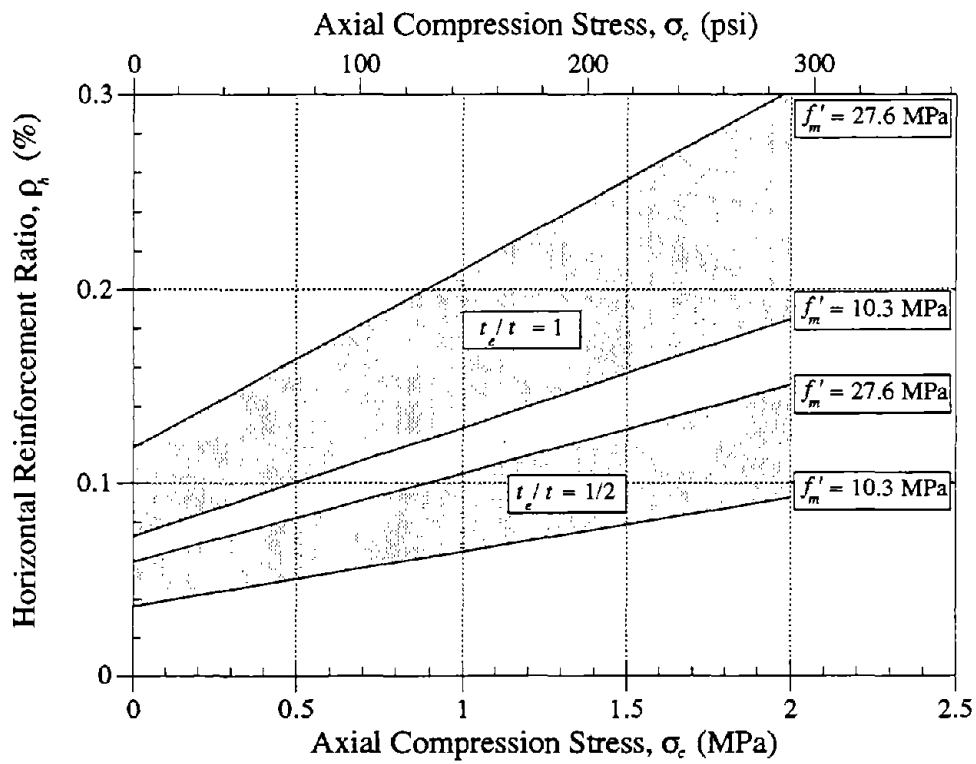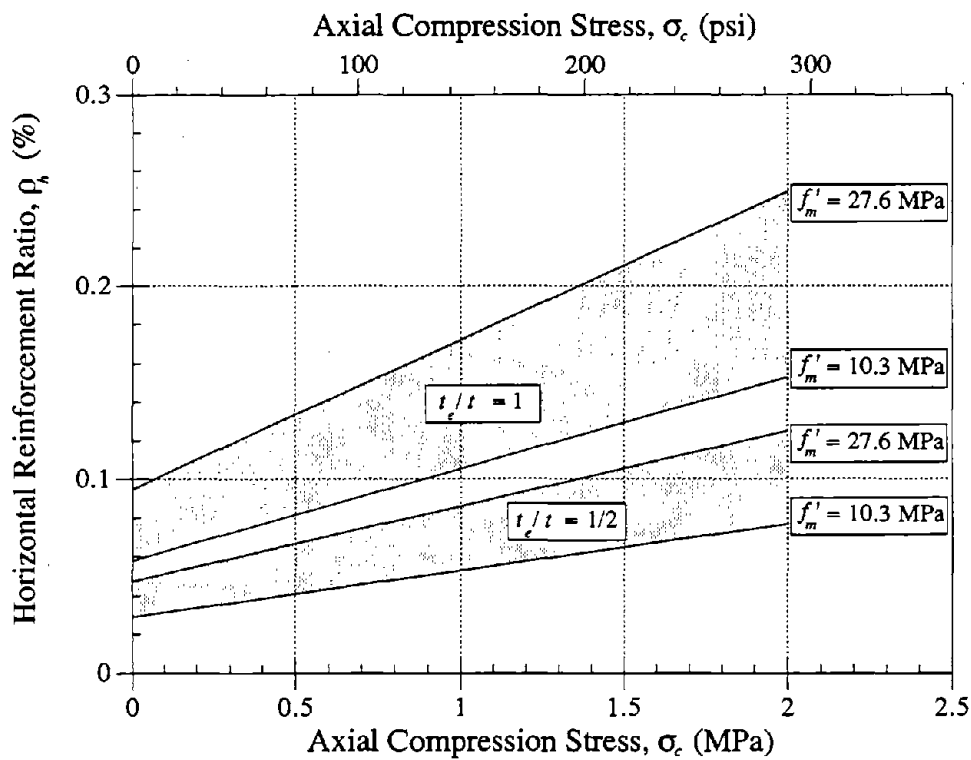Fig. A.3 Stress-Strain Curve for Reinforcing Steel

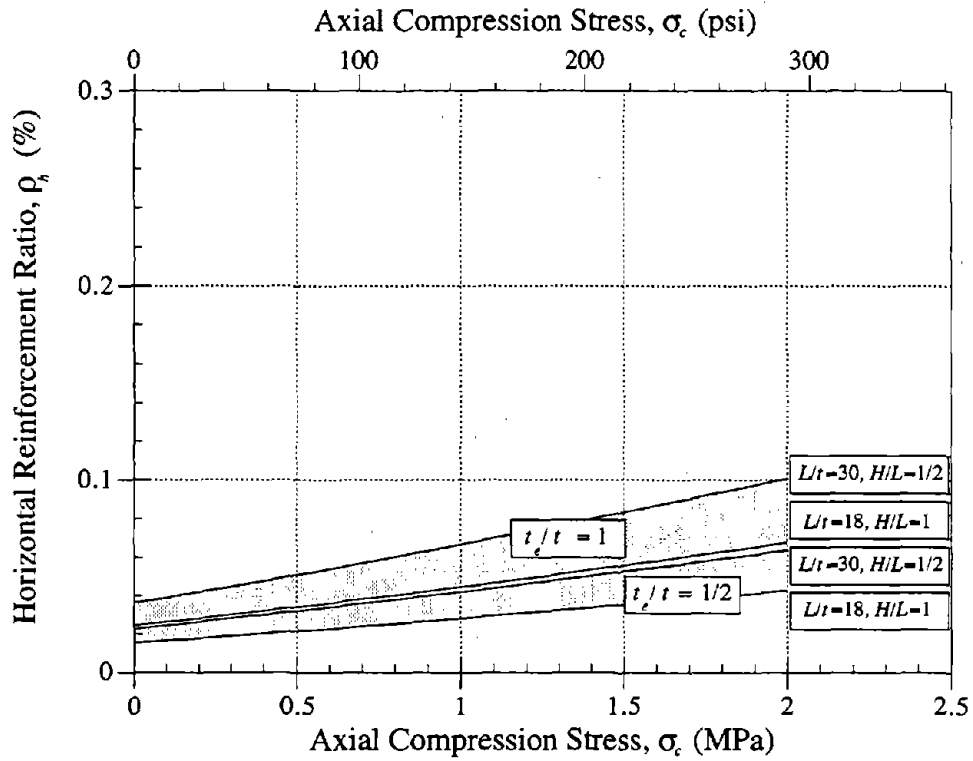Fig. A.4 Stresses and Strains for Grids with Cross Wires
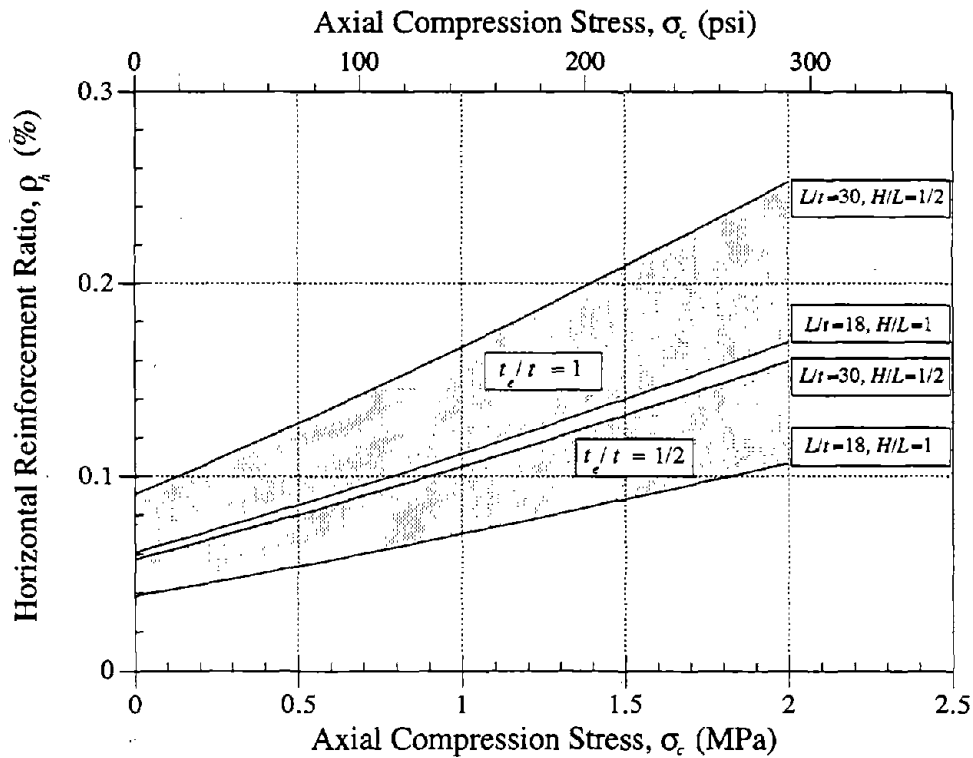
a) Hot-Rolled Reinforcing Bar (f_{yh} = 414 MPa)

b) Wire Reinforcing Grid (f_{yh} = 552 MPa)

Fig. A.5 Minimum Horizontal Reinforcement Ratios for the Strength Criterion

97

a) Hot-Rolled Reinforcing Bar (f_{yh} = 414 MPa, u_b = 10.3 MPa, μ_ε = 75)

b) Wire Reinforcing Grid (f_{yh} = 552 MPa, u_b = 4.1 MPa, μ_ε = 19)

Fig. A.6 Minimum Horizontal Reinforcement Ratios for the Energy Criterion

APPENDIX B. POTENTIAL DIRECTIONS FOR FUTURE RESEARCH

This appendix briefly discusses potential topics for future research on seismic behavior and design of masonry walls. Some of these topics were identified in an industry workshop held at NIST in conjunction with the Council for Masonry Research (Fattal, 1993b). Other topics were identified after the workshop, as Structure Division staff at NIST continued to interact with masonry producers, practicing structural engineers, and code writing bodies.

B.1 Prestressed Masonry

Prestressed masonry is a promising load-resisting system in need of practice-oriented research and development (Schultz and Scolforo, 1992a). In prestressed masonry, vertical reinforcing bars are replaced with prestressing tendons (bar or strand). As such, prestressed masonry requires less vertical reinforcement than reinforced masonry because it utilizes tendons with effective yield stresses of at least 620 MPa (90 ksi) instead of hot-rolled reinforcing bars with a yield strength of 414 MPa (60 ksi). Besides increasing in-plane and out-of-plane flexural strength of masonry shear walls through the reduction of flexural tension, prestressing also enhances in-plane and out-of-plane shear strength by taking advantage of friction. This effect is particularly beneficial for low-rise construction in which axial stress from vertical loads is almost always low. In the case of clay masonry, the usually high compression strength of this material may enable prestressing to extend load capacity markedly.

Prestressed masonry applications have been proposed for seismic and wind design of new construction, as well as strengthening of existing structures (Schultz and Scolforo, 1992a). Issues that need to be investigated include identification of shear wall response and failure modes, optimal magnitude of vertical prestressing, spacing of tendons, expected toughness in seismic events, techniques to improve toughness, optimal amount of horizontal reinforcement, type of horizontal reinforcement, and techniques for corrosion protection. Another advantage offered by prestressed masonry is ungrouted construction, whereby the cost and weight of the structure are reduced as compared to fully-grouted or partially-grouted masonry. A particularly attractive variant combines ungrouted vertical tendons with bed joint reinforcement, thereby eliminating all grouting. This form of construction represents the next logical step in the progression of masonry structural systems which follow the partially-grouted masonry walls in the present research program.

It is impossible for the masonry industry in the U.S. to fund all of the research and development needed to propel prestressed masonry into use. Yet, without this investment, practicing engineers and building officials are unwilling to experiment with its use. Building code provisions have been suggested for use in the U.S.A. (Schultz and Scolforo, 1992b; 1992c), and the Masonry Standards Joint Committee is currently drafting recommended standards for the design of prestressed masonry. Unfortunately, these provisions arise primarily from gravity load and wind load design considerations, and precious little information is available regarding earthquake loading.

B.2 Composite Walls

Composite walls comprising wythes of different types of masonry (usually clay brick and concrete block) have enjoyed some increase in popularity in the aftermath of the problems associated with light metal stud backup systems. Bond failure of the collar joint between wythes may be induced by long-term differential movements between the two materials. However, the use of metal ties to connect the wythes has been shown to maintain integrity of the wythes (Drysdale et al., 1994). If it can also be shown that composite walls can be proportioned to improve earthquake resistance, say for a small amount of vertical and horizontal joint reinforcement a significant and consistent increase in resistance is gained, then this may become an even more appealing architectural/structural system. However, experimental verification of this lateral strength, and reliable methods for its computation, are needed.

B.3 Higher Strength Masonry

The current research plan identifies a single value of compression strength for each type of masonry (clay or concrete). Mean values for nominal compression strength equal to 27.6 MPa (4000 psi) and 13.8 MPa (2000 psi) for clay and concrete masonry, respectively, are adopted in the plan. The resulting range of compression strengths is not broad, and it may become necessary, at a later time, to investigate higher-strength masonry. Current technology facilitates easy and economical manufacture of high strength clay or concrete units, but existing code provisions for determining f_m from masonry unit and mortar strengths underestimate the actual capacity of masonry. Improvements in mortar mixtures and confining devices for high-compression regions further enhance the mechanical behavior of masonry in compression. Recognized higher compression strengths of masonry can extend the range of lateral load applicability of masonry walls.

B.4 Biaxial Lateral Load

Biaxial lateral loading effects should be studied, as such load combinations have proven to be more damaging than uniaxial lateral loads for other structural materials. Corners of masonry buildings are vulnerable to biaxial loading effects, and Fattal's recommendation regarding the placement of vertical reinforcement in outer cells (1993b) may prove to be well suited to mitigate damage from biaxial lateral loading. Out-of-plane racking loads from cross walls and diaphragms, particularly if the latter are not fully fixed to the walls, also give rise to biaxial lateral loading.

B.5 Variable Axial Load

All of the masonry shear wall tests identified by Yancey et. al. (1991) appear to have been conducted with constant axial forces to simulate vertical stress from dead loads. At some juncture, however, the behavior of masonry shear walls under variable axial load histories should be investigated. Dramatic changes in the seismic performance of laterally-loaded reinforced concrete columns under variable axial loads have been observed experimentally and analytically. Two general classes of axial load histories should be considered. Axial loads generated in masonry piers by overturning are approximately proportional to (i.e. synchronous with) the lateral load history. On the other hand, axial loads from vertical acceleration histories are independent of (i.e. asynchronous with) the lateral load history.

B.6 Grout Replacement

The Council for Masonry Research has identified grout replacement as a valid and timely subject for practice-oriented research. The issue of greatest interest is the replacement of pumping with pouring as the choice method for grout placement. Replacement of grout with mortar is also identified by industry as a topic in need of research. In both cases, the issues at stake concern the impact of material properties on structural behavior, and the requirements are such that the resulting material may differ considerably from that specified in ASTM C476 (ASTM, 1983). It is possible that grout replacement may have an impact on lateral load response of masonry shear walls. If further enhancement to seismic load resistance is sought, then the use of metal or plastic fibers, in conjunction with superplasticized grout or mortar, may be pursued as a means of increasing the toughness of masonry under compression.